

# **Postsynaptic Signaling Mechanisms by the NMDA-Receptor and CaMKII**

Dissertation

In partial fulfillment of the requirements for the degree of  
*Doctor rerum naturalium* (Dr. rer. nat.)

Presented to the Department of Chemistry at the  
University of Bielefeld

by

Sebastian Ivar Stein

Bielefeld 2012



Reviewer: Prof. Dr. Johannes Hell  
Department of Pharmacology  
University of California, Davis

Prof. Dr. Gabriele Fischer von Mollard  
Biochemistry III, Department of Chemistry  
University of Bielefeld

<b>1</b>	<b>Introduction .....</b>	<b>1</b>
1.1	LTP .....	2
1.2	The Role of CaMKII in LTP .....	3
1.3	The Role of CaMKII in Learning and Memory .....	5
1.4	The Structure of CaMKII and its Activity-dependent Translocation to the PSD .....	7
1.5	The CaMKII/GluN2B Interaction .....	10
1.6	The CaMKII/GluN2B Interaction in Learning and Memory .....	13
1.7	The N-methyl-D-aspartate Receptor (NMDAR) .....	14
1.8	The Regulation of the NMDAR by Phosphorylation via the cAMP/PKA Pathway.....	16
1.9	Aim of this Work .....	17
<b>2</b>	<b>Material and Methods.....</b>	<b>19</b>
<b>2.1</b>	<b>Animal Procedures .....</b>	<b>19</b>
2.1.1	Animal Husbandry.....	19
2.1.2	GluN2B KI Mice .....	19
2.1.3	Genotyping.....	21
2.1.3.1	Tail Tip Digest .....	21
2.1.3.2	Polymerase Chain Reaction (PCR) .....	22
2.1.3.3	PCR Digest.....	23
2.1.3.4	Agarose Gel Electrophoresis .....	23
2.1.4	Behavior .....	24
2.1.4.1	Morris Water Maze (MWM).....	24
2.1.4.2	Barnes Maze .....	24
2.1.4.3	Elevated Plus Maze (EPM) .....	25
2.1.4.4	Contextual Fear Conditioning.....	26
<b>2.2</b>	<b>Cell Culture and Molecular Biological Methods .....</b>	<b>26</b>
2.2.1	DNA Purification.....	26
2.2.2	Preparation and Coating of Coverslips with Poly-L-Lysine .....	27
2.2.3	Hippocampal Cultures .....	27
2.2.4	Transfection of Hippocampal Cultures with Lipofectamine2000 .....	29
2.2.5	Fixation of Hippocampal Cultures.....	29

## Table of contents

---

2.2.5.1	Methanol Fixation .....	30
2.2.5.2	Paraformaldehyde (PFA) Fixation.....	30
2.2.6	Immunostaining of Hippocampal Cultures.....	31
2.2.7	Surface Staining of Hippocampal Cultures.....	32
2.2.8	LDH Cytotoxicity Assay .....	33
<b>2.3</b>	<b>Protein Biochemistry.....</b>	<b>33</b>
2.3.1	Preparation of Acute Slices .....	33
2.3.2	Protein Extraction from Whole Tissue .....	35
2.3.3	Protein Quantification with the BCA (Bicinchoninic Acid) Assay.....	38
2.3.4	Immunoprecipitation (IP).....	38
2.3.5	Preparation of the Postsynaptic Density Fraction (PSD).....	39
2.3.6	<i>In vitro</i> Phosphorylation/Dephosphorylation .....	41
2.3.6.1	PKA Phosphorylation .....	41
2.3.6.2	CaMKII Phosphorylation .....	41
2.3.6.3	CIP Dephosphorylation .....	42
2.3.7	<sup>32</sup> P Labeling and Overlay Analysis .....	42
2.3.8	Western Blot (WB) Analysis.....	43
2.3.8.1	SDS-PAGE.....	43
2.3.8.2	Wet Transfer.....	43
2.3.8.3	Immunodetection.....	43
2.3.8.4	Quantification of Immunoblot Signals .....	44
<b>2.4</b>	<b>Antibodies .....</b>	<b>46</b>
2.4.1	List of Antibodies Used for WB and Immunocytochemistry (ICC)....	46
<b>2.5</b>	<b>Statistical Analysis .....</b>	<b>47</b>
<b>3</b>	<b>Results .....</b>	<b>48</b>
<b>3.1</b>	<b>The Role of the CaMKII/GluN2B Interaction in Learning and Memory .....</b>	<b>48</b>
3.1.1	Spatial Learning and Memory is not Affected in the Barnes Maze ..	49
3.1.2	Single Day Spatial Learning in the Morris Water Maze is Impaired in GluN2BKI Mice .....	51
3.1.3	Basal Anxiety Levels in the GluN2B KI Mice are Normal .....	53
3.1.4	Learning and Memory in Contextual Fear Conditioning is not Affected in GluN2B KI.....	54

3.1.5	Contextual Fear Conditioning Performance is Independent of the Stimulus Strength.....	55
<b>3.2</b>	<b>The Activity-dependent Translocation of CaMKII .....</b>	<b>57</b>
3.2.1	Interactions of Autophosphorylated CaMKII in the Brain .....	58
3.2.2	Concentration-dependent Displacement of the CaMKII/NMDAR Complex by CN21.....	59
3.2.3	Time Course of CaMKII $\alpha$ Clustering.....	61
3.2.4	Time Course of CaMKII $\beta$ Clustering.....	64
3.2.5	The Persistence of the CaMKII $\alpha$ Translocation.....	67
3.2.6	Brief Stimulation with Glutamate is Sufficient to Induce CaMKII $\alpha$ Translocation .....	69
3.2.7	The Role of Neurogranin in the Activation and Translocation of CaMKII .....	71
3.2.8	The Translocation of CaMKII is Independent of GluN1 .....	75
<b>3.3</b>	<b>PKA-dependent Regulation of the NMDAR.....</b>	<b>79</b>
3.3.1	PKA Induces phosphorylation of GluN2B S1166 <i>In Vitro</i> .....	79
3.3.2	Phosphorylation of S1166 is Enriched in the PSD .....	80
3.3.3	$\beta$ -Adrenergic-Receptor Stimulation of Acute Forebrain Slices Increases S1166 Phosphorylation.....	81
3.3.4	$\beta$ -Adrenergic-Receptor Stimulation-induced Increase of S1166 Phosphorylation is Independent of AKAP150 .....	82
3.3.5	Forced Swim Stress Induces S1166 Phosphorylation <i>In Vivo</i> .....	84
3.3.6	I.P. Injection of Propranolol Reduces Forced Swim-induced Phosphorylation of S845 but not S1166 .....	86
3.3.7	D <sub>1</sub> /D <sub>5</sub> Receptor Stimulation of Acute Forebrain Slice Induces S1166 Phosphorylation .....	88
3.3.8	I.P. Injection of the D <sub>1</sub> /D <sub>5</sub> Receptor Antagonist SCH23390 does not Reduce Forced Swim-induced Phosphorylation .....	89
3.3.9	A Combination of the Antagonists Propranolol and SCH23390 Reduces Basal Phosphorylation Levels of S1166 <i>In Vivo</i> .....	91
3.3.10	I.P. Injection of a Combination of Propranolol and SCH23390 has no Effect on the Forced Swim-induced Increase in Phosphorylation of S1166.....	91

3.3.11	I.P. Injection of the Adenosine A <sub>2A</sub> Receptor does not Affect Stress-induced Regulation of S1166.....	93
3.3.12	Reduced Forced Swim Stress Results in Reduced Receptor Phosphorylation Levels.....	95
3.3.13	Hippocampal Injection of PKA Antagonist Rp-8-Br-cAMPs Reduces Basal and Forced Swim-induced S1166 Phosphorylation .....	97
<b>3.4</b>	<b>Side Effects of Cell Penetrating Peptides (CPP) .....</b>	<b>99</b>
3.4.1	The 11R Cell Penetrating Peptide Induces Cytotoxicity in a Concentration-dependent Manner.....	100
3.4.2	The 11R Cell Penetrating Peptide Inhibits CaMKII Activity in a Concentration-dependent Manner.....	102
3.4.3	The 11R Cell Penetrating Peptide Inhibits PKA Activity in a Concentration-dependent Manner, with no Effect of the Tat Sequence or Myristoylation .....	105
<b>4</b>	<b>Discussion .....</b>	<b>108</b>
4.1	The Role of the CaMKII/GluN2B Interaction in Learning and Memory .....	108
4.2	The Activity-dependent Translocation of CaMKII .....	112
4.3	PKA-dependent Regulation of the NMDAR.....	120
4.4	Side Effects of Cell Penetrating Peptides (CPP) .....	126
<b>5</b>	<b>Summary .....</b>	<b>129</b>
5.1	Summary.....	129
5.2	Zusammenfassung .....	131
<b>6</b>	<b>References .....</b>	<b>133</b>
	<b>Figures .....</b>	<b>150</b>
	<b>Acknowledgements/Danksagung.....</b>	<b>152</b>
	<b>Curriculum Vitae .....</b>	<b>154</b>
	<b>Erklärung .....</b>	<b>156</b>

## 1 Introduction

Memory is the process by which acquired information is encoded, stored and retrieved if needed. It is absolutely essential for managing our everyday lives and chores and, even more importantly, our memories and experiences make and define us as individuals.

One of the pioneers of the still ongoing journey to understand learning and memory and the underlying molecular mechanism was the Spanish physician Santiago Ramón y Cajal who was able to visualize individual neurons using a staining procedure developed shortly before by Camillo Golgi. Based on his findings Cajal argued that nerve cells are independent entities and as such the functional unit of the brain (Swanson et al., 2007). In the 1950s the Canadian psychologist Donald O. Hebb took Cajal's finding a step further and developed a theory about how these individual neurons function and adapt in complicated processes like learning. Hebb's cell assembly theory describes the basic mechanism of synaptic plasticity: "*When an axon of cell A is near enough to excite cell B and repeatedly or persistently takes part in firing it, some growth process or metabolic change takes place in one or both cells such that A's efficiency, as one of the cells firing B, is increased.*" (Hebb, 1949). Experimental evidence for this phenomenon, where coordinated activation of two cells results in synaptic strengthening of those cells, was found in the 1970s when Terje Lømo and Tim Bliss described long-term potentiation (LTP) in the hippocampus (Bliss and Lomo, 1973). The hippocampus itself is one of the major model systems for synaptic plasticity and learning and memory. Findings in patients and later on in animal studies show that the hippocampus is important for the formation of episodic memory. The most famous patient, H.M., suffered from anterograde amnesia after, in an attempt to remedy his epileptic seizures, he underwent experimental bilateral medial temporal lobe resection that included both hippocampi. He was unable to form new episodic memories, but was still able to partially recall old ones (Scoville and Milner, 1957; Squire, 2009). These observations and subsequent studies (Squire, 1992) showed that the hippocampus is essential

for the formation of new episodic memories and that at least part of these memories are transferred to other brain regions for long-term storage.

## 1.1 LTP

LTP is one of the best studied forms of synaptic plasticity. This permanent increase in the strength of synaptic transmission after brief patterns of high-frequency stimulation (HFS) was first observed in the hippocampus (Bliss and Lomo, 1973) and is thought to be the cellular equivalent of learning and memory. LTP can be induced in the living animal and last for at least several months (Abraham et al., 2002).

The most striking evidence that memories are encoded by strengthening of synaptic transmission in an LTP-like process comes from a study showing that the learning-induced synaptic potentiation in the hippocampus actually occluded subsequent HFS induced LTP (Whitlock et al., 2006). Also, the induction of LTP in a large fraction of hippocampal synapses after Morris water maze (MWM) learning disrupted the memory trace, presumably by interfering with the ability of retrieving memory from the network, where it is stored in a distributed pattern of potentiated synapses (Brun et al., 2001).

Synaptic transmission in over 90% of the synapses in the brain is mediated by the excitatory neurotransmitter glutamate. The increase in synaptic strength is predominantly mediated by increased sensitivity of the glutamate receiving postsynaptic sites (Malenka and Bear, 2004). The signal promoting these plastic changes in the postsynapses is calcium entering the cell through an ionotropic glutamate receptor, the N-methyl-D-aspartate receptor (NMDAR), which is essential for this type of LTP. Calcium is an important second messenger for LTP as well as learning and memory. Upon entering the postsynaptic site through the NMDAR, calcium regulates many enzymes and proteins including the calcium/calmodulin-dependent protein kinase II (CaMKII) (Hudmon and Schulman, 2002). CaMKII is activated by calcium influx through the NMDAR and is subsequently recruited to the postsynaptic density (PSD) where it directly interacts with the NMDAR (Lee

and Silva, 2009; Lisman et al., 2012; Malenka and Bear, 2004). CaMKII binds to the GluN1 and GluN2B subunit of the NMDAR (Leonard et al., 1999; Strack et al., 2000a). Particularly the interaction with the GluN2B subunit is critical for the induction of LTP (Barria and Malinow, 2005; Halt et al., 2012; Zhou et al., 2007)

Interestingly transgenic mice which over express the GluN2B subunit in the forebrain (*doogie* mouse) show enhanced hippocampal LTP and superior performance in different hippocampus-dependent learning and memory paradigms (Tang et al., 1999).

## 1.2 The Role of CaMKII in LTP

Synaptic strengthening after LTP is due to the potentiation of the  $\alpha$ -amino-3-hydroxy-5-methyl-4-isoxazole propionic acid receptor (AMPA) mediated excitatory postsynaptic current (EPSC). AMPARs mediate most of the excitatory glutamatergic synaptic transmission in the brain. The number of functional AMPARs in the synapse is tightly linked to synaptic strength and the activity-dependent regulation of the synaptic AMPAR content is the mechanism underlying synaptic plasticity (Lisman and Raghavachari, 2006; Martin et al., 2000). The recruitment of AMPARs during LTP involves exocytosis at extra- and/or peri-synaptic sites, lateral diffusion into the synapse, and subsequent diffusional trapping in the PSD (Opazo and Choquet, 2011). The trapping of AMPARs at synaptic sites is mediated bidirectionally by phosphorylation of the auxiliary subunit stargazin, which mediates the interaction of the AMPAR complex with the postsynaptic scaffolding protein PSD-95. In its C-terminal tail Stargazin contains a polybasic region consisting of eight arginine residues, which interact with the negatively charged lipid bilayer. This polybasic region is surrounded by nine serine residues which can be phosphorylated in an activity-dependent manner and thereby disrupt the electrostatic interaction with the membrane. The subsequent dissociation from the lipids allows the C-terminal interaction with PSD-95, resulting in the diffusional trapping of the AMPAR at the PSD (Sumioka et al., 2010; Tomita et al., 2005).

During the early phase of LTP the phosphorylation of stargazin is mediated by CaMKII. The translocation of CaMKII to the PSD brings the activated enzyme close to the AMPAR complex, where it is responsible for this activity-dependent phosphorylation of the C-terminal tail of stargazin and the GluA1 subunit of the AMPAR itself (Opazo et al., 2010). CaMKII phosphorylates S831 of the GluA1 subunit of the AMPAR, thereby increasing the average conductance of the channel (Barria et al., 1997; Kristensen et al., 2011; Lee et al., 2000).

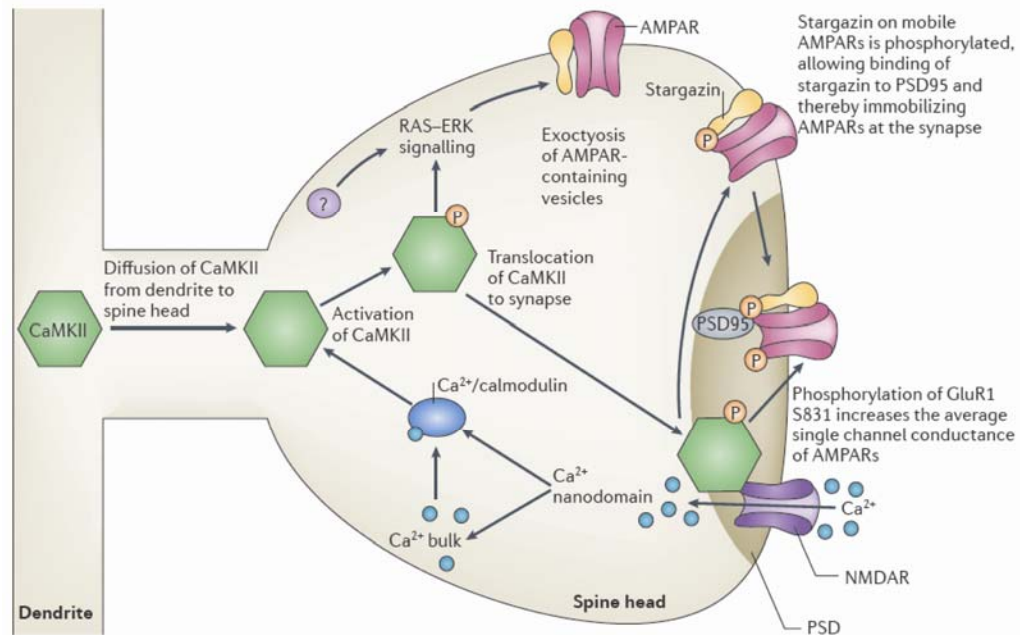


**Figure 1.1: The Role of CaMKII during early LTP.** The Ca<sup>2+</sup>-influx through the NMDAR and the subsequent binding of CaM in the nanodomain of the channel, as well as in the bulk of the cytoplasm leads to activation of CaMKII. The activated and autophosphorylated CaMKII then translocates to the PSD, where it enhances AMPAR mediated excitatory postsynaptic potentials (EPSC) by direct phosphorylation of the GluA1 (formerly GluR1) subunit and phosphorylation of stargazin. Phosphorylation of S831 of GluA1 enhances the single channel conductance, while phosphorylation of stargazin and the subsequent interaction with PSD-95 increases the number of synaptic AMPARs. Figure from Lisman et al., 2012.

CaMKII contributes to the increase in AMPAR mediated EPSCs during early long-term potentiation (Fig. 1.1) in at least two ways: through the increase in single channel conductance and the number of functional receptors at the PSD. Its role during LTP maintenance, however, is not clear.

In individual dendritic spines the majority of CaMKII was only active for about one minute after LTP induction (Lee et al., 2009). This brief window of CaMKII activity could mean two things for its involvement during LTP. CaMKII

may only be important for the induction of LTP and play a transient role in the activation of downstream processes maintaining LTP. Alternatively the ubiquitous, dodecameric CaMKII holoenzyme may have a structural role. CaMKII is anchored at the PSD by interacting with the NMDAR in an activity-dependent manner (Bayer et al., 2006; Halt et al., 2012; Leonard et al., 1999). It was reported that the CaMKII/NMDAR complex itself might control synaptic strength independent of kinase activity, supporting the idea for a structural role of CaMKII during LTP maintenance (Sanhueza et al., 2011; Sanhueza et al., 2007).

Unlike the early-phase of LTP which relies on posttranslational modifications, the late-phase of LTP requires transcription and synthesis of new proteins, together with spine enlargement and growth of the synapse itself (Malenka and Bear, 2004; Ostroff et al., 2002).

The overexpression of active CaMKII holoenzymes leads to an increase in spine size as seen following LTP induction. Remarkably, even overexpression of the autonomous,  $\text{Ca}^{2+}$ /CaM independent form of CaMKII (T286D) without kinase activity (K42R) increases spine size (Pi et al., 2010a), further arguing for a structural role independent of kinase activity. In addition, CaMKII $\alpha$  mRNA levels are high in dendrites (Burgin et al., 1990). Consequently, tetanic stimulation results in a translation-dependent increase of dendritic CaMKII $\alpha$  levels (Ouyang et al., 1999). Removal of the dendritic targeting signal on the CaMKII $\alpha$  mRNA in an *in vivo* mouse model resulted in decreased postsynaptic CaMKII $\alpha$  levels, reduced late-phase LTP and deficits in spatial memory tasks (Miller et al., 2002).

### 1.3 The Role of CaMKII in Learning and Memory

The accumulating evidence that the NMDAR and CaMKII represent two of the key players involved in memory and learning as well as in the LTP model (best studied in the CA1 region of the hippocampus) led to the generation of various mouse mutants to better understand the molecular basis of these phenomena. Notably, CaMKII with its calcium independent activity and multiple levels of regulation through autophosphorylation on T286 and

TT305/306 (amino acid positions are given in reference to CaMKII $\alpha$ ) received a lot of attention. The first mutant described was the CaMKII $\alpha$  knock-out mouse. It is deficient in LTP and impaired in spatial learning in the MWM (Silva et al., 1992a; Silva et al., 1992b). This learning deficit is overcome after more intensive training, likely due to a compensatory translocation of CaMKII $\beta$  (Elgersma et al., 2002). Knock-in mice with mutations in the endogenous CaMKII $\alpha$  gene allowed the specific role of CaMKII $\alpha$  in LTP, learning and memory to be addressed, without compensation by the  $\beta$ -subunit. Many of the mutations focused on the regulation of CaMKII through autophosphorylation on T286 and T305/306. Phosphorylation of T286 renders CaMKII constitutive active independent of calcium and it was observed that T286 autophosphorylation is increased after chemical LTP and tetanic stimulation (Lengyel et al., 2004; Ouyang et al., 1997). Calcium-independent activity was also enhanced in rats after spatial learning in the Morris water maze (Tan and Liang, 1996). T286A CaMKII mutant mice exhibit no hippocampal NMDAR-dependent LTP and have impaired MWM learning (Giese et al., 1998). The rapid acquisition of fear conditioning is affected, but can be rescued by more extensive training. Memory formation after this extended training is normal in T286A mice (Irvine et al., 2005), arguing that T286 autophosphorylation is important for acquisition but not memory recall and consolidation.

In comparison to the T286A mice, the T286D mutation and the results from the KI mouse are harder to interpret. For instance, the autophosphorylation-mimicking aspartate mutation (T286D) has no effect on high-frequency stimulation induced LTP (100 Hz), but affects 5 Hz LTP in an expression level dependent manner. Low-level expression enhances 5 Hz LTP while high expression levels of the T286D mutant induce LTD and impair spatial learning in the Barnes Maze (Bach et al., 1995; Bejar et al., 2002; Mayford et al., 1996; Mayford et al., 1995). Though initially surprising, these findings are in line with a later study in organotypic hippocampal slice cultures, which found that autonomous T286D CaMKII is shifting the balance either towards LTP or LTD, depending on the phosphorylation state of T305/T306 (Pi et al., 2010b). *In vitro* studies showed that T305/T306 phosphorylation succeeds T286 phosphorylation (Jama et al., 2009; Lou and

Schulman, 1989) and that this phosphorylation regulates PSD association (Shen et al., 2000; Strack et al., 1997b). These findings were confirmed in TT305/306 mutant mice. Phosphomimetic T305D mutants displayed deficits in MWM learning and memory and disrupted contextual fear conditioning, explainable by reduced levels of PSD associated CaMKII and impaired LTP. The non-phosphorylatable TT305/306VA mutants, in contrast exhibited increased PSD associated CaMKII levels and a shift of the frequency-dependence of plasticity towards LTP, allowing LTP after 10 Hz stimulation. General spatial learning seemed to be normal, but less adaptable as seen in reduced reversal learning and missing discrimination during contextual fear conditioning (Elgersma et al., 2002).

#### **1.4 The Structure of CaMKII and its Activity-dependent Translocation to the PSD**

CaMKII is a dodecameric holoenzyme that constitutes up to 1% of total protein in the forebrain and 2% in the hippocampus (Erondu and Kennedy, 1985). CaMKII is encoded by four different genes,  $\alpha$ - $\delta$ , and each of the isoforms has multiple splice variants (Hudmon and Schulman, 2002).  $\alpha$  and  $\beta$  are the predominant isoforms in the brain. In the early postnatal brain up to postnatal day ten CaMKII has low expression levels, followed by a huge increase in expression coinciding with the most important time of synaptic network formation (Yamauchi, 2005). The relative expression levels of the two isoforms are changed during development and are modified by synaptic activity. The fact that CaMKII $\alpha$  mRNA in contrast to  $\beta$  can be found in dendrites corresponds with the activity-dependent local upregulation of CaMKII $\alpha$  (Ouyang et al., 1999; Thiagarajan et al., 2002).  $\alpha/\beta$  heteromers as well as  $\alpha$  homomers have been found in brain tissue and the individual isoform ratios in the holoenzyme are dependent on tissue- and cell-specific expression patterns (Brocke et al., 1999). In the adult forebrain the ratio of  $\alpha$  to  $\beta$  subunit is roughly 3:1, whereas a ratio of 1:4 is seen in the cerebellum (McGuinness et al., 1985).

Apart from the sheer abundance of CaMKII in the brain, the fact that autophosphorylation on T286 confers autonomous activity independent of the presence of  $\text{Ca}^{2+}/\text{CaM}$  caused a lot of interest and made CaMKII a central molecule of research in LTP and learning and memory. Each CaMKII subunit consists of an N-terminal catalytic domain, an autoinhibitory domain followed by a variable segment (linker region) and the C-terminal association (hub) domain. The catalytic domain contains the ATP binding site, the substrate binding site (S-site) and the so called T-site, which interacts in the inactive conformation with the segment surrounding T286 and serves in the open active conformation as a platform for multiple protein interactions. The autoinhibitory domain encloses the T286 segment and the pseudosubstrate region, which interacts with the S-site and blocks access to the catalytic domain and therefore kinase activity.  $\text{Ca}^{2+}/\text{CaM}$  bind to a region in the autoinhibitory domain including T305/T306 and partially overlapping with the pseudosubstrate segment. The binding of  $\text{Ca}^{2+}/\text{CaM}$  results in a conformational change that displaces the pseudosubstrate segment and the T286 segment from the S- and T-site. This conformational change renders the kinase active and exposes the region around T286 to phosphorylation by the neighboring subunit (Fig. 1.2). The inter subunit autophosphorylation on T286 precludes the interaction with the T-site and thereby functions as a wedge, keeping the S-site open and the kinase active (Griffith, 2004; Hudmon and Schulman, 2002; Lisman et al., 2002; Merrill et al., 2005). Autophosphorylation at T286 and the underlying conformational change not only keeps the kinase active, but also increases the affinity for  $\text{Ca}^{2+}/\text{CaM}$  by a factor of 1000, resulting in the so called “CaM trapping” (Meyer et al., 1992).

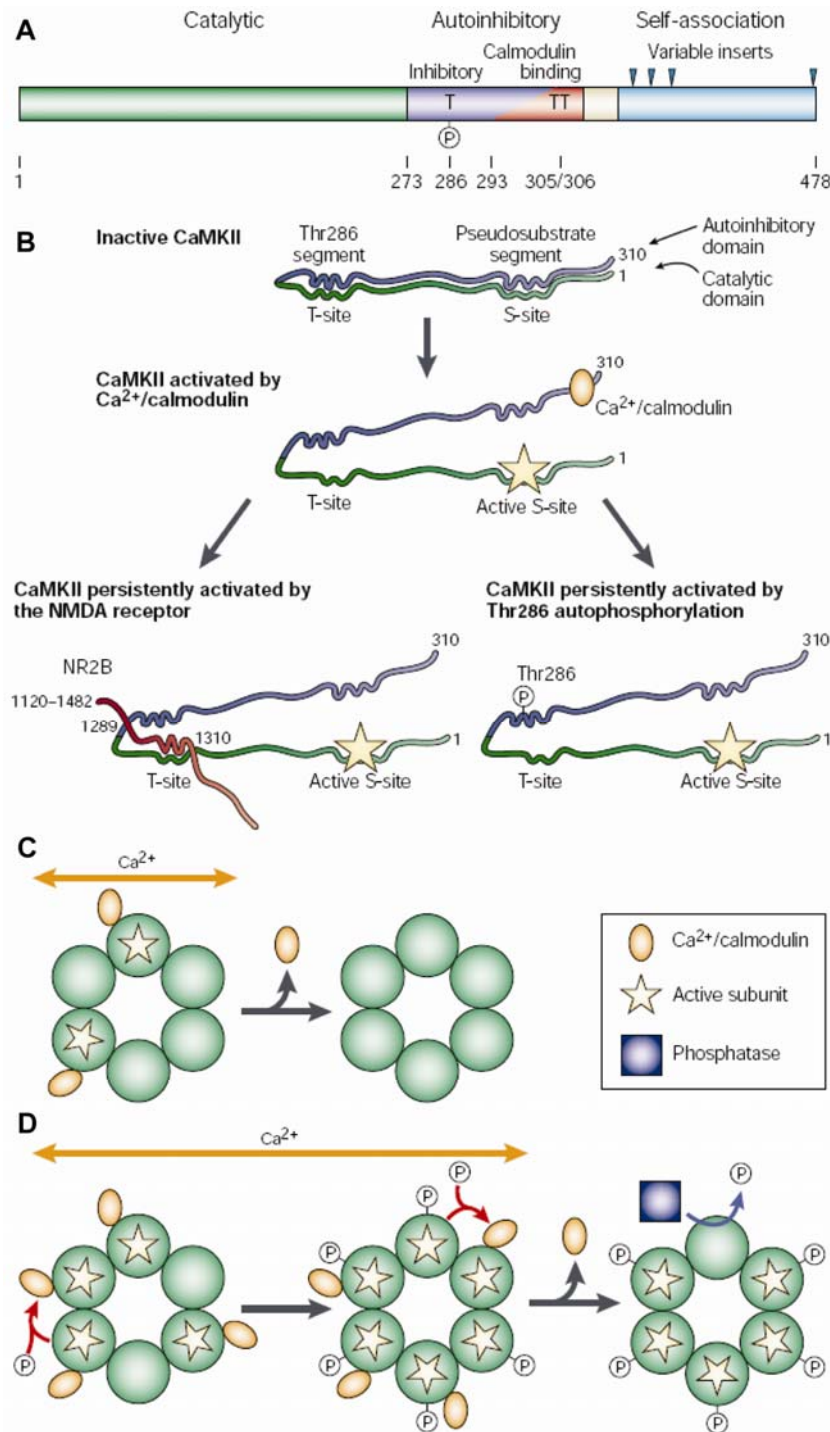


**Figure 1.2: CaMKII Subunit Structure and Activation.** (A) Primary structure of a CaMKII $\alpha$  subunit with the functional domains depicted. (B) In its closed/inactive conformation access of the substrate binding site (S-site) is obstructed through an interaction of the autoinhibitory domain with the S- and T-site of the catalytic domain. The binding of Ca<sup>2+</sup>/CaM activates or opens the kinase by displacing the pseudosubstrate segment and the T286 segment from the S- and T-site respectively. Autophosphorylation at T286 or interaction with the GluN2B (formerly NR2B) subunit of the NMDAR are sufficient to prevent the re-association of the autoinhibitory domain and keep the kinase active even after dissociation of Ca<sup>2+</sup>/CaM. (C) Brief or weak stimuli only keep the kinase active while Ca<sup>2+</sup>/CaM is bound, because of the low probability of simultaneous activation of two neighboring subunits (continued on next page)

(Figure 1.2 continued) which could result in autophosphorylation. **(D)** Short-term persistent activation and the associated  $\text{Ca}^{2+}$ -influx lead to T286 autophosphorylation and persistent activity of CaMKII even after intracellular calcium levels dropped. Autonomous CaMKII activity declines with increasing dephosphorylation. Modified from Lisman et al., 2002.

CaMKII $\beta$  possesses a higher calmodulin affinity than  $\alpha$  (Brocke et al., 1999), but the most important difference between the two isoforms is an insert in the variable region of CaMKII $\beta$  that mediates binding to F-actin. This activity-dependent regulated interaction targets the entire holoenzyme to F-actin (Shen and Meyer, 1999; Shen et al., 1998). Activation of the kinase upon neuronal activity disrupts the interaction and allows translocation to the synapse. A recent study (using CaMKII $\beta$  null mice) showed that the  $\beta$  subunit is essential for hippocampal LTP and learning. CaMKII $\beta$  played a crucial, activity-independent structural role by targeting CaMKII holoenzymes to the F-actin cytoskeleton in spines (Borgesius et al., 2011). In addition to the role in targeting the  $\alpha$  subunit to the spine, CaMKII $\beta$  can function as an F-actin bundling protein and regulate actin assembly and spine structure (O'Leary et al., 2006; Okamoto et al., 2007; Sanabria et al., 2009).

Neuronal activity leads to a translocation of CaMKII from the cytoplasm and its F-actin bound pool to the synapse. This activity-dependent redistribution is synapse specific and persistent (Otmakhov et al., 2004; Zhang et al., 2008). Upon induction of LTP, there is not only an activity-dependent increase in the amount of PSD-bound CaMKII, but the stimulation also induces spine growth and F-actin assembly which results in a further subsequent recruitment of CaMKII to the spine (Ahmed et al., 2006; Okamoto et al., 2004; Otmakhov et al., 2004).

## 1.5 The CaMKII/GluN2B Interaction

The translocation of CaMKII depends on activation of its cytoplasmic pool, including mobilization of the F-actin bound fraction, for diffusion to the synaptic site. There the holoenzyme gets trapped, as its open active conformation allows its interaction with binding partners in the PSD. The interaction that was first described and is most interesting in the context of learning, memory and LTP, is with the NMDAR. Not only does this interaction

allow anchoring of CaMKII in the PSD, it also brings the NMDAR together with CaMKII, both of which are essential for LTP and learning and memory.

By now, multiple binding partners for CaMKII in the PSD have been identified, but the NMDAR emerged as the critical interaction partner. Initially, interactions were reported with the GluN2B, GluN1 and GluN2A subunit (Gardoni et al., 1998; Leonard et al., 1999; Strack and Colbran, 1998). Subsequent work revealed a strong, activity-dependent binding to GluN2B with only weak, if any, contribution of the GluN2A site and so far no definite function for GluN1.

CaMKII interacts with amino acid residues (aa) 1290-1309 of the GluN2B subunit (Strack et al., 2000a) and requires activation by  $Ca^{2+}/CaM$  or T286 autophosphorylation (Bayer et al., 2001). This interacting region contains S1303, a high affinity substrate for CaMKII (Omkumar et al., 1996), and generally shows high homology to the autoinhibitory segment around T286 (Figure 1.3 A) of CaMKII. Binding to this region renders the kinase active, independent of T286 phosphorylation (Strack et al., 2000a). The observation, that the interaction with GluN2B prevents autoinhibition of CaMKII, without blocking access to the S-site, led to the hypothesis, that the interaction is mediated via the T-site. Peptide competition assays confirmed this interaction. The NMDAR can be displaced by a peptide derived from the autoinhibitory region surrounding T286, but not by the classical CaMKII substrate syntide-2 (Strack et al., 2000a). A later study then reported the transition from a reversible interaction of GluN2B with the S-site to a persistent interaction with the T-site (Bayer et al., 2006). Consistent with a role for the T-site in the interaction, an I205K mutation within the T-site blocked the GluN2B interaction as well as the activity-dependent translocation (Bayer et al., 2001; Bayer et al., 2006; Strack et al., 2000a). Site directed mutagenesis showed L1298, R1300 and S1303 were specifically important for CaMKII binding (Fig. 1.3 B). Notably the single point mutants L1298A and R1300Q completely abrogated the interaction *in vitro* (Strack et al., 2000a).



to target CaMKII to spines and that the interaction with the GluN2B subunit in the PSD is required for synaptic translocation.

## 1.6 The CaMKII/GluN2B Interaction in Learning and Memory

NMDAR and CaMKII, as well as their specific interaction, are crucial for LTP. Therefore, this interaction is likely to play an important role in learning and memory, of which LTP is generally regarded to be the physiological correlate.

The different CaMKII mutant mouse models do not disagree with a role of this interaction in learning and memory because the changes in CaMKII expression levels or modifications of the autophosphorylation supposedly all alter the association of CaMKII with the PSD or, more specifically, the association with the NMDAR required for anchoring CaMKII at the PSD. As previously discussed, overexpression of the GluN2B subunit in the *doogie* mouse resulted in enhanced hippocampal LTP and superior performance in various spatial learning paradigms (Tang et al., 1999).

Two different studies tried to address the question what happens if the interaction is disrupted *in vivo*. The first study is based on a mouse with an inducible fusion protein of the GluN2B C-terminus. The disruption of the CaMKII/GluN2B interaction (associated with the expression of the fusion protein) resulted in reduced LTP and spatial learning deficits in the MWM (Zhou et al., 2007). This study is limited, however, in that it does not exclude potential side effects of the C-terminal fusion protein on other protein-protein interactions besides CaMKII. For example, the C-terminus of GluN2B anchors the receptor at the PSD by interacting with PSD-95, the central scaffolding protein in the PSD (Bard et al., 2010). A second and more recent report from our lab investigated a GluN2B KI mouse containing the two point mutations L1298A and R1300Q that specifically interrupt the interaction between GluN2B and CaMKII *in vitro* (Strack et al., 2000a). This study confirmed *in vivo*, that these two point mutations entirely abrogated the activity-dependent increase in the interaction with the NMDAR, reduced LTP by 50% and resulted in a MWM memory deficit, whereas spatial learning was normal (Halt

et al., 2012). This specific observation of a memory deficit is similar to the heterozygous CaMKII $\alpha$  KO mice, which learn normally, but show impaired MWM memory recall if tested 10 or 17 days after the last training session (Frankland et al., 2001).

## 1.7 The N-methyl-D-aspartate Receptor (NMDAR)

NMDARs are ionotropic glutamate receptors, permeable to sodium, potassium and calcium. Besides mediating excitatory synaptic transmission, the calcium influx through the NMDAR is essential for synaptic function and involved in neuronal development, synaptic plasticity and excitotoxicity/cell survival. Dysregulation of NMDARs is implicated in neurodegenerative and psychiatric diseases (Lau and Zukin, 2007).

The calcium influx through the NMDAR is required for the induction of long-term potentiation (LTP) as well as long-term depression (LTD). It has been proposed that high levels of calcium influx trigger the activation of LTP pathways including activation and recruitment of CaMKII, while a modest increase in postsynaptic calcium levels induces activation of LTD pathways (Fetterolf and Foster, 2011). The NMDAR is well suited for the induction of long-term plasticity, due to its magnesium block at resting membrane potentials. The Mg<sup>2+</sup> block of the channel pore is voltage dependent and removed by postsynaptic depolarization. When postsynaptic depolarization coincides with presynaptic glutamate release, resulting in binding to the NMDAR (together with its co-agonists glycine or D-serine), the receptor gets activated and the resulting calcium influx is able to trigger plasticity mechanisms (Sanz-Clemente et al., 2012).

The NMDAR consists of a diverse family of different subunits, GluN1 and GluN2A-D being the most relevant, with the GluN1 subunit giving rise to eight different splice variants, further increasing variation. NMDARs are heterotetrameric assemblies of two essential GluN1 subunits and two GluN2 subunits (Paoletti, 2011; Sanz-Clemente et al., 2012). Deletion of the GluN1 gene is neonatally lethal, while conditional knockout studies demonstrated

that the GluN1 subunits are crucial for the expression of functional receptors, as individual GluN2 subunits were retained in the ER (Fukaya et al., 2003).

The GluN2 subunits confer different physiological and pharmacological properties on the receptor and have differential expression patterns during development and in different tissues. In the forebrain the prevalent subunits are GluN2A and GluN2B. Neonatally GluN2B is the dominant isoform and GluN2A expression gradually increases during the first postnatal weeks till mature synapses contain both GluN2A and GluN2B (Flint et al., 1997; Paoletti, 2011; Sheng et al., 1994). Usually, NMDARs are di-heteromeric consisting of two GluN1 and two GluN2A or GluN2B subunits, but they are also able to form tri-heteromeric GluN1/GluN2A/GluN2B complexes. Indeed, in the adult hippocampus 15-40% of the GluN2A and 2B subunits are found in GluN1/GluN2A/GluN2B triheteromeric receptor assemblies (Al-Hallaq et al., 2007).

The membrane domain configuration of the NMDAR is common to all eukaryotic glutamate receptors, consisting of three transmembrane domains (M1, M3 and M4) and a re-entrant loop (M2). M2 lines the pore of the functional channel and includes a critical asparagine residue, controlling ion pore selectivity and magnesium affinity. The N-terminal domain consisting of the first ~380 amino acids is important for subunit assembly and allosteric modulation. Additionally, a part of it (S1 segment) contributes together with the long extracellular loop between M3 and M4 (S2 segment) the agonist binding site. Glutamate binds to the S1/S2 domains of the GluN2 subunit, while the GluN1 subunit forms the binding site for the required co-agonist glycine or D-serine (Fig. 1.4). The intracellular C-terminal tail varies in size depending on the subunit and is involved in receptor regulation, trafficking and anchoring. In case of the GluN2 subunits it constitutes nearly half of the protein (Cull-Candy and Leszkiewicz, 2004) and creates the first level of protein-protein interactions in the PSD.

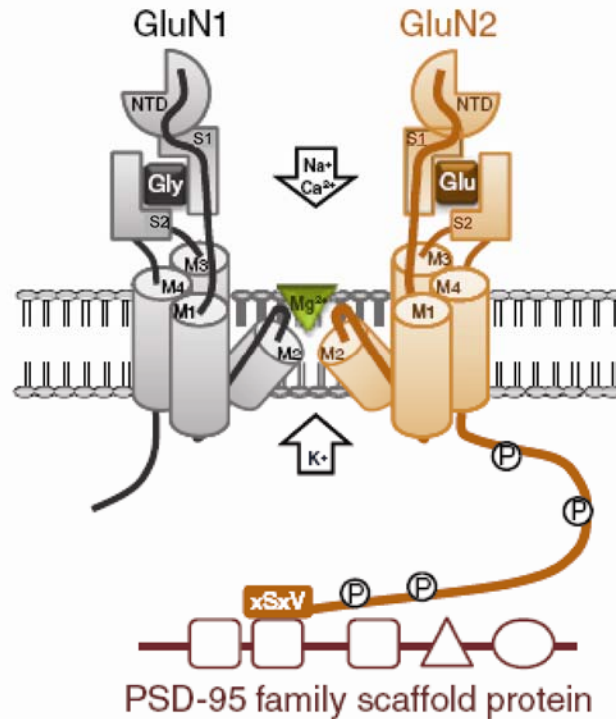


**Figure 1.4: The Molecular Organization of the NMDAR.** The N-terminus of the NMDAR includes the amino-terminal domain (NTD), a potential site of allosteric modulation and the S1 segment part of the agonist binding site (glutamate for GluN2 and glycine/D-serine for GluN1). The other part of the binding site is contributed by S2, the large extracellular loop between the transmembrane segments M3 and M4. The re-entrant loop M2 lines the channel pore and is important for ion selectivity and the affinity for  $Mg^{2+}$ , which occludes ion flux through the pore at resting membrane potentials. The very end of the long C-terminal tail of the GluN2 subunits interacts with the PDZ domain of synaptic scaffolding proteins of the PSD-95 family. Modified from Bard and Groc, 2011.

## 1.8 The Regulation of the NMDAR by Phosphorylation via the cAMP/PKA Pathway

The calcium influx through the NMDAR is critical for synaptic function and mediates most of its physiological and pathogenic effects. Notably modulation of synaptic plasticity including the induction of LTP and LTD is, as previously stated, dependent on the NMDAR activation and the resulting intracellular calcium levels. Fast control mechanisms through posttranslational modifications such as protein phosphorylation could be important to tip dynamics in the direction of either potentiation or depression (Lau et al., 2009). The NMDAR is phosphorylated by PKA (Leonard and Hell, 1997; Tingley et al., 1997), which is an interesting candidate mechanism for

modulating NMDAR activity. In fact the NMDAR is indirectly coupled to PKA (protein kinase A or cAMP-dependent kinase) and phosphatases over A-kinase anchoring proteins (AKAPs), offering competitive regulation of channel activity. More precisely, the AKAP Yotiao, which is directly interacting with the C-terminus of GluN1 links NMDARs to PKA and PP1, while AKAP150, which binds via PSD-95 to the GluN2 subunits, links them to PKA, PKC and PP2B (Colledge et al., 2000; Sanderson and Dell'Acqua, 2011; Wong and Scott, 2004). It has been shown that phosphatases decrease open probability of NMDARs, while phosphatase inhibitors or PKA activation can overcome the constitutive downregulation and enhance NMDAR currents (Wang et al., 1994; Westphal et al., 1999). Direct modulation of G-protein coupled receptors like the  $\beta$ -adrenergic receptor or the  $D_1/D_5$  dopamine receptor, which activate the cAMP/PKA signaling pathway, also enhance NMDAR current and facilitate induction of LTP (Otmakhova and Lisman, 1996; Raman et al., 1996; Thomas et al., 1996). Additionally, calcium influx through the NMDAR in the striatum is bidirectionally regulated through the  $D_2$  dopamine and the  $A_{2A}$  adenosine receptor in a PKA dependent manner. Activation of the  $G_{\alpha i}$  coupled  $D_2$  receptor lowers cAMP resulting in PKA inhibition. The resulting reduction of NMDAR dependent calcium signaling can be counteracted by simultaneous activation of the  $A_{2a}$  adenosine receptor, which is positively coupled to cAMP production over  $G_{\alpha s}$  (Higley and Sabatini, 2010).

It was demonstrated that PKA controls the activity-dependent calcium signaling in dendritic spines and regulates LTP induction at hippocampal synapses by modulating these calcium levels (Skeberdis et al., 2006). The modulation of activity dependent calcium signaling through the NMDAR by the cAMP/PKA pathway depicts an interesting possibility for bi-directional modification of synaptic plasticity by transmitters and hormones (Lau et al., 2009).

## 1.9 Aim of this Work

Glutamate is the major excitatory neurotransmitter in the brain. The N-methyl-D-aspartate-type glutamate receptor (NMDAR) and the

calcium/calmodulin-dependent protein kinase II (CaMKII) are at the heart of long lasting potentiation of excitatory synaptic transmission. CaMKII and the NMDAR are not only essential for hippocampal LTP, but also for spatial learning and memory formation. The aim of this thesis was to elucidate the implications of the activity-dependent interaction between CaMKII and the NMDAR, as well as to characterize the PKA dependent regulation of the NMDAR.

The importance of the CaMKII/NMDAR interaction for spatial learning and memory formation was investigated using a GluN2B KI mutant mouse model. These mice carry two point mutations, specifically disrupting the critical interaction between CaMKII and the GluN2B subunit of the NMDAR. GluN2B KI mice and WT litter controls were studied in a series of spatial and contextual learning paradigms.

On a molecular level the activity-dependent translocation of endogenous CaMKII to synaptic sites in hippocampal cultures was examined. It was particularly studied how the translocation is modulated through interactions with the NMDAR as well as the stimulation length and the local calmodulin availability.

PKA regulated calcium influx through the NMDAR is crucial for synaptic plasticity. The modulation of the novel PKA phosphorylation site S1166 on the GluN2B subunit was biochemically investigated in acute forebrain slices, as well as in response to *in vivo* elicited stress and pharmacological dissection of this stress response.

## **2 Material and Methods**

Throughout this thesis numbers are depicted with a decimal point according to the U.S. convention.

### **2.1 Animal Procedures**

#### **2.1.1 Animal Husbandry**

All animal procedures were approved by the UC Davis Institutional Animal Care and Use Committee (IACUC) and followed NIH guidelines.

The animals were housed in a pathogen-free facility on a 12 h light/dark cycle. The mice were housed in individually ventilated cages on corn cob bedding with Envivo-dri nesting material and with free access to food (PicoLab diet) and water.

For breeding purposes heterozygous mice of at least 5 weeks of age were put into mating cages. The offspring was weaned at 21 days of age, tagged by ear punch and 0.1-0.5 cm of the tail clipped for genotyping purposes.

For all behavioral experiments the mice were transferred to the UC Davis Mouse Behavioral Assessment Lab (MBAL). The experiments were conducted with litter matched wild-type (WT) and GluN2B KI (KI) mice with age differences of no more than 4 weeks within each experiment and a general age of 3-6 months. Upon arrival at MBAL the mice were housed individually and acclimated for at least one week. After the acclimation period, but before the training and testing the mice were extensively handled (1-2 min on 7-10 different days).

#### **2.1.2 GluN2B KI Mice**

To generate the L1298A and R1300Q mutations in the GluN2B KI mice three point mutations were introduced in exon 13 of the GluN2B gene, simultaneously creating a BssHII site for diagnostic purposes. The targeting vector used to introduce these point mutations within the GluN2B gene via homologous recombination contained a Neomycin resistance gene flanked by two loxP sites for positive selection and two copies of the HSV thymidine

kinase gene for negative selection. The Neomycin resistance gene was flanked by a 2.3 kb 5' short arm containing exon 13 with the three point mutations and the stop codon of the GluN2B gene and a 3.1 kb 3' long arm containing the remaining 3' untranslated region as well as part of the intron. Two copies of the HSV thymidine kinase gene were attached 5' to the short arm. The targeting construct was linearized by enzymatic digestion using NotI and electroporated into the E14 ES cell line. The cells were selected for homologous recombination in the presence of the aminoglycoside antibiotic G418 (positive selection) and Ganciclovir (negative selection against random integration). Positive clones were injected into C57BL/6 blastocytes and the founder chimeras were backcrossed for 9 generations with C57BL/6 mice, all obtained from Taconic (Hudson, NY). The Neomycin resistance gene was removed by backcrossing with E1a-cre mice.

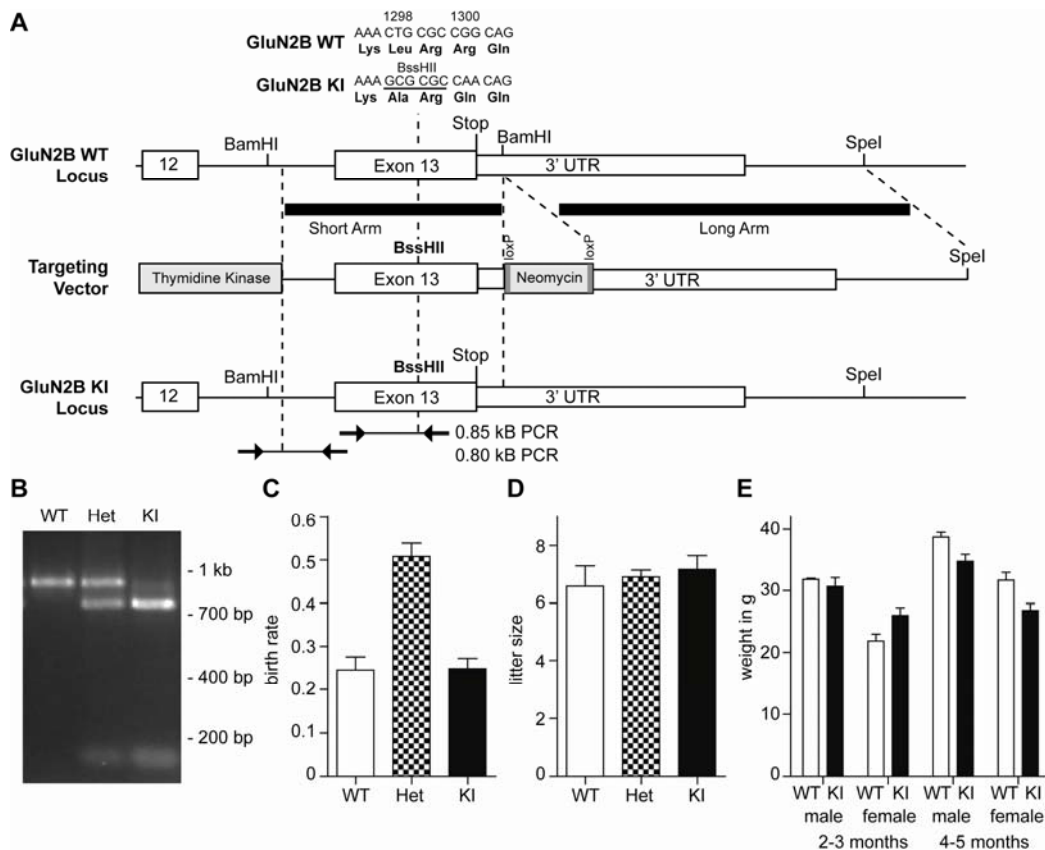


**Figure 2.1 Creation and genotyping of GluN2B KI mice.** (A) Targeting vector and homologous recombination are displayed. A Neomycin resistance gene flanked by two loxP sites was inserted downstream of the last exon (exon 13) of the GluN2B gene. Two copies of the HSV thymidine kinase gene were inserted into the intron preceding exon 13. Three point mutations created L1298A and R1300Q mutant GluN2B and a BssHII site for diagnostic purposes. (continued on next page)

(Figure 2.1 continued) E14 ES cells were electroporated with linearized vector and homologously recombined cells were treated with G418 (positive selection) and Ganciclovir (negative selection). The positive homologous recombination was confirmed by diagnostic PCR before injection for germline transmission. **(B)** Routine PCR genotyping identified homozygous WT mice by a single 853 bp undigested fragment, homozygous KI mice by 2 bands with 709 and 144 bp due to the complete digestion of the amplified fragment by BssHII, and heterozygous (het) mice by the presence of all 3 bands. **(C)** Normal birth rate of wild type, heterozygous and homozygous GluN2B KI mice from heterozygous breeders following Mendelian genetics as monitored between June 2010 and April 2011 after 10 back crossings with C57BL/6J from Taconic. **(D)** Normal offspring size from homozygous C57black/6 WT, heterozygous and homozygous GluN2B KI breeders as monitored between June 2010 and April 2011. **(E)** Normal weight of homozygous GluN2B KI mice vs. litter mate WT mice for different sexes and ages as monitored between June 2010 and April 2011. Modified from Halt et al., 2012.

## 2.1.3 Genotyping

### 2.1.3.1 Tail Tip Digest

The clipped tails were incubated overnight in 0.5 mL lysis buffer, 20 µg/mL RNase A and 500 µg/mL of Proteinase K under constant shaking at 37 °C. After incubation the samples were pelleted at room temperature (RT) for 3 min at 20.000 xg and ~ 300 µL of the supernatant containing the genomic DNA transferred over into a new, clean 1.5 mL microcentrifuge tube. To inactivate any remaining Proteinase K activity the samples were heated for 15 min to 95 °C and stored afterwards at -20 °C until needed for the genotyping PCR.

#### Reagents

Lysis buffer

	Stock	Volume (50 mL)	Concentration
Tris-Cl pH 8.5	1 M	5 mL	100 mM
NaCl	5 M	4 mL	400 mM
SDS	10%	1 mL	0.2%

Add 40 mL ddH<sub>2</sub>O (Gibco).

Tail digestion mix

	Volume
Lysis buffer	0.5 mL
RNase A (Fermentas, 10 mg/mL stock)	1 µL
Proteinase K (New England Biolabs, 20 mg/mL stock)	12.5 µL

### 2.1.3.2 Polymerase Chain Reaction (PCR)

To distinguish between the different genotypes the genomic DNA obtained from the tail digestion was used as a PCR template and the fragment in the GluN2B gene carrying the three point mutations was amplified via PCR.

PCR reaction mix:

	Stock	Volume (50 $\mu$ L)
Tail lysate		3 $\mu$ L
ThermoPol buffer	10x	5 $\mu$ L
dNTPs	10 mM	1 $\mu$ L
Forward primer	5 $\mu$ M	2 $\mu$ L
Reverse primer	5 $\mu$ M	2 $\mu$ L
Taq DNA polymerase		0.5 $\mu$ L

Add 36.5  $\mu$ L ddH<sub>2</sub>O (Gibco).

PCR conditions:

Initial Denaturation	95 °C	2 min	
Denaturation	95 °C	30 sec	36x
Annealing	60 °C	1 min	
Elongation	72 °C	1 min	
Final Elongation	72 °C	5 min	

#### Reagents

Taq DNA polymerase (5 U/ $\mu$ L, New England BioLabs)

10x ThermoPol buffer (New England BioLabs)

Deoxynucleotide solution mix (10 mM, New England BioLabs)

Primer

Name	Gene	Sequence
F-seq 2BKI	GluN2B	5'CATCTCCACGCATACTGTCAC3'
Rev-seq 2BKI	GluN2B	5'CAGCTGGCATCTCAAACATATGG3'

### 2.1.3.3 PCR Digest

The PCR amplified DNA fragments were overnight digested with the restriction enzyme BssHII at 50°C.

PCR digestion mix (per sample):

	Stock	Volume (15 $\mu$ L)
PCR product		6 $\mu$ L
NEBuffer 3 (New England BioLabs)	10x	1.5 $\mu$ L
BSA	100x	0.15 $\mu$ L
BssHII (New England BioLabs)	4U/ $\mu$ L	1 $\mu$ L

Add 6.5  $\mu$ L ddH<sub>2</sub>O (Gibco).

### 2.1.3.4 Agarose Gel Electrophoresis

The overnight digested DNA fragments were diluted with 6x DNA loading dye and analyzed via agarose gel electrophoresis. The samples were run together with a marker on a 2% (w/v in 1x TAE buffer) agarose gel for 75 min at 80 V. The whole gel was soaked and the DNA fragments stained in a Sybr Gold (1:10.000 dilution in 1x TAE buffer) bath for 15-30 min at RT and made visible with a blue light transilluminator and analyzed using the Kodak 1D imaging software. The PCR amplified WT DNA fragment is not digested by BssHII and should run at approximately 853 base pairs (bp). The DNA fragment from the KI mice is digested by BssHII and two bands should be visible at approximately 709 and 144 bp. The DNA from heterozygous mice should display all bands at approximately 853, 709 and 144 bp (Fig. 2.1).

#### Reagents

SYBR Gold nucleic acid gel stain (10.000x concentrate, Invitrogen)

6x DNA loading dye

	50 mL	Concentration (w/v)
Bromphenol Blue	0.125 g	0.25%
Xylene Cyanol	0.125 g	0.25%
Sucrose	20 g	40%

Add ddH<sub>2</sub>O to 50 mL.

50x TAE (Tris-acetate-EDTA) buffer

	MW (g/mol)	1 L	Concentration
Tris-Cl	121.14	242 g	2 M
Na <sub>2</sub> EDTA · 2H <sub>2</sub> O	372.24	18.6 g	50 mM
Glacial acetic acid		57.1 mL	

Add ddH<sub>2</sub>O to 1 L.

## 2.1.4 Behavior

### 2.1.4.1 Morris Water Maze (MWM)

The water maze apparatus itself is a circular, enamel coated steel tank, 94 cm in diameter filled with water at 22-24 °C. For the visible trial a black labeled square platform (6 x 6 cm) emerging 2 cm out of the opaque (through addition of nontoxic paint) water surface is used, while the clear acrylic glass Plexiglas square platform (6 x 6 cm) for the training trials is submerged 2 cm below the opaque water surface. On the first day the mice were trained in one visible trial followed by 12 consecutive training trials, while the platform was kept in a fixed position. The mice were always placed facing the wall of the pool and started randomly from three different starting positions that are equally distributed around the perimeter and are not located within the target quadrant. The mice were allowed to swim freely for 90 s to find the platform, if they failed to locate the platform within time they were gently guided to it. After the mice climbed on the platform they were allowed to remain 30 s on the platform before they were removed from the pool and placed in their home cage for an inter-trial time of 6-10 min. The mice were returned to the pool for a 90 s probe test without the platform 1 day and 7 days after the training day. The training session and probe trials were monitored and analyzed using the SMART (Version 2.5.19) real-time video-tracking system.

### 2.1.4.2 Barnes Maze

The Barnes maze was executed according to (Berta et al., 2007). In short, the maze consists of a circular platform (92 cm diameter) with 20 equally spaced holes (5 cm diameter; 7.5 cm between holes) and was

elevated 105 cm above the floor. All holes are 2 cm away from the perimeter of the platform and a dark escape box (10.16 cm x 12.7 cm x 12.7 cm) is located beneath one of the holes.

The mouse was placed in a cylindrical black start chamber (10.16 cm x 12.7 cm x 12.7 cm) in the middle of the maze. After 10 s the chamber was lifted and the mouse exposed to bright light. For the habituation trial on day 1 the animal was gently guided to the escape box and once it entered, the entry hole was covered and the mouse kept for 2 min in the dark escape box. Between each mouse, before the next trial, the platform was cleaned with a 10% Nolvasan solution to avoid residual olfactory cues. During the acquisition phase, after the start chamber was lifted, the mouse was allowed to explore the maze for 3 min. The trial ended when the mouse entered the escape box or after 3 min had elapsed. Immediately after the mouse entered the escape box, the entry hole was covered and the animal stayed for 1 min in the dark escape box. If the mouse did not reach the target hole/escape box within 3 min, it was gently guided to it. After 1 min in the escape box the mouse was placed back in its home cage until the next trial. Each mouse received 4 training trials per day with an inter-trial interval of 10-15 min on 4 consecutive days.

On day 5, 24 h after the last training day and for long-term retention on day 12 the probe trial was conducted. During the probe test the escape box was removed and the mouse was allowed to explore the maze for a fixed time of 90 s. The number of pokes (errors) in each hole and the latency and path length to reach the virtual target hole was measured using the SMART (Version 2.5.19) real-time video-tracking system.

#### **2.1.4.3 Elevated Plus Maze (EPM)**

The elevated plus maze is a four arm maze with each arm measuring 30 x 5 cm and the central platform measuring 5 x 5 cm. One set of arms, opposing one another, are enclosed completely by side walls (15 cm high) while the other set is open with a ledge of 0.5 cm on either side of the arms. The maze was elevated two feet from the floor and the mice were placed on the central platform, facing a closed arm, and allowed to freely explore the

maze for 5 min. The SMART (Version 2.5.19) real-time tracking software was used to record locomotor activity including the time spent on both the closed and the open arms during the test.

#### **2.1.4.4 Contextual Fear Conditioning**

Contextual fear conditioning was conducted using the Video Tracking of Fear Conditioning System and the Video Freeze Software (MED Associates Inc.). The experimentally naïve mice were placed in the conditioning chamber and received the first foot shock at the end of a 3 min habituation period. The mice remained for 1 additional min in the chamber after the last foot shock was delivered. For the 5 shock conditioning protocol, the mice received an electric foot shock (0.75 mA, 1 s) at the end of the 3<sup>rd</sup>, 4<sup>th</sup>, 5<sup>th</sup>, 6<sup>th</sup>, and 7<sup>th</sup> min. During the milder 3 shock (0.5 mA, 1 s) paradigm the shock was received at the end of the 3<sup>rd</sup>, 4<sup>th</sup> and 5<sup>th</sup> min, while for the 4 day training protocol only one shock (0.75 mA, 1 s) per day was delivered. For recall the mice were placed back for 5 min in the same chamber after the indicated periods of time. If the mice were exposed to a different context, the chamber geometry was changed (from square to curved wall), the lights were dimmed, the rod-flooring was covered with white linoleum, and the scent was changed from 0.01% bleach to bubble gum. Using the Video Freeze Program freezing time (in %) was determined for each minute and was defined as an absence of movement except motion that was necessary for respiration.

## **2.2 Cell Culture and Molecular Biological Methods**

### **2.2.1 DNA Purification**

For purification of small amounts of DNA for analytical purposes 5 mL bacterial cultures (*E. coli*) were grown overnight with constant shaking at 37 °C. The next day, the DNA was isolated from the pelleted cells using the QIAprep Spin Miniprep Kit (QIAGEN), according to the QIAprep Miniprep Handbook.

Preparative amounts of DNA, for transfection of eukaryotic cells, were purified from 500 mL bacterial cultures (*E. coli*) with the NucleoBond Xtra Maxi EF

(Macherey-Nagel) Kit, according to the Endotoxin-free plasmid DNA purification user manual.

### 2.2.2 Preparation and Coating of Coverslips with Poly-L-Lysine

400-500 coverslips were incubated overnight under constant shaking with concentrated nitric acid at RT. The next day, the coverslips were washed with ddH<sub>2</sub>O until the pH was neutral, followed by an additional 3 washes for 5 min at RT. Afterwards, the coverslips were washed 3x for 5 min at RT with 95% EtOH and kept in the last EtOH wash until flaming. Finally, the flamed coverslips were autoclaved and stored for fresh coating with Poly-L-Lysine before each experiment. The coverslips were covered with 1 mg/mL Poly-L-Lysine dissolved in borate buffer and coated overnight in the tissue culture incubator. The next day, the coating solution was removed and the coverslips were washed overnight with sterile, endotoxin free water. After the water was removed the coverslips were covered and incubated with Neurobasal (NB) complete medium until the next day when the medium was removed and new hippocampal cultures were plated on the coverslips.

#### Reagents

Poly-L-Lysine Hydrobromide (Peptide Institute Inc.)

Borate buffer

	MW (g/mol)	500 mL	Concentration
H <sub>2</sub> O (TC tested, Sigma-Aldrich)		500mL	
Boric acid (H <sub>3</sub> BO <sub>3</sub> )	61.83	2.38 g	20 mM
Borax (Na <sub>2</sub> B <sub>4</sub> O <sub>7</sub> · 10H <sub>2</sub> O)	381.4	1.27 g	1.7 mM

### 2.2.3 Hippocampal Cultures

Hippocampal neurons were isolated from embryonic day 18 (E18) rat embryos. The pregnant mother rat was anesthetized with Isoflurane and euthanized by cervical dislocation. Under a Bunsen burner the uterus (filled with the embryos) was removed by caesarian section and transferred into a sterile 100 mm culture dish, which was then transferred in the biological safety cabinet (BSC) for the following procedures. The embryos were decapitated and the brain isolated. For the isolation the head was fixed by inserting

Dumont forceps through the eyes and angled spring scissors were used to cut the skull open along the sagittal suture (from caudal to rostral), and the brain was carefully removed with a spatula. The isolation of the brain as well as the storage of the embryo heads, brains and later the dissection of the hippocampi and their storage were all performed in Hanks' Balanced Salt Solution (HBSS, stored at RT). Using a dissecting microscope the meninges were removed from the cerebral hemispheres and the hippocampi isolated. After one hemisphere of the cerebral cortex was gently peeled back, the hippocampus was visible and freed from the surrounding tissue. The dissected hippocampi were transferred into a 0.3 mg/mL Trypsin (in HBSS) solution and incubated for 12-15 min at 37 °C. Then the hippocampi were transferred with a moistened Pasteur pipette in a 15 mL conical tube containing 10 mL of Neurobasal complete medium with 5% horse serum to inactivate any remaining Trypsin. After two washes with HBSS the hippocampi were transferred into 5 mL of HBSS and dissociated by repeatedly pipetting them up and down with first a regular and then a flame constricted Pasteur pipette. The dissociated cells were allowed to sit for 1 min to let any remaining debris settle down. Subsequently, the supernatant was transferred to a new 15 mL conical tube and spun down for 5 min at 1.100 rpm at RT. The pelleted cells were resuspended in 3 mL of Neurobasal complete medium with 5% horse serum and the cell density determined with a hemocytometer. For immunostaining and imaging purposes the cells were plated on the coated coverslips with a density of 30.000 cells/mL, 60.000 cells per 35 mm dish. After 4 h the plating medium containing 5% horse serum was removed and replaced by Neurobasal complete medium.

### Reagents

Neurobasal complete medium

	Stock	500 mL	Concentration
Neurobasal (-glutamine, Gibco)		500 mL	
NS21 (Chen et al., 2008)		10 mL	
L-glutamine (Gibco)	200 mM	1.25 mL	0.5 mM
HEPES (Gibco)	1 M	5 mL	10 mM

Hanks' Balanced Salt Solution (HBSS -CaCl<sub>2</sub>, -MgCl<sub>2</sub>, -MgSO<sub>4</sub>, Gibco)

Trypsin (cell culture tested, Sigma-Aldrich)

Horse serum (Gibco)

#### **2.2.4 Transfection of Hippocampal Cultures with Lipofectamine2000**

The transfection of the neurons was carried out at 4-7 days in vitro (DIV) (Dalby et al., 2004; Ohki et al., 2001). The neurons were generally cultured on coverslips in 35 mm dishes with 2 mL of NB complete medium. Per 35 mm dish/2 mL of medium 3 µg of purified DNA and 4 µg of Lipofectamine 2000 were used. In short: 3 µg of purified, sterile DNA were resuspended in 400 µL Opti-MEM (modification of Eagle's Minimum Essential Medium, Gibco), mixed and incubated for 5 min at RT. 4 µg of Lipofectamine 2000 were resuspended as well in 400 µL Opti-MEM, mixed gently and let sit for 5 min at RT. After 5 min the two solutions were combined, gently mixed and incubated for 30 min at RT. The NB complete medium of the hippocampal cultures was adjusted to 1.2 mL and the 800 µL Lipofectamine-DNA mix in Opti-MEM was added drop wise on the cells and the dish gently rocked. After 4-5 h of incubation the transfection medium was removed and replaced with normal culturing medium (NB complete).

##### **Reagents**

Opti-MEM (reduced serum medium, Gibco)

Lipofectamine 2000 Transfection Reagent (Invitrogen)

#### **2.2.5 Fixation of Hippocampal Cultures**

Hippocampal cultures were grown at a density of 30.000 cells/mL, 60.000 cells per 35 mm dish, and kept in culture till the desired developmental stage. Unless otherwise stated, cultures of 18-21 DIV with fully mature synapses at dendritic spines were used. At the desired age and/or after the stated drug treatment the hippocampal cultures were fixed.

### 2.2.5.1 Methanol Fixation

The culture medium was removed and the cells were rinsed once with Dulbecco's Phosphate Buffered Saline (DPBS, Gibco) and subsequently fixed with -20 °C water-free methanol for 10 min at -20 °C. After the 10 min the methanol was removed and the cells washed 3 times with DPBS. The coverslips were directly used for an immunostaining or stored in the third wash with DPBS and 0.05% sodium azide at 4 °C.

#### Reagents

Methanol (Optima LC/MS, Fisher)

Dulbecco's Phosphate Buffered Saline (DPBS -CaCl<sub>2</sub>, 10x, Gibco)

Sodium azide (Sigma-Aldrich)

	25 mL	Concentration (w/v)
Sodium azide	5 g	20%

Add ddH<sub>2</sub>O to 25 mL.

### 2.2.5.2 Paraformaldehyde (PFA) Fixation

The culture medium was removed and the cells were rinsed once with DPBS and subsequently fixed with 4% PFA/4% sucrose in DPBS for 10 min at RT. After the 10 min incubation, the fixation solution was removed and the cells were washed 3 times with DPBS. The coverslips were either directly used for immunostaining or were stored in the third wash with DPBS and 0.05% sodium azide at 4 °C.

#### Reagents

8% Paraformaldehyde (Fisher)

	800 mL	Concentration (w/v)
Paraformaldehyde	64 g	8%

Add ddH<sub>2</sub>O to 800 mL.

The solution was heated to 60 °C and the pH adjusted to 7.2-7.6 with 5 M NaOH. Afterwards 10 mL aliquots were frozen and stored for future use at -20 °C.

## 8% Sucrose in 2x DPBS

	100 mL	Concentration (w/v)
Sucrose	8 g	8%
10x DPBS	20 mL	2x

Add ddH<sub>2</sub>O to 100 mL.

## Fixation solution (4% PFA/4% sucrose in 1x DPBS)

	20 mL
8% PFA	10 mL
8% Sucrose in 2x DPBS	10 mL

**2.2.6 Immunostaining of Hippocampal Cultures**

Unless stated otherwise, the hippocampal cultures were fixed with PFA. The PFA fixed neurons (after 3 washes with DPBS, 5 min at RT) were permeabilized with 0.25% Triton X-100 in DPBS for 10 min at RT. After 2 washes with DPBS for 5 min at RT blocking solution was applied and the cells were blocked for 2 h at RT to prevent non-specific binding and reduce background staining. The primary antibodies were diluted in blocking solution, applied to the cells and incubated overnight at 4 °C. Following the overnight incubation unbound primary antibody was removed by washing 3x for 5 min and 1x for 15 min with DPBS at RT. Before application of the fluorescence labelled secondary antibodies the neurons were blocked again for 30 min at RT. The fluorescence labelled antibodies were also diluted in blocking solution and were applied to the cells for 1 h at RT. Before mounting the cells were washed 3x for 5 min and 1x for 15 min with DPBS and 2x for 5 min with water at RT. The coverslips were mounted on glass slides using Prolong Antifade Gold Reagent (Molecular Probes) dried overnight at RT and stored in the dark until imaging. All procedures involving the secondary fluorescence labelled antibodies were carried out in the dark. If neurons were transfected with fluorescent proteins or fluorescently labelled proteins, the whole fixation and staining process was completed in the dark.

**Reagents**

20% Triton X-100 (Alfa Aesar)

	50 mL	Concentration (v/v)
Triton X-100	10 mL	20%

Add ddH<sub>2</sub>O to 50 mL.

Permeabilization Solution (0.25% Triton X-100 in DPBS)

	100 mL	Concentration (v/v)
20% Triton X-100	1.25 mL	0.25%

Add DPBS to 100 mL.

50% Glycerol (Fisher)

	50 mL	Concentration (v/v)
Glycerol	25 mL	50%

Add ddH<sub>2</sub>O to 50 mL.1 M NH<sub>4</sub>Cl (Fisher)

	MW (g/mol)	50 mL	Concentration
NH <sub>4</sub> Cl	53.49	2.67 g	1 M

Add ddH<sub>2</sub>O to 50 mL.

Blocking Solution

	25 mL	Concentration
50% Glycerol	1 mL	2%
1 M NH <sub>4</sub> Cl	1.25 mL	50 mM
Fetal Bovine Serum (FBS)	1.25 mL	5%
Goat Serum	0.5 mL	2%

Add DPBS to 25 mL.

**2.2.7 Surface Staining of Hippocampal Cultures**

In the case of surface staining the permeabilization step with 0.25% Triton X-100 in DPBS was skipped and the immunostaining was carried out as previously described. For co-staining against intracellular epitopes, the

cells were washed after application of the primary surface antibody and fixed again for 2-3 min at RT. After fixation of the extracellular bound primary antibody, the fixation solution was washed off and the cells were permeabilized and the staining procedure continued as previously described.

### **2.2.8 LDH Cytotoxicity Assay**

The LDH cytotoxicity assay was performed with the detection kit from Takara according to the manufacturer's specifications. The method is based on the measurement of lactate dehydrogenase (LDH) enzyme activity, which is released from the cytoplasm of damaged cells. The tissue culture supernatant was collected and the LDH activity determined in a colorimetric assay through the catalyzed reduction of tetrazolium salt to formazan.

## **2.3 Protein Biochemistry**

### **2.3.1 Preparation of Acute Slices**

Mice were sacrificed by decapitation and the brain rapidly dissected. The cerebellum was removed and the forebrain containing the hippocampal formation was mounted in the slicing chamber using instant all purpose glue (cyanoacrylate). During the slicing procedure the forebrain was bathed in ice cold low  $\text{Ca}^{2+}$ /high  $\text{Mg}^{2+}$  artificial cerebrospinal fluid (ACSF) saturated with 95%  $\text{O}_2$  and 5%  $\text{CO}_2$ . 350  $\mu\text{m}$  thick transverse forebrain slices were cut using a Leica VT1000S vibrating microtome. The slices containing the hippocampal formation were immediately transferred in a chamber with low  $\text{Ca}^{2+}$ /high  $\text{Mg}^{2+}$  ACSF gassed with 95%  $\text{O}_2$ /5%  $\text{CO}_2$  and recovered for 45-60 min at 30 °C and an additional 45-60 min at RT. For stimulation and drug treatments the slices were transferred to oxygenated high  $\text{Ca}^{2+}$ /low  $\text{Mg}^{2+}$  ACSF at 30 °C and equilibrated for 30 min before the stimulation. After the stimulation the slices were frozen immediately in liquid nitrogen and stored at -80 °C until further processing.

**Reagents**1.1 M CaCl<sub>2</sub> (Sigma-Aldrich)

	MW (g/mol)	50 mL	Concentration
CaCl <sub>2</sub> · 2H <sub>2</sub> O	147.01	8.09 g	1.1 M

Add ddH<sub>2</sub>O to 50 mL.

1 M MgSO<sub>4</sub> (Sigma-Aldrich)

	MW (g/mol)	50 mL	Concentration
MgSO <sub>4</sub> · 7H <sub>2</sub> O	246.47	12.32 g	1 M

Add ddH<sub>2</sub>O to 50 mL.

10x ACSF stock without Ca<sup>2+</sup> and Mg<sup>2+</sup>

	MW (g/mol)	1 L	Concentration
NaCl (Fisher)	58.44	74.22 g	1.27 M
NaHCO <sub>3</sub> (Fisher)	84.01	21.84 g	260 mM
KH <sub>2</sub> PO <sub>4</sub> (Fisher)	136.09	1.63 g	12 mM
KCl (Sigma-Aldrich)	74.55	1.42 g	19 mM

Add ddH<sub>2</sub>O to 1 L.

Low Ca<sup>2+</sup>/high Mg<sup>2+</sup> ACSF

	MW (g/mol)	Stock	1 L	Concentration
NaCl		10x	100 mL	127 mM
NaHCO <sub>3</sub>		10x	100 mL	26 mM
KH <sub>2</sub> PO <sub>4</sub>		10x	100 mL	1.2 mM
KCl		10x	100 mL	1.9 mM
D-glucose	180.16		1.8 g	10 mM
CaCl <sub>2</sub>		1.1 M	1 mL	1.1 mM
MgSO <sub>4</sub>		1 M	2 mL	2 mM

Add ddH<sub>2</sub>O to 1 L and check pH. If not at pH7.4 adjust with HCl/NaOH.

High Ca<sup>2+</sup>/low Mg<sup>2+</sup> ACSF

		MW (g/mol)	Stock	1 L	Concentration
NaCl	10x ACSF		10x	100 mL	127 mM
NaHCO <sub>3</sub>			10x	100 mL	26 mM
KH <sub>2</sub> PO <sub>4</sub>			10x	100 mL	1.2 mM
KCl			10x	100 mL	1.9 mM
D-glucose		180.16		1.8 g	10 mM
CaCl <sub>2</sub>			1.1 M	2 mL	2.2 mM
MgSO <sub>4</sub>			1 M	1 mL	1 mM

Add ddH<sub>2</sub>O to 1 L and check pH. If not at pH7.4 adjust with HCl/NaOH.

### 2.3.2 Protein Extraction from Whole Tissue

The extraction of protein from whole tissue was done immediately upon dissection or from frozen tissue (shock frozen in liquid nitrogen and stored at -80 °C). The tissue was directly dissolved in 1% deoxycholate buffer or in case of whole forebrain extracts, crude membrane fractions were prepared and the sedimented membranes solubilized in 1% deoxycholate buffer.

One mouse forebrain was homogenized (using 10-15 strokes with a motor-driven glass-Teflon homogenizer) in 2.5-5 mL of sucrose buffer and centrifuged at low speed (2 min at 5.000 xg) to remove remaining cell debris and the nuclear fraction. The crude membrane fraction was pelleted by high speed centrifugation (30 min at 110.000 xg) and solubilized in 2.5 mL 1% deoxycholate buffer.

Smaller tissue samples like forebrain slices or isolated hippocampi were directly homogenized in 0.2-1 mL 1% deoxycholate buffer with an insulin syringe.

The deoxycholate lysates were cleared by ultra-centrifugation (30 min at 110.000 xg) and directly used for further analysis or stored at -80 °C.

**Reagents**

## Sucrose buffer

	Stock	10 mL	Concentration
Sucrose		1.03 g	300 mM
Tris-Cl pH 7.4	1 M	100 $\mu$ L	10 mM
EGTA	500 mM	200 $\mu$ L	10 mM
EDTA	500 mM	200 $\mu$ L	10 mM
NaPP <sub>i</sub> pH 7.4	250 mM	1 mL	25 mM
NaF	800 mM	312.5 $\mu$ L	25 mM
Pepstatin A	1.46 mM	10 $\mu$ L	1.46 $\mu$ M
Leupeptin/Aprotinin	21 mM/3.1 mM	1 $\mu$ L	2.1/0.31 $\mu$ M
PNPPi	1 M	10 $\mu$ L	1 mM
Microcystin	400 $\mu$ M	50 $\mu$ L	2 $\mu$ M
PMSF	195 mM	10 $\mu$ L	195 $\mu$ M

Add ddH<sub>2</sub>O to 10 mL.

## 1% Deoxycholate buffer

	Stock	10 mL	Concentration
Tris-Cl pH 8.5	1 M	500 $\mu$ L	50 mM
EGTA	500 mM	200 $\mu$ L	10 mM
EDTA	500 mM	200 $\mu$ L	10 mM
NaPP <sub>i</sub> pH 7.4	250 mM	1 mL	25 mM
NaF	800 mM	312.5 $\mu$ L	25 mM
Deoxycholate	10%	1 mL	1%
Pepstatin A	1.46 mM	10 $\mu$ L	1.46 $\mu$ M
Leupeptin/Aprotinin	21 mM/3.1 mM	1 $\mu$ L	2.1/0.31 $\mu$ M
PNPPi	1 M	10 $\mu$ L	1 mM
Microcystin	400 $\mu$ M	50 $\mu$ L	2 $\mu$ M
PMSF	195 mM	10 $\mu$ L	195 $\mu$ M

Add ddH<sub>2</sub>O to 10 mL.

Ethylene glycol-bis(2-aminoethylether)-N,N,N',N'-tetraacetic acid (EGTA, RPI Corp)

	MW (g/mol)	250 mL	Concentration
EGTA	380.35	47.54 g	500 mM

Add ddH<sub>2</sub>O to 250 mL and adjust pH to 8.

Ethylenediaminetetraacetic acid disodium salt dihydrate (EDTA, Sigma-Aldrich)

	MW (g/mol)	250 mL	Concentration
EDTA	372.24	46.53 g	500 mM

Add ddH<sub>2</sub>O to 250 mL and adjust pH to 8.

250 mM NaPP<sub>i</sub> (Sigma-Aldrich)

	MW (g/mol)	50 mL	Concentration
NaPP <sub>i</sub> · 10 H <sub>2</sub> O	446.1	5.58 g	250 mM

Add ddH<sub>2</sub>O to 50 mL and adjust pH to 7.4.

800 mM NaF (Sigma-Aldrich)

	MW (g/mol)	50 mL	Concentration
NaF	41.99	1.68 g	800 mM

Add ddH<sub>2</sub>O to 50 mL.

Pepstatin A (Sigma-Aldrich)

	MW (g/mol)	10 mL	Concentration
Pepstatin A	685.89	10 mg	1.46 mM

Add MeOH to 10 mL.

Leupeptin/Aprotinin (Sigma-Aldrich)

	MW (g/mol)	1.5 mL	Concentration
Leupeptin	475.6	15 mg	21 mM
Aprotinin	~6500	30 mg	3.1 mM

Add ddH<sub>2</sub>O to 1.5 mL.

Phenylmethylsulfonyl fluoride (PMSF, RPI Corp.)

	MW (g/mol)	10 mL	Concentration
PMSF	174.2	0.34 g	195 mM

Add EtOH to 10 mL.

4-Nitrophenylphosphate di(tris) salt (PNPP<sub>i</sub>, Sigma-Aldrich)

	MW (g/mol)	1 mL	Concentration
PNPP <sub>i</sub>	461.36	0.46 g	1 M

Add ddH<sub>2</sub>O to 1 mL.

Microcystin-LR (Calbiochem)

	MW (g/mol)	1268 μL	Concentration
Microcystin-LR	995.2	500 μg	400 μM

Add DMSO to 1268 μL.

### 2.3.3 Protein Quantification with the BCA (Bicinchoninic Acid) Assay

The total amount of protein in the protein extracts was determined with the Thermo Scientific Pierce BCA Protein Assay Kit, according to the manufacturer's protocol. From a 2 mg/mL BSA stock solution a protein standard with 0, 1, 2, 5 and 10 μg of BSA was prepared in a 96 well plate. To the standard as well as to a serial dilution of the samples (all in triplicate) 200 μL of the BCA working reagent mix was added and incubated for 30 min at 37 °C before the OD<sub>562</sub> was measured in a Synergy 2 Multi-Mode Microplate Reader (Biotek). The calibration curve of the protein standard was used to calculate the concentration of the samples.

### 2.3.4 Immunoprecipitation (IP)

In order to detect changes in the level of phosphorylation or changes in protein-protein interaction an IP or a co-immunoprecipitation was performed. For an IP 500-1000 μg of total protein was incubated with 1-5 μg of antibody (1-2 μL of serum) and 20 μL of bead slurry, consisting of protein A conjugated

agarose (IPA300, Repligen) and Sepharose CL-4B beads (Sigma), at 4 °C overnight. After the incubation the beads were washed three times with Tris buffered saline (TBS) containing 0.1% Triton X-100 and one time with TBS for 20 min at 4 °C. To mitigate unspecific binding, a washing step with 1% Triton X-100 and a high salt wash (900 mM NaCl, 20 mM Tris-Cl pH 7.4) were included (only if high non-specific co-IPs made these steps necessary). The precipitated proteins were eluted with 30  $\mu$ L of 1.5x SDS sample buffer, heated for 5 min at 95 °C, separated by sodium dodecyl sulfate polyacrylamide gel electrophoresis (SDS-PAGE) and transferred onto a polyvinylidene difluoride (PVDF) membrane for immunoblotting.

### Reagents

10x TBS

	MW (g/mol)	Stock	1 L	Concentration
Tris-Cl pH 7.4		1 M	200 mL	200 mM
NaCl	58.44		87.7 g	1.5 M

Add ddH<sub>2</sub>O to 1 L.

1x TBS + 0.1% Triton X-100

	Stock	1 L	Concentration
TBS	10x	100 mL	1x
Triton X-100	20%	5 mL	0.1%

Add ddH<sub>2</sub>O to 1 L.

### 2.3.5 Preparation of the Postsynaptic Density Fraction (PSD)

The isolation of the PSD fraction from brain (Carlin et al., 1980) was conducted on ice or at 4 °C. Four forebrains were homogenized in 5 mL solution A and centrifuged (1.400 xg, 10 min). The pellet was re-extracted in the same volume of buffer A and the combined supernatants from both steps were centrifuged at low speed (710 xg, 10 min), followed by a high speed spin (13.800 xg, 20 min) of the supernatant (to obtain the synaptic membrane enriched P2 pellet). The P2 pellet was resuspended in 3.1 mL solution A without MgCl<sub>2</sub> and loaded onto a 0.85/1/1.25 M sucrose step gradient, and centrifuged (82.500 xg, 2 h). The synaptosome enriched fraction at the

1/1.25 M interface was extracted with an equal volume of Triton-X-100 buffer (0.5% final concentration) for 15 min and pelleted (35.000 xg, 30 min). The pellet was resuspended in 1 mL solution A without MgCl<sub>2</sub> and layered on top of a 1/1.5/2 M sucrose gradient. Following centrifugation (225.000 xg, 2 h) the PSD enriched fraction at the 1.5/2 M interface was collected. The protein concentrations were determined with the BCA assay and 10 µg of total protein of each fraction analyzed by immunoblotting.

### Reagents

#### Buffer A

	Stock	40 mL	Concentration
Sucrose		4.38 g	0.32 M
Tris-Cl pH 7.4	1 M	40 µL	1 mM
MgCl <sub>2</sub> · 6 H <sub>2</sub> O	200 mM	200 µL	1 mM
Leupeptin/Aprotinin	21 mM/3.1 mM	4 µL	2.1/0.31 µM
Pepstatin A	1.46 mM	40 µL	1.46 µM
PMSF	195 mM	40 µL	195 µM
Microcystin	400 µM	200 µL	2 µM

Add ddH<sub>2</sub>O to 40 mL.

#### Triton-X-100 buffer

	Stock	20 mL	Concentration
Triton-X-100	20%	1 mL	1%
Tris-Cl pH 8.0	1 M	240 µL	12 mM
KCl	1 M	38 µL	1.9 mM
Leupeptin/Aprotinin	21 mM/3.1 mM	2 µL	2.1/0.31 µM
Pepstatin A	1.46 mM	20 µL	1.46 µM
PMSF	195 mM	20 µL	195 µM
Microcystin	400 µM	100 µL	2 µM

Add ddH<sub>2</sub>O to 20 mL.

## Sucrose buffers

	MW (g/mol)	In 50 mL
0.85 M	342.3	14.55 g
1 M	342.3	17.11 g
1.25 M	342.3	21.39 g
1.5 M	342.3	25.67 g
2 M	342.3	34.33 g

**2.3.6 *In vitro* Phosphorylation/Dephosphorylation****2.3.6.1 PKA Phosphorylation**

For the *in vitro* phosphorylation with PKA the purified catalytic subunit was purchased from Sigma and reconstituted according to the data sheet. The *in vitro* phosphorylation was conducted for 3 min at 30 °C in the following reaction mix:

	MW (g/mol)	Stock	Concentration
HEPES, pH 7.4	238.3	200 mM	20 mM
MgCl <sub>2</sub> · 6 H <sub>2</sub> O	203.3	200 mM	2 mM
KCl	74.56	1 M	100 mM
DTT (Dithioereitol)	154.25	20 mM	0.2 mM
ATP, Disodium Salt	551.1	10 mM	0.5 mM
PKA, catalytic subunit			4 U

As substrate the immuno precipitated NMDA receptor or a GST fusion protein of the GluN2B or the GluA1 C-terminus was used. The reaction was stopped by the addition of 5x SDS sample buffer and denaturing for 5 min at 95 °C. The induced phosphorylation was detected and determined with phospho specific antibodies.

**2.3.6.2 CaMKII Phosphorylation**

Purified CaMKII $\alpha$  was a generous gift from Dr. Andy Hudmon and the *in vitro* phosphorylation also was conducted for 3 min at 30 °C in the following reaction mix (next page):

	MW (g/mol)	Stock	Concentration
HEPES, pH 7.4	238.3	500 mM	50 mM
MgCl <sub>2</sub> · 6 H <sub>2</sub> O	203.3	1 M	10 mM
CaCl <sub>2</sub> · 2 H <sub>2</sub> O	147	100 mM	1 mM
CaM (Calmodulin)		40 μM	1 μM
ATP, Disodium Salt	551.1	10 mM	0.25 mM
CaMKII-α			30 nM

A GST fusion protein of the GluA1 C-terminus served as substrate and the reaction was again stopped by the addition of 5x SDS sample buffer and denaturing for 5 min at 95 °C. The induced phosphorylation was detected and determined with phospho specific antibodies.

### 2.3.6.3 CIP Dephosphorylation

The *in vitro* dephosphorylation with alkaline phosphatase (New England BioLabs) was performed for 1 h at 37 °C in 1x NEBuffer 3 (50 mM Tris-Cl, 100 mM NaCl, 10 mM MgCl<sub>2</sub>, 1 mM Dithiothreitol) and stopped through the addition of 5x SDS sample buffer and denatured via a 5 min incubation at 95 °C.

### 2.3.7 <sup>32</sup>P Labeling and Overlay Analysis

Purified CaMKIIα was autophosphorylated at T286 in the presence of calcium/calmodulin and [ $\gamma$ -<sup>32</sup>P]-ATP (3000 Ci/mmol). The *in vitro* phosphorylation was conducted for 90 s on ice in the following reaction mix:

	MW (g/mol)	Stock	Concentration
HEPES, pH 7.4	238.3	500 mM	50 mM
MgCl <sub>2</sub> · 6 H <sub>2</sub> O	203.3	1 M	10 mM
CaCl <sub>2</sub> · 2 H <sub>2</sub> O	147	100 mM	1 mM
CaM (Calmodulin)		40 μM	2 μM
ATP, Disodium Salt	551.1	100 μM	6 μM
[ $\gamma$ - <sup>32</sup> P]-ATP (3000 Ci/mmol)		1.67 μM	0.33 μM
CaMKII-α			0.9 μM

After 90 s the reaction was stopped by the addition of 1.25  $\mu\text{L}$  500 mM EDTA ( $\sim 12.5$  mM final concentration) and incubated for a few minutes on ice. For desalting, the reaction mix was loaded on 200  $\mu\text{L}$  of packed, swelled and degassed Sephadex G50 beads. The eluted (with TBS + 12.5 mM EDTA) autophosphorylated,  $^{32}\text{P}$ -labeled CaMKII $\alpha$  was diluted in blocking solution (2% BSA in TBS-T + 12.5 mM EDTA) and overlaid overnight at 4  $^{\circ}\text{C}$  on the to be analyzed blots. The next day, after extensive washing, the blots were analyzed via autoradiography.

### **2.3.8 Western Blot (WB) Analysis**

#### **2.3.8.1 SDS-PAGE**

After the protein extracts or IP samples were dissolved in SDS sample buffer and denatured for 5 min at 95  $^{\circ}\text{C}$ , they were separated according to their molecular weight by SDS-PAGE. To increase the resolution of the protein separation a discontinuous buffer system was used. The proteins were concentrated in the stacking gel and separated in the lower resolving gel.

#### **2.3.8.2 Wet Transfer**

The proteins were transferred from the electrophoresis gel to the surface of a PVDF membrane via tank transfer (Mini Trans-Blot Cell, Biorad). For the wet transfer the methanol activated PVDF membrane and the gel were equilibrated in transfer buffer and pressed together in a transfer sandwich consisting of sponge/Whatman paper/PVDF membrane/gel/Whatman paper/sponge in a gel holder cassette. The transfer was performed at 4  $^{\circ}\text{C}$  for roughly 10 h (exact time depending on the molecular weight of the protein of interest) at 50 V.

#### **2.3.8.3 Immunodetection**

After the transfer, unspecific binding sites on the PVDF membrane were blocked with 2% BSA in TBS with Tween 20 (TBS-T) for 1 h at RT. The primary antibody was diluted in blocking solution and incubated with the membrane for 2 h at RT or overnight at 4  $^{\circ}\text{C}$ . Afterwards, the membrane was washed 3 x 5 min and 2 x 15 min with TBS-T at RT and incubated in blocking solution with diluted horseradish peroxidase (HRP) conjugated secondary

antibody for 1 h at RT. Following the incubation with the secondary antibody the membrane was washed 3 x 5 min, 2 x 20 min and 1 x 30 min with TBS-T and 1 x 5 min with TBS. Finally, a standard enhanced chemiluminescent (ECL) substrate was used for detection of HRP activity using X-ray film and a Konica Minolta SRX-101A processor.

#### 2.3.8.4 Quantification of Immunoblot Signals

The chemiluminescent immunosignals were digitalized by scanning the films and quantified with Adobe Photoshop. To measure the intensity of the individual pixels (dark bands on film), the images were inverted in Adobe Photoshop (intensity settings are from 0-255, darkest to whitest). Individual bands were quantified for mean intensity by drawing equal sized boxes around each band and using the histogram function of Adobe Photoshop to calculate the mean intensity. A box of the same size was used to subtract the background from a nearby area on the film. The background generally consisted of no more than 5-10% of the total signal.

#### Reagents

SDS sample buffer

	1.5x	5x
SDS	2.25 g	7.5 g
Tris-Cl pH 7.4	0.834 g	2.811 g
Sucrose	7.5 g	25 g
DTT	0.233 g	0.772 g
Bromphenol Blue	0.003 g	0.01 g

Add ddH<sub>2</sub>O to 50 mL.

4x Tris-Cl-SDS resolving gel buffer, pH 8.8

	MW (g/mol)	500 mL	Concentration
Tris-Cl	121.14	90.86 g	1.5 M
SDS	288.38	2 g	0.4%

Add ddH<sub>2</sub>O to 500 mL and adjust pH to 8.8.

## 4x Tris-Cl-SDS stacking gel buffer, pH 6.8

	MW (g/mol)	500 mL	Concentration
Tris-Cl	121.14	30.3 g	0.5 M
SDS	288.38	2 g	0.4%

Add ddH<sub>2</sub>O to 500 mL and adjust pH to 6.8.

## SDS-PAGE gel (resolving gel 10 mL, stacking gel 5 mL)

	Resolving gel		Stacking gel
	7.5%	10%	
ddH <sub>2</sub> O	5 mL	4.17 mL	3.15 mL
4x Tris-Cl-SDS pH 8.8	2.5 mL	2.5 mL	
4x Tris-Cl-SDS pH 6.8			1.25 mL
30% acrylamide, 0.8% bis-acrylamide solution	2.5 mL	3.33 mL	0.6 mL
10% Ammonium persulfate (APS)	50 µL	50 µL	50 µL
TEMED (N,N,N',N'-tetramethylethylenediamine)	15 µL	15 µL	15 µL

## 10x SDS electrophoresis buffer

	MW (g/mol)	1 L	Concentration
Tris-Cl	121.14	30.3 g	250 mM
Glycine	75.07	143.25 g	1.92 M
SDS	288.38	10 g	1%

Add ddH<sub>2</sub>O to 1 L and adjust pH to 8.8.

## Transfer buffer

	MW (g/mol)	1 L	Concentration
Tris-Cl	121.14	3.03 g	25 mM
Glycine	75.07	14.4 g	192 mM
Methanol		150 mL	15%

Add ddH<sub>2</sub>O to 1 L.

TBS-T (1x TBS + 0.05% Tween-20)

	Stock	1 L	Concentration
TBS	10x	100 mL	1x
Tween-20	20%	2.5 mL	0.05%

Add ddH<sub>2</sub>O to 1 L.

## 2.4 Antibodies

### 2.4.1 List of Antibodies Used for WB and Immunocytochemistry (ICC)

Antibody: anti-	Source/Company	WB	ICC
$\alpha$ -actinin	Santa Cruz	X	
Bassoon	Stressgen		X
CaMKII- $\alpha$ (CB $\alpha$ 2)	Invitrogen	X	X
CMKII- $\beta$ (CB $\beta$ 1)	Invitrogen	X	X
pT286 (CaMKII)	Promega	X	X
Densin-180 (Ab650)	(Jiao et al., 2008)	X	
GFP (N86/38)	Neuromab		X
GluA1	(Leonard et al., 1998)	X	
pS845 (GluA1)	(Leonard et al., 1998)	X	
pS831 (GluA1)	(Leonard et al., 1998)	X	
GluN1 (54.1)	Millipore	X	X
pS897 (GluN1)	Millipore	X	
GluN2A	(Leonard and Hell, 1997)	X	
GluN2B	(Leonard and Hell, 1997)	X	
pS1166 (GluN2B)	PhosphoSolutions (custom made)	X	
PSD-95	Neuromab	X	X
Shank	Neuromab		X
Synapsin	Synaptic Systems		X
Synaptophysin	Epitomics	X	
VGLUT1	Synaptic Systems		X

## **2.5 Statistical Analysis**

Statistical analysis was performed using GraphPad Prism version 5.01 for Windows (GraphPad Software, Inc.). Means and SEMs were calculated from three or more independent experiments (unless stated otherwise). Statistical significance was calculated using (as indicated) the appropriate t-test or one-way or two-way analysis of variance (ANOVA) followed by the stated post-test.

### 3 Results

#### 3.1 The Role of the CaMKII/GluN2B Interaction in Learning and Memory

*In vitro* data clearly established a strong and activity dependent interaction between CaMKII and the GluN2B subunit of the NMDA receptor (Leonard et al., 1999; Strack and Colbran, 1998; Strack et al., 2000a). The formation of the CaMKII/NMDAR complex is essential for the induction of LTP in organotypic hippocampal slices (Barria and Malinow, 2005). Pharmacological inhibitors and CaMKII mutant mice also established a role for the NMDAR and CaMKII itself during LTP and learning and memory (Elgersma et al., 2004; Malenka et al., 1989; Malinow et al., 1989; Morris et al., 1986).

The exact role of the CaMKII/GluN2B interaction for CaMKII binding to the NMDAR and anchoring at the PSD as well as its importance for learning and memory only started to be recently addressed by the generation of GluN2B KI mice that contain two point mutations in the GluN2B C-terminus (L1298A and R1300Q). Each of these mutations abolished CaMKII binding to this site nearly completely (Strack et al., 2000a). In the GluN2B KI mice the activity dependent increase of the NMDAR interaction is entirely abrogated and the activity induced synaptic clustering of CaMKII is missing. Various forms of LTP at the Schaffer collateral synapses in CA1 are reduced by 50%. Nevertheless, working memory in the win-shift 8 arm maze task and learning of the Morris water maze (MWM) task was normal in the KI mice. The GluN2B KI learned to escape to a hidden platform as fast and to the same extent as the WT controls in a spaced six-day MWM training protocol. In addition, normal performance was assessed by probe trials 1 h after training sessions on day 3 and day 5. Despite this normal learning, recall of the task was impaired in the KI mice during the period of early memory consolidation, tested 1 d and 3 d after the last training session (Halt et al., 2012). To further dissect the precise timing of this deficit in early consolidation or retrieval

GluN2B KI mice were trained and tested in various spatial and contextual learning paradigms including Barnes maze, MWM and contextual fear conditioning.

### **3.1.1 Spatial Learning and Memory is not Affected in the Barnes Maze**

We trained and tested two independent cohorts of GluN2B KI mice and WT litter-matched controls in the Barnes maze. The Barnes maze is a less aversive spatial learning paradigm, which unlike the MWM allows the mice to move freely and explore the environment under conditions that are less stressful than the MWM. It is solely based on the motivation of the mice to avoid prolonged exposure to an open area under light and to search for a dark and safe hideout, the escape box. Interestingly, the GluN2B KI showed no detectable deficits in either learning or early memory (Fig. 3.1) contrasting what had been seen before after spaced MWM learning that had been conducted over a period of 6 days (Halt et al., 2012). Over the 16 training trials, which were executed on 4 consecutive days (4 trials per day) the latency to locate and enter the escape box decreased equally fast for both genotypes and saturated on the fourth day (Fig. 3.1 A). During the probe test one day after the last training session there was no difference in the primary escape latency (Fig. 3.1 B, left), covered distance (Fig. 3.1 B, middle) or mean velocity (Fig. 3.1 B, right). Both WT and KI mice searched preferentially in the target area and the surrounding holes (areas +1 and -1), indicating that they clearly remembered the former location of the escape box (Fig. 3.1 B, lower part). The overall number of zone entries and time in zones for GluN2B KI mice showed a slight increase compared to WT mice, which is probably a reflection of the statistically non-significant increased activity of KI as seen in the covered distance and mean velocity (Fig. 3.1 B). The performance in the probe test seven days after the last training session mirrored the results of the one-day probe test. There was no significant difference in the primary escape latency (Fig. 3.1 C, left), covered distance (Fig. 3.1 C, middle) and mean velocity (Fig. 3.1 C, right). The slightly increased activity of the GluN2B KI

mice is again reflected by an increased number of zone entries and by the time spent in the zones (Fig. 3.1 C, bottom).

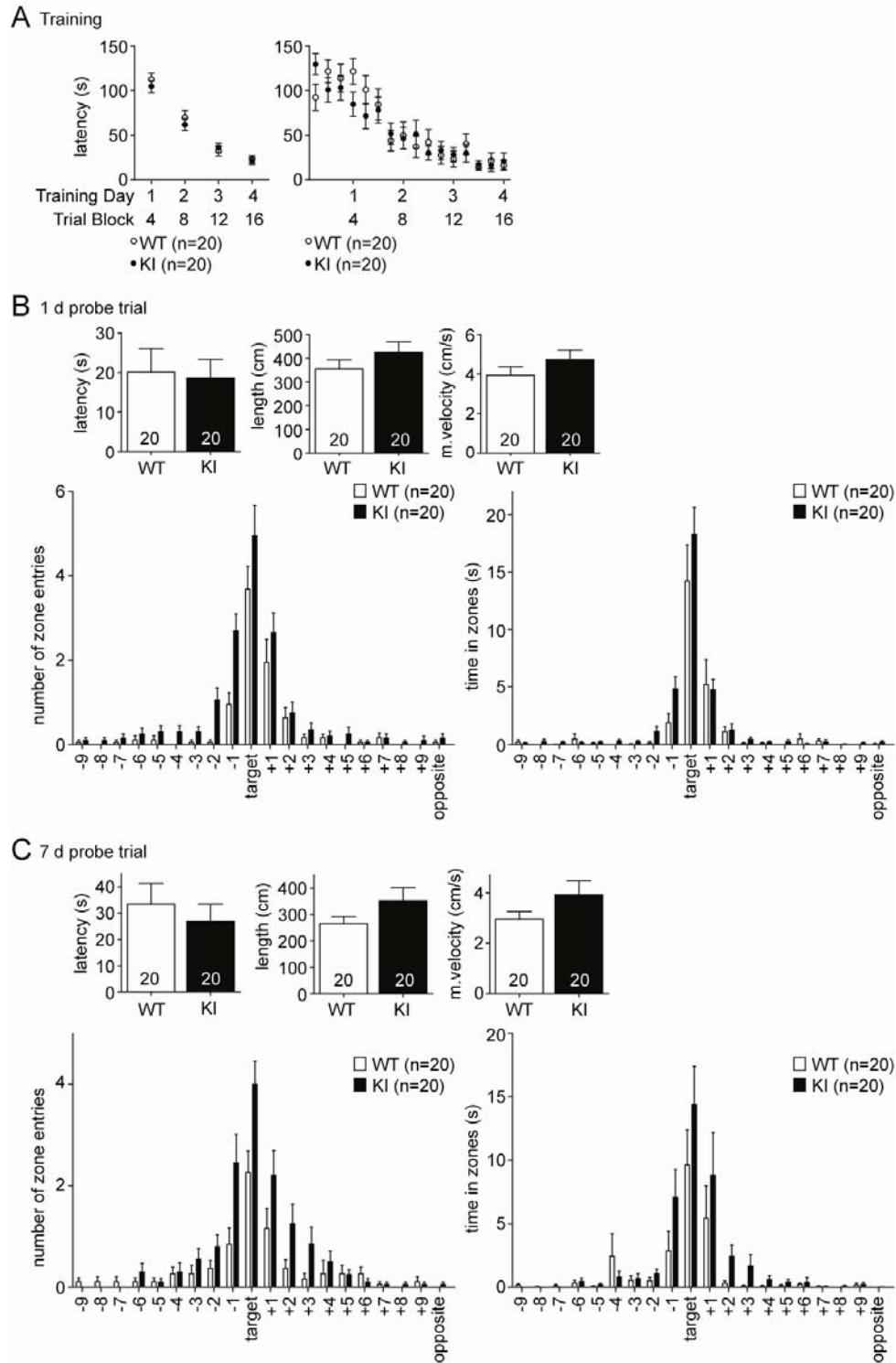


**Figure 3.1 Spatial learning and memory is unaffected in the Barnes maze.** The Barnes maze task was evaluated with two cohorts of naïve litter-matched WT and GluN2B KI mice (10 mice per genotype in each cohort). **(A)** The escape latency for both genotypes decreases equally over the 16 training trials (continued on next page)

(Figure 3.1 continued) and saturates on the fourth day (WT:  $22.99 \pm 4.08$  s, KI:  $20.95 \pm 3.95$  s; left panel depicts average latencies over each of the 4 training days whereas right panel shows averages from all mice for each individual trial). **(B)** The primary escape latency during the probe test one day after the last training session is not different (left; WT:  $20.11 \pm 6.02$  s, GluN2BKI:  $18.68 \pm 4.72$  s). KI mice searched like the WT mice preferentially in and around the target area for the escape box (bottom panels). The covered distance (middle; WT:  $355.70 \pm 37.25$  cm, GluN2BKI:  $426.60 \pm 43.64$  cm) and mean velocity (right; WT:  $3.95 \pm 0.41$  cm/s, GluN2BKI:  $4.74 \pm 0.48$  cm/s) is slightly, but not significantly increased in KI mice. **(C)** The probe test seven days after the last training session shows like the one day test no difference in the avg. primary escape latency (left; WT:  $33.37 \pm 7.98$  s, KI:  $26.80 \pm 6.61$  s) and the KI mice again exhibited the tendency to increased covered distance (middle; WT:  $265.40 \pm 26.47$  cm, GluN2BKI:  $353.00 \pm 49.42$  cm) and mean velocity (right; WT:  $2.95 \pm 0.29$  cm/s, GluN2BKI:  $3.92 \pm 0.55$  cm/s). Both genotypes searched in the right location in and around the target area (bottom panels). Data represent mean  $\pm$  SEM.

### 3.1.2 Single Day Spatial Learning in the Morris Water Maze is Impaired in GluN2BKI Mice

In order to further dissect the exact time course of the memory deficit observed during the initial MWM experiment (Halt et al., 2012), two different cohorts of GluN2B KI mice and their WT littermate controls underwent a massed training protocol on a single day in the MWM. Such a compressed training protocol has the potential to reveal deficits in early- versus late-phase consolidation and in memory recall, by testing multiple cohorts on various days after training. This massed training also further challenges the animals by testing for the capacity to learn and remember during a brief but intensive training session. After habituation on the first day (training day) mice underwent one visible platform trial followed by 12 consecutive training trials, while the no longer visible platform was kept in a fixed position. The initial trial with a marked visible platform is a hippocampus-independent task. It was conducted to rule out changes in motivation, coordination, or sensory processing in GluN2B KI mice. The latency in reaching the visible platform was not different between the two genotypes (Fig. 3.2 A). In the following 12 consecutive trials with a submerged platform the KI mice started to show deficits in spatial learning around trial 6, roughly the onset of learning in the WT mice. For statistical analysis, latencies for the 12 training trials were split up into blocks of four (Fig. 3.2 B, left) or 6 trials (Fig. 3.2 B, right). The GluN2B KI mice displayed significantly decreased average escape latencies during the last four and the last six training trials compared to their WT littermates.

During the probe test one day after training the WT mice required significantly less time to reach the original location of the platform as reflected by faster primary escape latency (Fig. 3.2 C, left). The KI mice also entered less often the target quadrant D (where the platform had been positioned) compared to WT (Fig. 3.2 C, right) and displayed a more random search for the platform. The performance in the probe test 7 days after training was similar to the one day test. The GluN2B KI mice still showed an increased primary escape latency (Fig. 3.2 D, left) and crossed significantly less over into the target quadrant in search for the platform (Fig. 3.2 D, right).

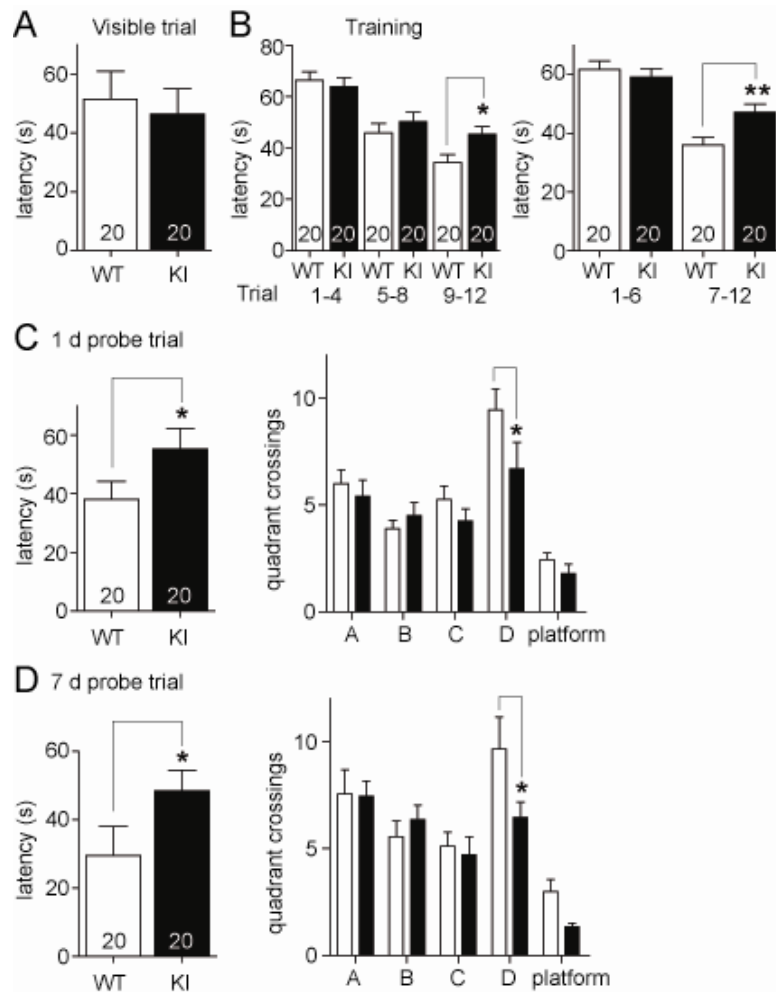


**Figure 3.2 Spatial learning in the Morris water maze (MWM) is impaired in GluN2B KI mice.** The effect of massed training of the MWM task was evaluated with the same cohorts of litter-matched WT and GluN2B KI mice (10 mice per genotype in each of the two cohorts) that had been analyzed with the Barnes maze task in Fig. 2. **(A)** WT and KI mice displayed no difference in the average escape latency during the visible platform trial (WT:  $51.48 \pm 9.50$  s, KI:  $46.46 \pm 8.60$  s). **(B)** The GluN2B KI mice showed a deficit during acquisition of the hidden platform task. The avg. escape latency is significantly increased for KI versus WT mice when comparing the averages of the last four (left; WT:  $34.35 \pm 3.07$  s, KI:  $45.27 \pm 3.08$  s,  $p < 0.05$ , unpaired two-tailed t-test) or (continued on next page)

(Figure 3.2 continued) the last six (right; WT:  $35.93 \pm 2.64$  s, KI:  $47.19 \pm 2.65$  s,  $p < 0.01$ , unpaired two-tailed t-test) training trials. **(C)** During the probe test one day after the training the KI mice exhibited a decreased primary avg. escape latency (left; WT:  $38.09 \pm 6.15$  s, KI:  $55.32 \pm 6.91$  s;  $p < 0.05$ , two-tailed unpaired t-test) and showed significantly fewer crossings into the target quadrant D (right; WT:  $9.45 \pm 0.98$ , KI:  $6.70 \pm 1.22$ ;  $p < 0.05$ , two-way-ANOVA with Bonferroni post test), the former location of the submerged platform. **(D)** The KI mice showed a similar deficit during the seven day probe test, with an extended primary avg. escape latency (left; WT:  $29.50 \pm 8.59$  s, KI:  $48.50 \pm 5.98$  s;  $p < 0.05$ , two-tailed unpaired t-test) and diminished crossings into target quadrant D (right; WT:  $9.67 \pm 1.49$ , KI:  $6.46 \pm 0.73$ ;  $p < 0.05$ , two-way-ANOVA with Bonferroni post test; A: adjacent right quadrant to D; B: quadrant opposite to quadrant D; C: adjacent left quadrant to D). Data represent mean  $\pm$  SEM.

### 3.1.3 Basal Anxiety Levels in the GluN2B KI Mice are Normal

Based on the fact that the GluN2BKI mice displayed a deficit in the more aversive MWM but not in the less frightening Barnes maze, we assessed basal anxiety levels in the GluN2B KI mice using the elevated plus maze (EPM). The EPM relies on the rodents' innate fear of heights and open spaces and their preference for dark and enclosed rooms (Walf and Frye, 2007). Basal anxiety levels in the GluN2B KI mice were not different compared to their WT litter-matched controls. During exposure to the elevated plus maze the GluN2B KI mice spent most of the time in the closed arms, like the WT controls, and rarely stayed in the open arms or center (Fig. 3.3 A). Both genotypes covered comparable minimal distances in the open arms (Fig. 3.3 B), while the WT mice had the tendency to be more active in the closed arms. This tendency is displayed in an increase in covered distance (Fig. 3.3 B) and a higher mean velocity in the closed arms (Fig. 3.3 C). The overall mean velocity was not different between genotypes (Fig. 3.3 C). The observed normal basal anxiety levels concur with earlier findings in the open field analysis and the same innate fear reaction to trimethyl-thiazoline (TMT) (Halt et al., 2012).

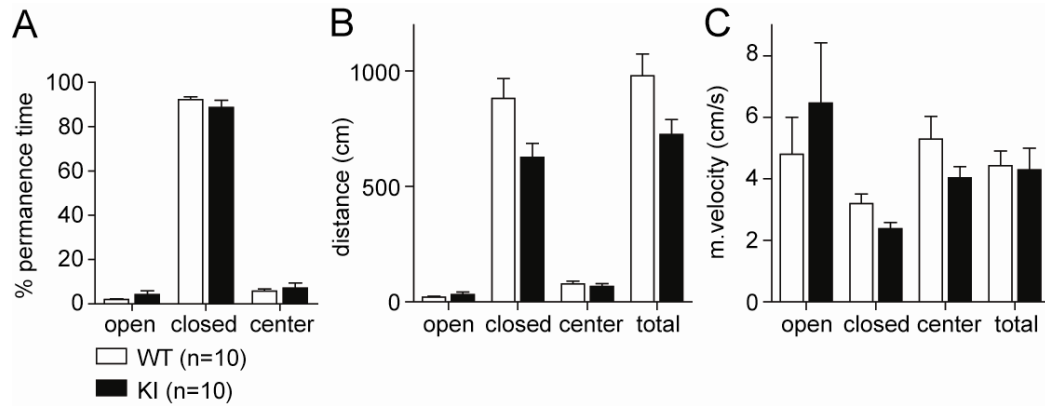


**Figure 3.3 Basal anxiety levels in the GluN2B KI mice are normal.** Basal anxiety levels were evaluated with the second cohort of litter-matched WT and GluN2B KI mice (10 mice per genotype) that had been analyzed in Barnes maze in Fig. 3.1 and for massed MWM training in Fig. 3.2. **(A)** The % of time the mice spent in the open and closed arms (WT:  $92.30 \pm 1.16\%$ , KI:  $88.68 \pm 3.27\%$ ) as well as the center is not different between WT and KI. **(B)** Both genotypes covered the same minimal distances in the open arms (WT:  $20.63 \pm 3.96$  cm, GluN2B KI:  $31.62 \pm 10.73$  cm), but WT mice covered greater distances than KI mice in the closed arms (WT:  $881.59 \pm 86.40$  cm, KI:  $626.92 \pm 59.24$  cm). **(C)** The overall mean velocity is not different between both genotypes, while the WT mice show a slightly increased mean velocity in the closed arm (WT:  $3.19 \pm 0.31$  cm, GluN2B KI:  $2.37 \pm 0.21$  cm/s) coinciding with the longer covered distance. Data represent mean  $\pm$  SEM.

### 3.1.4 Learning and Memory in Contextual Fear Conditioning is not Affected in GluN2B KI

With basal anxiety levels not being affected in the GluN2B KI mice (Fig. 3.3) (Halt et al., 2012), the role of the CaMKII/GluN2B interaction in contextual fear conditioning was investigated. The experimentally naïve mice were placed in the conditioning chamber and trained with 5 consecutive foot shocks (0.75 mA, 1 s duration; aversive unconditioned stimulus). The first foot shock was received at the end of a 3 min habituation period. Subsequent shocks were given at 1 min intervals. The observed freezing response to the foot shock is correlated to the degree of learning, the strength of the aversive stimulus, and the number of presentations. It is defined as the absence of movement except for respiration (Curzon et al., 2009). The GluN2B KI mice learned to the same extent and at the same speed as their WT litter-matched controls (Fig. 3.4 A, C). A total of four independent cohorts were trained. To be able to distinguish possible differences between memory recall and consolidation, two cohorts were tested after four days (Fig. 3.4 B) and the other two cohorts after fourteen days (Fig. 3.4 D). For the probe tests (after 4 or 14 days) the mice were placed back for 5 min into the conditioning

chamber and the freezing response to the context measured. There was no difference in the average time WT and KI mice spent freezing during the four and fourteen day probe test.

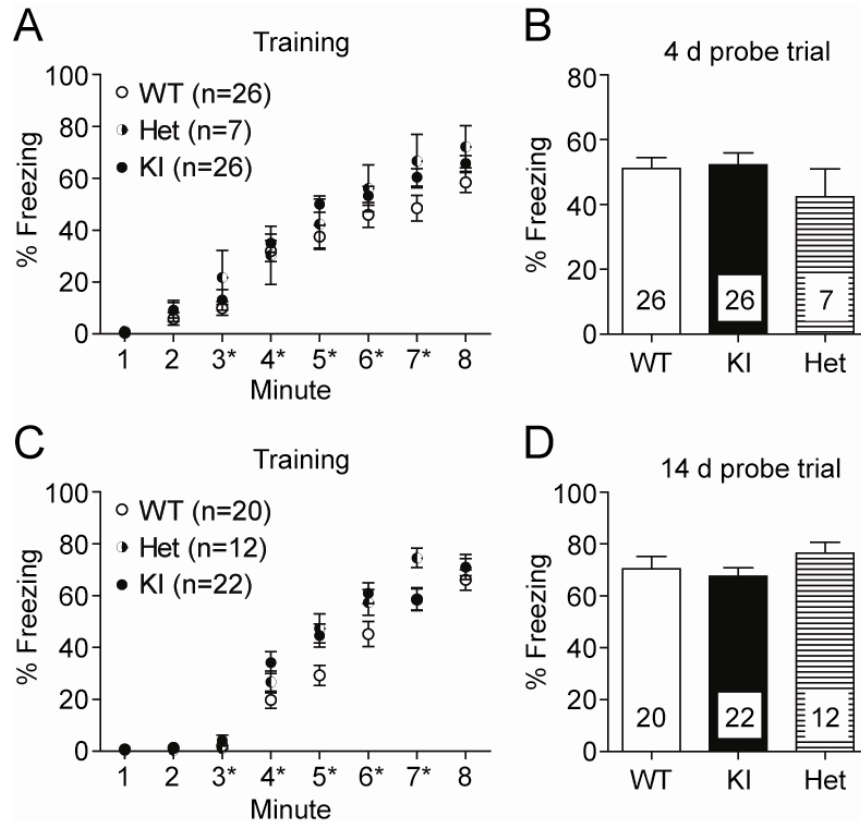


**Figure 3.4 Contextual fear conditioning and memory is unaffected in GluN2B KI mice.** Fear conditioning was evaluated 4 days after training of two different cohorts of naïve litter-matched WT, heterozygous, and GluN2B KI mice (12-14 WT and KI mice, and 3-4 heterozygous mice per cohort) and 14 days after training an additional two different cohorts of naïve litter-matched WT, heterozygous, and GluN2B KI mice (10 WT mice, 10-12 KI mice, and 5-7 heterozygous mice per cohort). **(A, C)** After the 3 min habituation phase, 5 shocks (0.75 mA, 1 s) were delivered at the end of 3<sup>rd</sup>, 4<sup>th</sup>, 5<sup>th</sup>, 6<sup>th</sup> and 7<sup>th</sup> min (asterisks). The increase in the fraction of time spent freezing during conditioning is not different between the GluN2B KI, heterozygous, and WT mice. **(B, D)** All genotypes also display a comparable fraction of time spent freezing during the 4 d (WT: 51.11 ± 3.37%, KI: 52.23 ± 3.77%) and the 14 d (WT: 70.48 ± 4.75%, KI: 67.51 ± 3.33%) probe test. Data represent percentage freezing (mean ± SEM).

### 3.1.5 Contextual Fear Conditioning Performance is Independent of the Stimulus Strength

CaMKII T286A mutant mice have impaired contextual short-term memory (STM) and long-term memory (LTM) formation after a single or three tone-shock pairings, while contextual STM and LTM formation after five

pairings are unaffected (Irvine et al., 2011; Irvine et al., 2005). To exclude the possibility that the mice were over trained with 5 consecutive foot shocks (0.75 mA, 1 s duration), we also tested two milder contextual fear conditioning paradigms. The milder conditioning might reveal defects in memory consolidation or recall in GluN2B KI mice that might have been masked before due to a potentially saturating training.

During the first paradigm, after two days of 3 min pre exposure to the conditioning chamber, 3 shocks (0.5 mA, 1 s) were delivered on day three at the end of the 3<sup>rd</sup>, 4<sup>th</sup> and 5<sup>th</sup> min. Conditioning and memory tested after four days were unaffected (Fig. 3.5 A, B). When the mice were exposed to a different context in the same chamber and room, the time spent freezing was reduced back to pre-conditioning levels and did not differ between the two genotypes (Fig. 3.5 C). LTM tested with the same cohort 11 days after the conditioning (Fig. 3.5 D) also showed no difference. Fig. 3.5 E depicts an overview of the whole experiment with three shocks on a single day.

In a multi day conditioning protocol the mice were pre exposed to the context on day one and conditioned on the following four days with one foot shock (each 0.75 mA, 1 s) per day (Fig. 3.5 F). The GluN2B KI and WT mice showed the same degree of conditioning over the four day training period. The KI displayed a reduction in freezing during the probe test on day 11, 6 days after training, which did not reach statistical significance (Fig. 3.5 F;  $p=0.1154$ ; two-tailed unpaired t-test). On day 12 (7 days after the last training) when the mice were exposed to a different context both genotypes exhibited reduced freezing levels similar to those observed before the conditioning. When the mice were re-exposed to the conditioning context on day 13 (8 day test), freezing was slightly reduced in KI and more so in WT mice compared to the day 11 test so that the tendency of differential recall seen on day 11 was minimized at that time point ( $p=0.5544$ ; two-tailed unpaired t-test) and with it the possibility of a real difference in recall on day 13 as well as day 11.

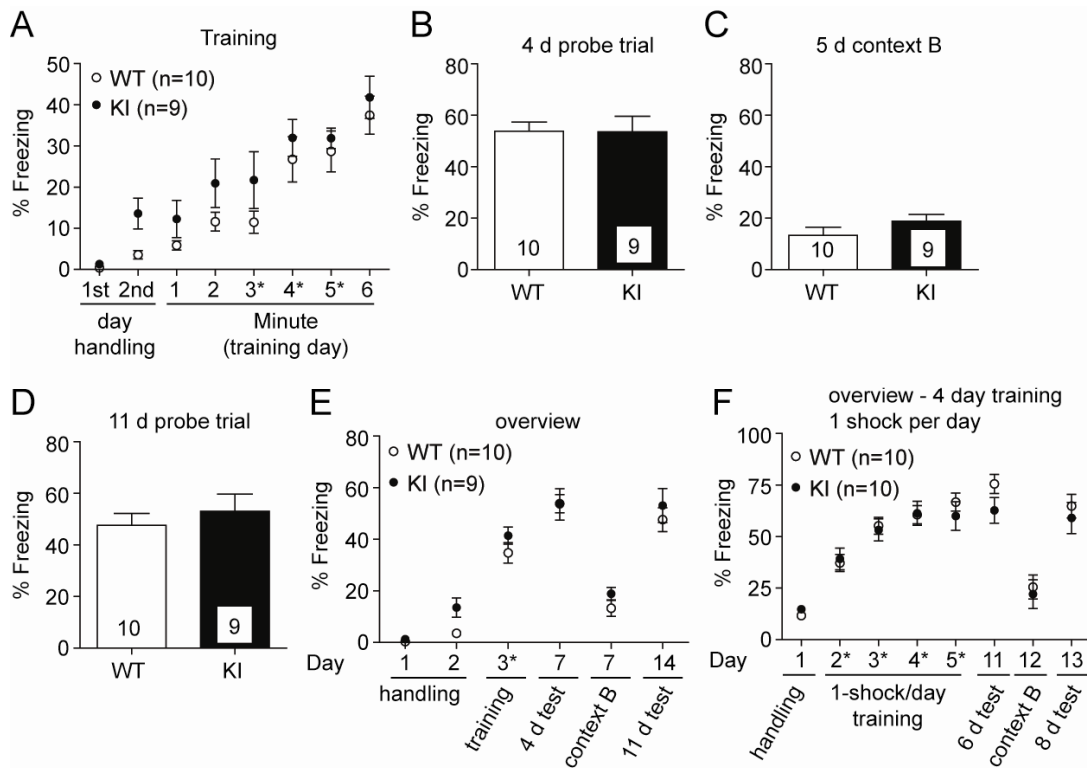


**Figure 3.5 Contextual fear conditioning with milder conditioning trials/stimuli is unaffected in GluN2B KI mice.** One cohort of naïve litter-matched GluN2B KI and WT mice (9-10 mice per genotype) was fear conditioned with three shocks on a single day and a different cohort of litter-matched GluN2B KI and WT mice (10 mice per genotype; same cohort as the first one tested in the Barnes maze in Fig. 3.1 and the MWM in Fig. 3.2) was fear conditioned with 4 shocks over a period of 4 days. **(A)** KI and WT mice acquired to the same extent fear conditioning as indicated by the time spent freezing after 3 consecutive mild foot shocks (0.5 mA, 1 s) at the end of the 3<sup>rd</sup>, 4<sup>th</sup> and 5<sup>th</sup> min (asterisks). **(B, D)** The time spent freezing during recall of context after 4 d (WT:  $53.82 \pm 3.55\%$ , KI:  $53.55 \pm 6.10\%$ ) and 11 d (WT:  $47.63 \pm 4.60\%$ , KI:  $53.08 \pm 6.60\%$ ) was not different between genotypes. **(C)** Exposure to a different context showed pre-conditioning freezing levels for both genotypes (WT:  $13.33 \pm 3.20\%$ , KI:  $18.90 \pm 2.55\%$ ). **(E)** Summary plot of the experimental data from A-D. **(F)** Summary plot of the experimental data of the 4 day training (1 shock, 0.75 mA, 1 s per day) experiment. WT and KI mice showed comparable learning curves during the 4 d conditioning. KI mice displayed less freezing than WT when tested 6 d later (WT:  $75.52 \pm 4.64\%$ , GluN2B KI:  $62.69 \pm 6.21$ ) and 8 d later (WT:  $64.75 \pm 5.68\%$ , KI:  $59.06 \pm 7.56\%$ ), although neither effect reached statistical significance ( $p=0.1154$  for 6 d and  $p=0.5544$  for 8 d trial; two-tailed unpaired t-test). Exposure to a different context, 7 d after the last training day revealed again pre-conditioning freezing levels (WT:  $25.56 \pm 5.85\%$ , KI:  $22.09 \pm 6.93\%$ ). Data represent percentage freezing (mean  $\pm$  SEM).

### 3.2 The Activity-dependent Translocation of CaMKII

Neuronal activity leads to CaMKII activation by calcium influx through the NMDAR and the subsequent recruitment of CaMKII to the PSD (Dosemeci et al., 2001; Otmakhov et al., 2004; Strack et al., 1997b), which can be

persistent and synapse specific (Lee et al., 2009; Zhang et al., 2008) (but see Rose et al., 2009). CaMKII binding to the NMDAR requires activation of CaMKII by  $\text{Ca}^{2+}/\text{CaM}$  or T286 autophosphorylation (Bayer et al., 2006; Leonard et al., 1999; Strack and Colbran, 1998). The activity-dependent translocation (Bayer et al., 2001; Hudmon et al., 2005; Shen and Meyer, 1999; Shen et al., 2000) depends on CaMKII binding to GluN2B (Halt et al., 2012), and is crucial for LTP (Barria and Malinow, 2005; Halt et al., 2012; Zhou et al., 2007).

The data presented here further investigate the physiological relevance of the interaction between CaMKII and its postsynaptic binding partners, particularly the NMDAR. The time course of the activity-dependent translocation of endogenous CaMKII and its persistence were studied in hippocampal cultures. Interestingly in *in vitro* binding assays and in HEK cells a dual mode of interaction between CaMKII and GluN2B was observed (Bayer et al., 2006). An initial reversible interaction by the S-site of CaMKII, converted with longer stimulations subsequently into a stable and persistent interaction with the T-site. To assess how relevant short vs. long stimulation is for the persistence of the translocation in the more physiological hippocampal culture system, CaMKII activation and its subsequent reversal of postsynaptic accumulation were investigated. In addition the role of neurogranin, which determines the local CaM availability, was investigated.

### 3.2.1 Interactions of Autophosphorylated CaMKII in the Brain

CaMKII interactions in the brain, particularly binding involving the NMDAR, were investigated by overlay. Purified CaMKII $\alpha$  (a generous gift from Andy Hudmon) was *in vitro* autophosphorylated on T286 with  $^{32}\text{P}$ -labeled ATP to serve as a probe, and overlaid on 400  $\mu\text{g}$  of brain lysate. Binding of  $^{32}\text{P}$ -labeled, autophosphorylated CaMKII $\alpha$  was detected via autoradiography and revealed three obvious interactions: two interactions at a molecular weight (Mr) of 170-190 kDa and one at  $\sim$ 110 kDa (Fig. 3.6). These three interactions correspond very well with the molecular weight of three known binding partners of CaMKII. One of the two bands detected at 170-190 kDa

presumably accounts for the well-defined and strong interaction with the GluN2B subunit (Mr ~190 kDa) of the NMDAR. The other two interactions at ~180 kDa and ~110 kDa correspond to the Mr of densin-180 and  $\alpha$ -actinin, respectively. CaMKII can form a ternary complex with densin-180 and  $\alpha$ -actinin (Strack et al., 2000b; Walikonis et al., 2001) and in agreement with our data GluN2B, densin-180 and  $\alpha$ -actinin were shown to bind comparable amounts of autophosphorylated CaMKII (Robison et al., 2005b). Notably, no interaction at ~130 kDa, corresponding to the Mr of GluN1, was observed.

P<sup>32</sup> -T286-CaMKII overlay

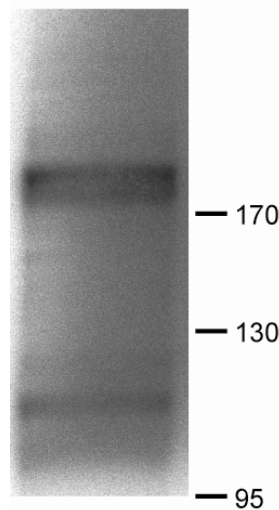


**Figure 3.6 Overlay of <sup>32</sup>P-labeled autophosphorylated CaMKII on brain lysate.** 400  $\mu$ g of brain lysate were separated by SDS-PAGE, transferred to a PVDF membrane and overlaid with 75 nM autophosphorylated CaMKII. The binding of autophosphorylated CaMKII was detected by autoradiography.

### 3.2.2 Concentration-dependent Displacement of the CaMKII/NMDAR Complex by CN21

As part of a collaboration to determine whether the formation of the CaMKII/NMDAR complex itself plays a role in the maintenance of synaptic strength, independent of CaMKII activity, the concentration dependent displacement of the complex through the CN21 peptide was investigated (Sanhueza et al., 2011). CN21 is derived from the endogenous specific CaMKII inhibitor CaM-KIIN (Chang et al., 1998, 2001) and represents the minimal region of CaM-KIIN (aa 43-63) that specifically and with full potency

inhibits CaMKII. CaM-KIIN or CN21 interact with the S-site and T-site of CaMKII (Vest et al., 2007).

Acute hippocampal slices were incubated with 5  $\mu$ M Tat-CN21, 20  $\mu$ M Tat-CN21 or the same concentration of Tat-SCR, a scrambled inactive version of the CN21 peptide, for 1 h. The cell membrane-penetrating peptide sequence from the transactivator of transcription (TAT) from HIV-1 (Deshayes et al., 2005) was attached to allow access to the cell interior. The peptide was washed out for 1 h and the slices frozen in liquid nitrogen for later co-immunoprecipitation analysis. The preparation and treatment of the acute hippocampal slices was performed by Magdalena Sanhueza and German Fernandez-Villalobos. The co-immunoprecipitation analysis including data analysis was conducted by Sebastian Ivar Stein.

Incubation of the hippocampal slices with 5  $\mu$ M Tat-CN21 had no effect on CaMKII binding to the NMDAR, compared to the scrambled control. This was illustrated by equal co-IP of GluN2B and GluN1 after a CaMKII $\alpha$  IP (Fig. 3.7 A, B). On the other hand, incubation with a higher concentration of Tat-CN21 (20  $\mu$ M) resulted in a persistent and significant reduction of the CaMKII/NMDAR complex, evident in reduced GluN2B and GluN1 co-IP levels. The interaction of CaMKII with  $\alpha$ -actinin, which was measured in parallel as a control for specificity of the peptides, was not affected at either CN21 concentration. The binding of CaMKII to  $\alpha$ -actinin is not activity dependent and not mediated over the T-site (Jalan-Sakrikar et al., 2012; Robison et al., 2005a; Robison et al., 2005b; Walikonis et al., 2001). Densin-180 is another CaMKII associated protein. It is enriched in the PSD and binds via a central domain to the T-site of CaMKII (Jiao et al., 2011). This activity dependent interaction was monitored at the same time, but due to the limited number of samples and the investigation of multiple interactions before densin-180 a definite conclusion could not be drawn. The results also suggest a reduction of the CaMKII/densin-180 interaction at a higher concentration of Tat-CN21 (20  $\mu$ M), and no effect at a concentration of 5  $\mu$ M, but need further clarification.

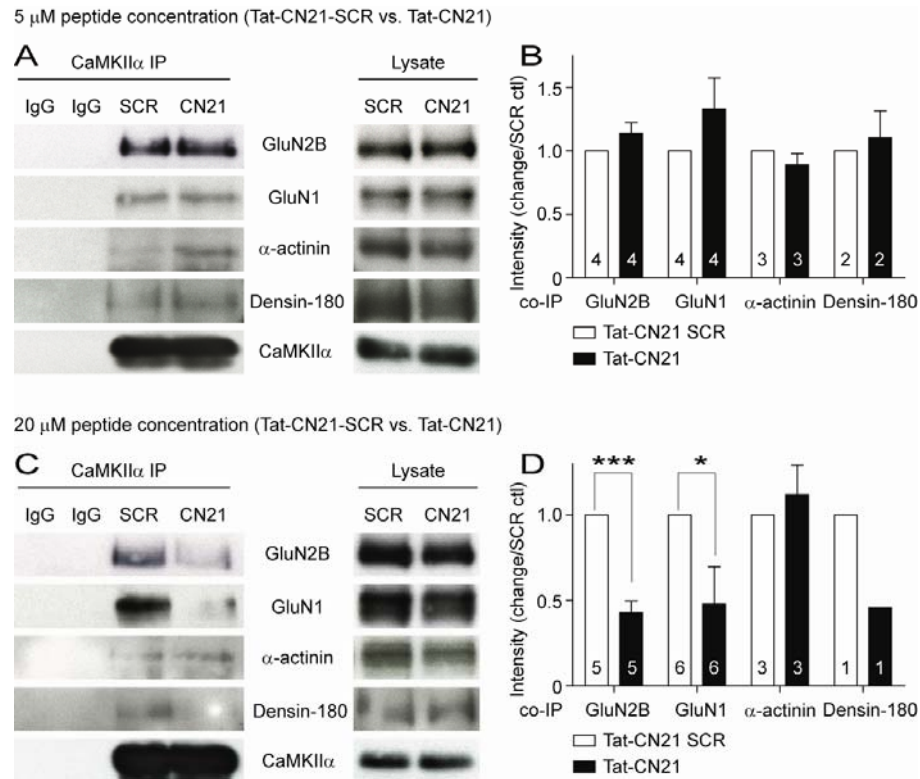


**Figure 3.7 Concentration dependent displacement of the CaMKII/NMDAR complex by Tat-CN21.** (A) The frozen hippocampal slices incubated with 5  $\mu$ M Tat-CN21 (CN21) were solubilized with 1% deoxycholate. The CaMKII/NMDAR complex was immunoprecipitated with a CaMKII $\alpha$  antibody or control IgG and immunoblotted for GluN2B, GluN1,  $\alpha$ -actinin, densin-180 and CaMKII $\alpha$ . (B) The immunosignals were analyzed by densitometry, corrected against CaMKII $\alpha$  for variations during the IP and the CN21 co-IP signals expressed as change compared to the scrambled control. (C, D) WB analysis and quantification of the samples incubated with 20  $\mu$ M Tat-CN21. Data represent mean  $\pm$  SEM. Statistical significance: paired t-test, \* $p$ <0.05, \*\*\* $p$ <0.001.

### 3.2.3 Time Course of CaMKII $\alpha$ Clustering

During neuronal activity CaMKII undergoes an activity-dependent redistribution from the cytosol and the F-actin bound pool to the synapse (Bayer et al., 2001; Bayer et al., 2006; Otmakhov et al., 2004; Shen and Meyer, 1999; Shen et al., 2000). The redistribution is driven by diffusion and subsequent trapping of activated CaMKII at the PSD. In hippocampal cultures from the GluN2B KI mice it was recently shown, that the interaction with GluN2B is critical for this activity-induced synaptic clustering (Halt et al., 2012).

To establish a time course for the redistribution of endogenous CaMKII $\alpha$ , hippocampal cultures were treated with 100  $\mu$ M glutamate/10  $\mu$ M

glycine for the indicated time points (Fig. 3.8), fixed immediately and immunostained for CaMKII $\alpha$  as well as Synapsin. Synapsin is associated with synaptic vesicles and serves as a synaptic marker. With increasing times of glutamate stimulation the CaMKII $\alpha$  staining changed from a smooth, even distribution to a more punctated, clustered one, coinciding with an increasing overlap of the presynaptic Synapsin puncta. The conversion from a smooth to a mainly clustered CaMKII $\alpha$  staining started at ~90 s (Fig. 3.8 J) and saturated after ~3 min of glutamate stimulation (Fig. 3.8 P). A similar time course of redistribution had been observed with ectopically expressed GFP-CaMKII $\alpha$  and  $\beta$  (Shen and Meyer, 1999).

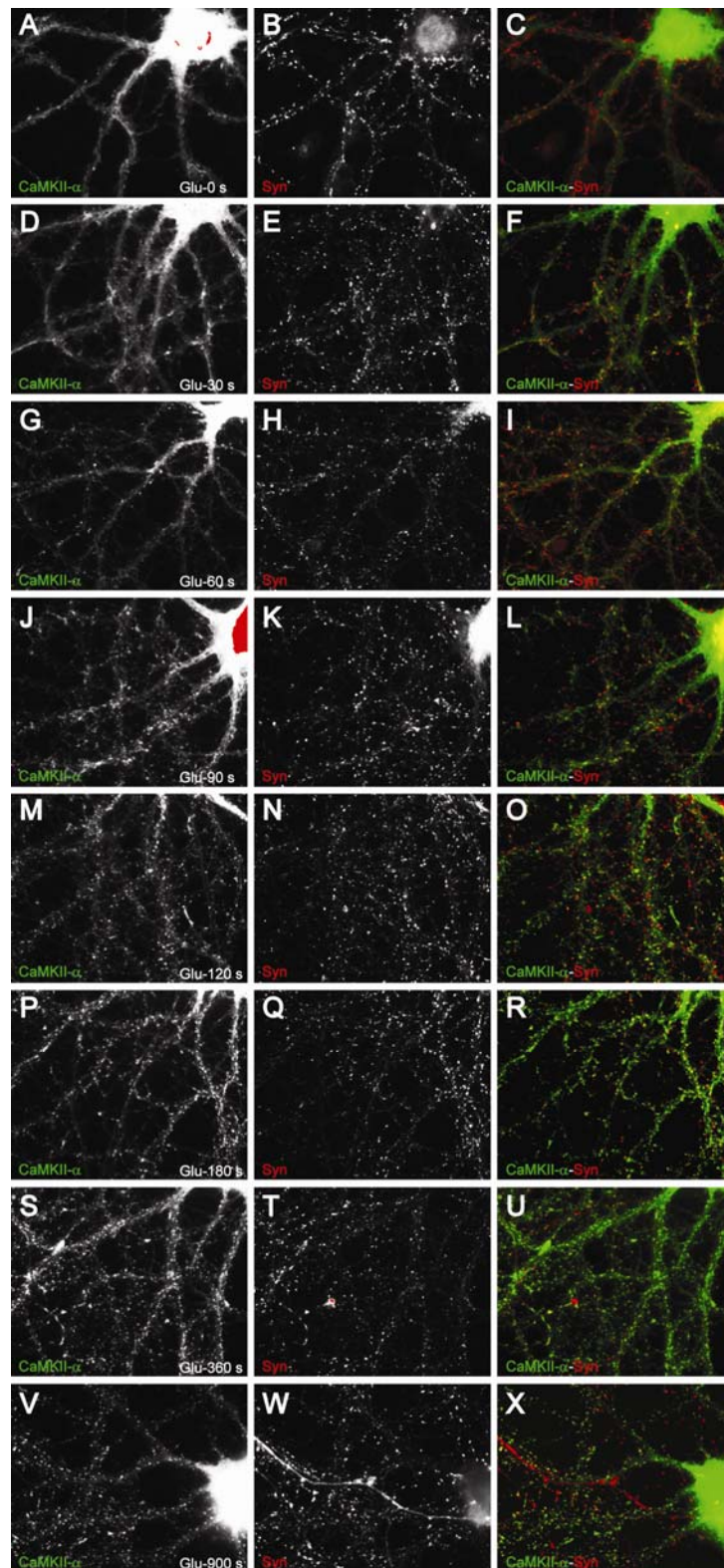


**Figure 3.8 CaMKII $\alpha$  clustering time course.** Mature (DIV 18-21) hippocampal cultures were treated for the indicated times with 100  $\mu$ M glutamate/10  $\mu$ M glycine (Glu). After treatment the cultures were immediately fixed with PFA and immunostained for CaMKII $\alpha$  and Synapsin (Syn), and labeled with Alexa fluor-coupled secondary antibodies.

### 3.2.4 Time Course of CaMKII $\beta$ Clustering

CaMKII $\alpha$  and  $\beta$  are the predominant isoforms in the brain and heteromers as well as  $\alpha$  homomers have been found in brain tissue. The individual isoform ratios in the holoenzyme (dodecamer) are dependent on tissue- and cell-specific expression patterns (Brocke et al., 1999). In the adult forebrain, including the hippocampus, the ratio of  $\alpha$  to  $\beta$  subunit is roughly 3:1 (McGuinness et al., 1985).

CaMKII $\beta$  possess, in contrast to the  $\alpha$  isoform, an insert in the variable region mediating binding to F-actin in an activity-dependent manner (Shen and Meyer, 1999; Shen et al., 1998). This interaction has an important structural role by targeting CaMKII holoenzymes to the F-actin structure in spines (Borgesius et al., 2011).

Hippocampal cultures were treated again with 100  $\mu$ M glutamate/10  $\mu$ M glycine for the indicated time points (Fig. 3.9), fixed immediately and immunostained for CaMKII $\beta$  and Synapsin. The translocation of CaMKII $\beta$ , observed as a change from a smooth even distribution to a more punctated clustered one, displayed the same time course as the previously shown CaMKII $\alpha$  staining. The onset of the clustering occurred around  $\sim$ 90 s (Fig. 3.9 J) and was complete after  $\sim$ 3 min of glutamate stimulation (Fig. 3.9 M, P). The fact, that CaMKII $\alpha$  and CaMKII $\beta$  displayed similar translocation kinetics, indicates that the majority of CaMKII holoenzymes exist as heteromers. Theoretically  $\alpha$  homomers, unable to bind F-actin, should be recruited faster from the cytoplasm to the PSD than  $\beta$  homomers or heteromers, which need to dissociate first from F-actin (Shen and Meyer, 1999).

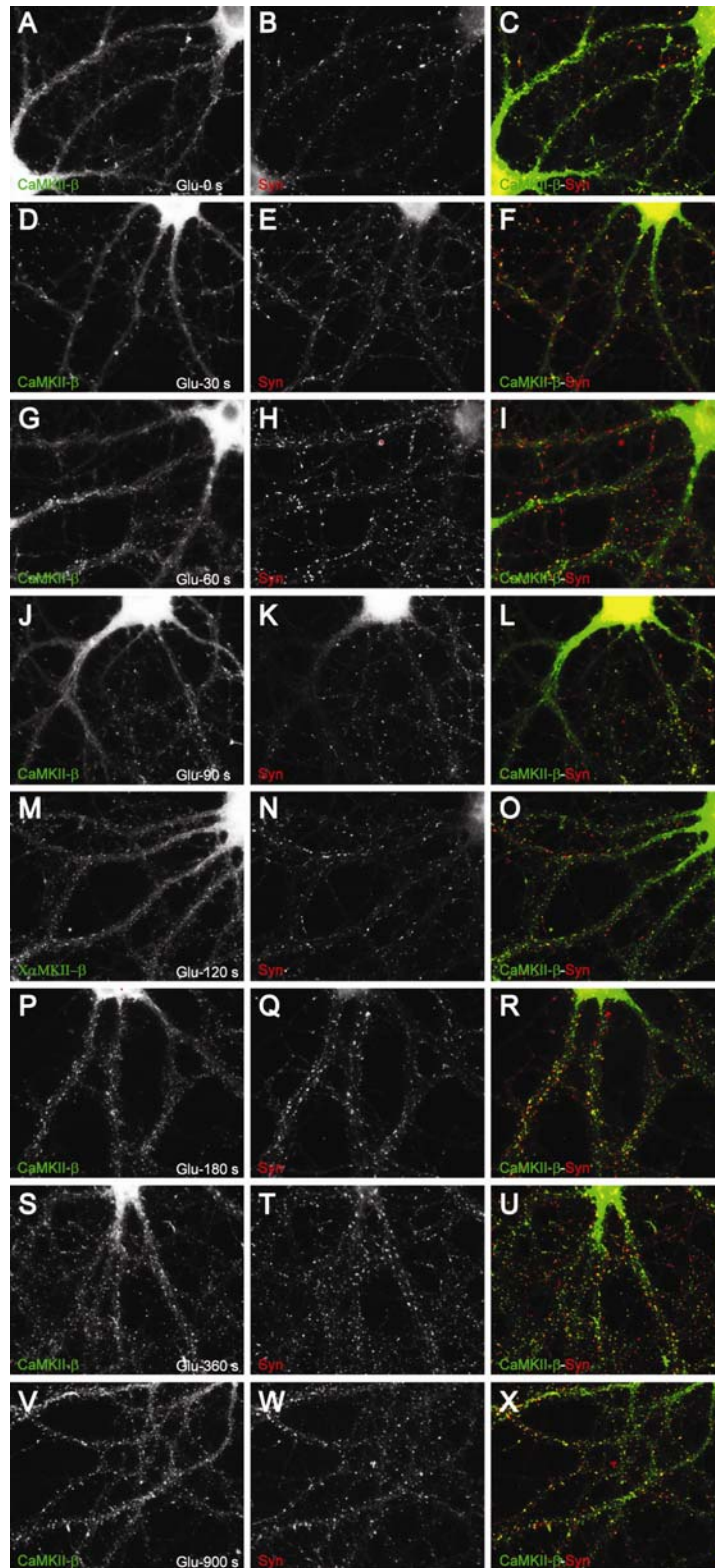


**Figure 3.9 CaMKII $\beta$  clustering time course.** Hippocampal cultures (DIV 18-21) were treated for the indicated times with 100  $\mu$ M glutamate/10  $\mu$ M glycine (Glu), fixed with PFA and immunostained for CaMKII $\beta$  and Synapsin (Syn), and labeled with Alexa fluor-coupled secondary antibodies.

The earlier CaMKII $\alpha$  and  $\beta$  time courses resulted in a slow onset of the clustering around 90 s of stimulation and seemed to be complete after ~3 min. To assess the exact time of saturated translocation more precisely, cultures were vehicle treated (ctl) or stimulated for 120, 150, 180, 210 and 240 s and counterstained with the postsynaptic scaffolding protein Shank. Confocal images were analyzed for changes in CaMKII $\beta$ . The Shank images were thresholded and used as a mask to measure CaMKII $\beta$  intensity in the Shank positive postsynaptic areas (all pictures within one experiment were taken using identical settings and within a time frame of 2 days. The threshold for Shank was kept constant across all conditions.). Fig. 3.10 A-F shows example pictures of the CaMKII $\beta$  and Shank staining for vehicle treatment and 100  $\mu$ M glutamate/10  $\mu$ M glycine stimulation for 240 s. Analysis of CaMKII $\beta$  fluorescence intensity revealed a time-dependent increase in intensity at synaptic sites (Shank positive areas) upon stimulation, reflecting the redistribution of CaMKII. Stimulation for 120 s showed a slightly increased CaMKII $\beta$  average (avg.) intensity, which was not statistically significant from control treatment. After 150 s of glutamate stimulation the avg. fluorescence intensity was significantly increased and was saturated after 180 s of stimulation (Fig. 3.10 G). Fig. 3.10 H shows the cumulative distribution of CaMKII $\beta$  fluorescence intensity for the different treatments and confirms the shift to increased CaMKII $\beta$  staining intensity with prolonged times of glutamate stimulation.

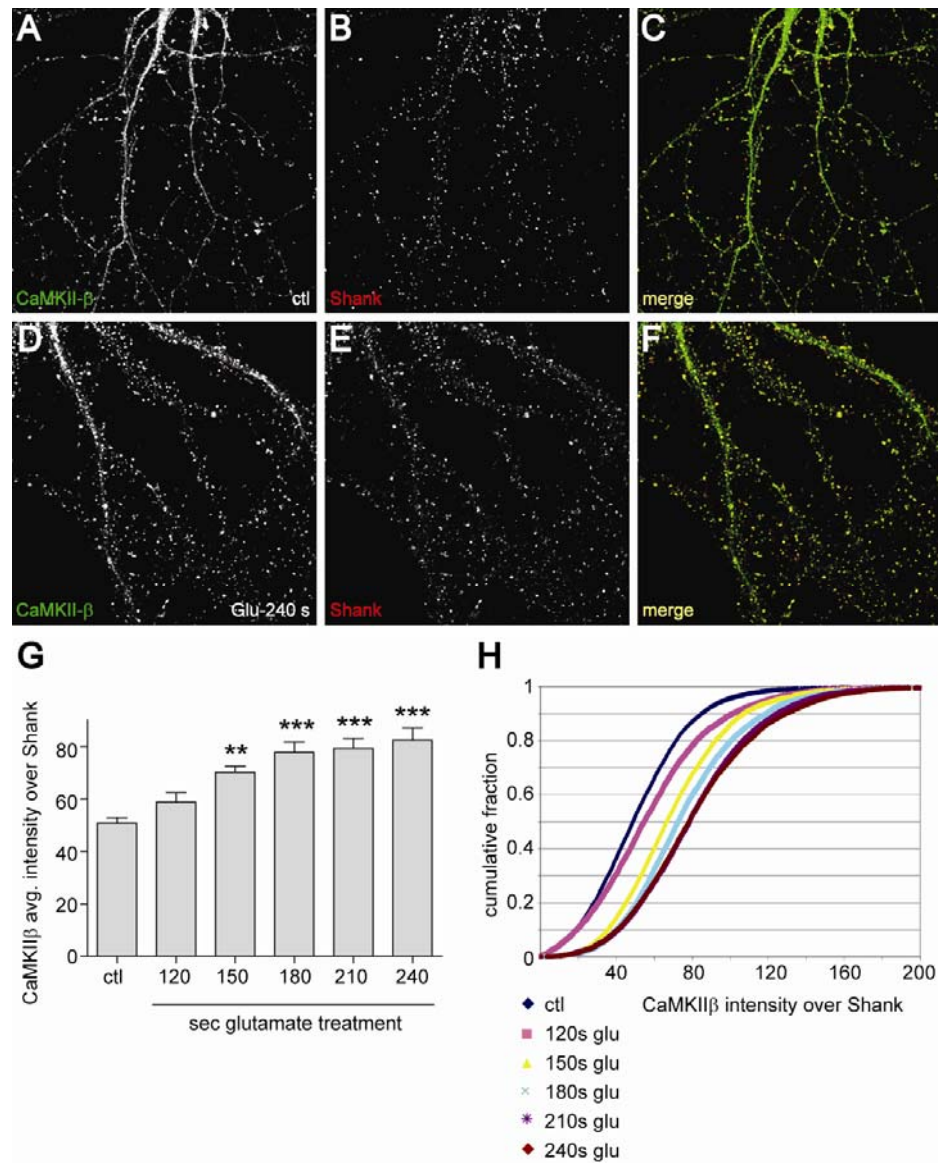


**Figure 3.10 Time-dependence of the increase in synaptic CaMKII $\beta$  intensity after glutamate stimulation.** Hippocampal cultures (18-21 DIV) were vehicle treated (ctl) or stimulated for the indicated time points with 100  $\mu$ M glutamate/10  $\mu$ M glycine. **(A-F)** Example pictures of CaMKII $\beta$  (in green), Shank (in red) and the overlay for control (ctl) and stimulated (240 s glutamate) conditions. **(G)** Analysis of CaMKII $\beta$  fluorescence intensity in Shank positive areas. Data represent mean  $\pm$  SEM. Statistical significance compared to ctl: one-way ANOVA with Tukey post test, \*\* $p < 0.01$ , \*\*\* $p < 0.001$ . **(H)** Analysis of CaMKII $\beta$  fluorescence intensity in Shank positive areas plotted as cumulative distribution.

### 3.2.5 The Persistence of the CaMKII $\alpha$ Translocation

The previous time course (Fig. 3.10) showed that the redistribution of CaMKII is measurable as an increase in CaMKII fluorescence intensity in postsynaptic Shank areas after 150-180 s of glutamate stimulation. The same

analysis was used to determine the persistence of the activity-induced translocation of CaMKII.

First, the finding of the CaMKII $\beta$  time course, of no distinct increase with glutamate stimulation up to 2 min, was confirmed for the  $\alpha$  subunit. Mature hippocampal cultures were vehicle treated or stimulated for 0, 30, 60, 90, 120 or 300 s with 100  $\mu$ M glutamate/10  $\mu$ M glycine. The cultures were immediately fixed (no chase) and stained for CaMKII $\alpha$  and Shank. Example pictures of vehicle treated (ctl) and glutamate stimulated (Glu) cultures show the activity-dependent redistribution of CaMKII, evident as a shift from a smoother to more punctate staining with increasing overlap of Shank (Fig. 3.11 A-F). Analysis of the CaMKII $\alpha$  fluorescence intensity over a Shank mask revealed no statistically significant increase in intensity compared to control (ctl, vehicle treatment) for all time-points up to 120 s, as observed earlier for CaMKII $\beta$ . Stimulation with glutamate for 300 s resulted in a statistically significant increase of CaMKII $\alpha$  fluorescence intensity (Fig. 3.11 G).

To investigate the persistence of anchoring of endogenous CaMKII at the PSD after the activity-dependent translocation, hippocampal cultures were vehicle treated or stimulated for 120 or 300 s with 100  $\mu$ M glutamate/10  $\mu$ M glycine. After removal of the glutamate containing medium and washing, the cultures were chased for 2, 5, 20 or 60 min, fixed, immunostained and the CaMKII $\alpha$  fluorescence intensity analyzed. The analysis revealed a significant increase of CaMKII $\alpha$  fluorescence intensity for both time points after a 2 min chase period. After a 5 min chase the translocation of CaMKII $\alpha$  was already partially reversed and no longer significantly differed from the control (Fig. 3.11 H). The reversal, however, was not complete; roughly 30% of the increase seen after the 2 min chase or the straight 5 min glutamate stimulation remained. Notably, the tendency of a slight remaining increase was persistent and still obvious after the 20 and 60 min chase period.

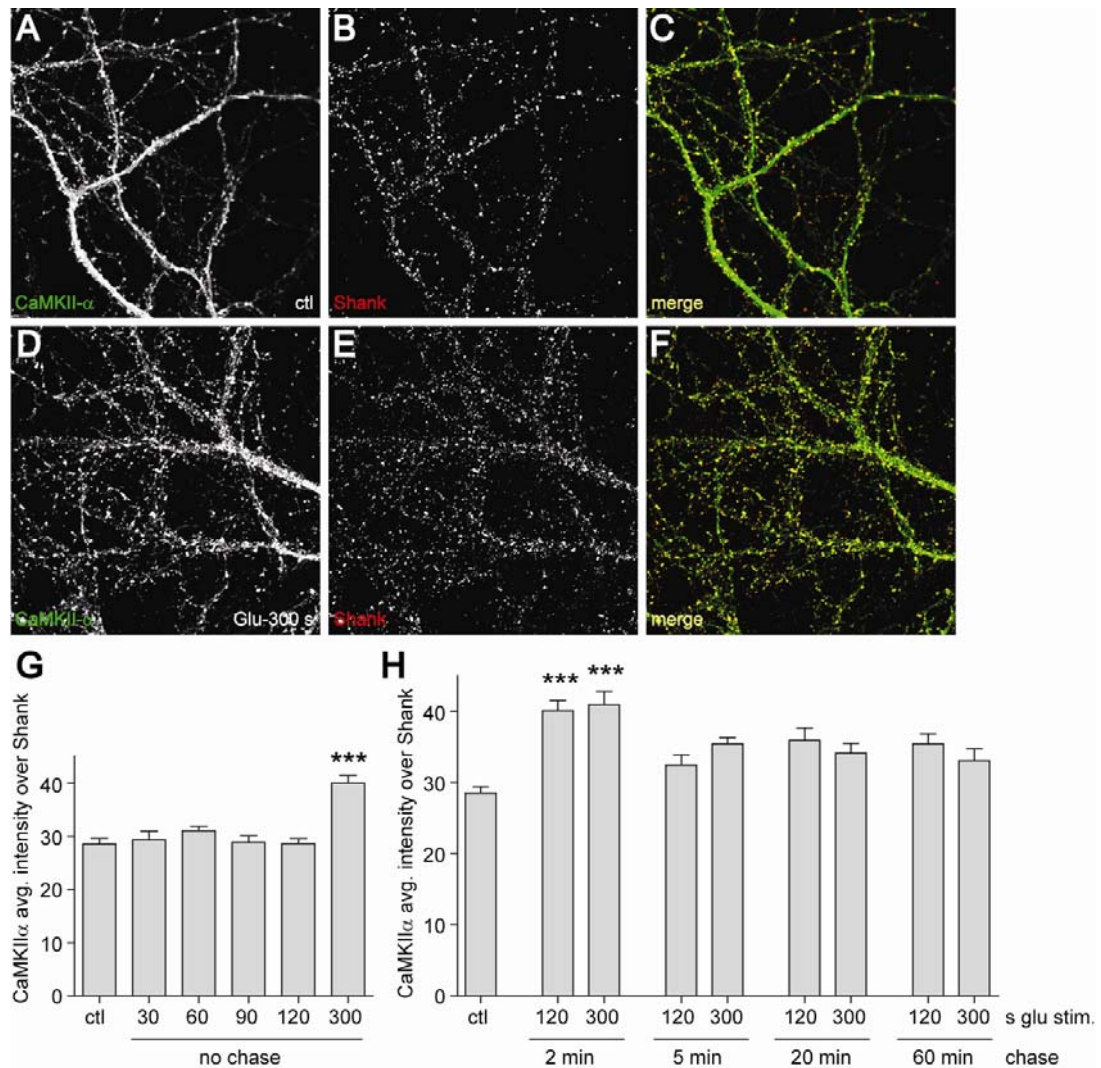


**Figure 3.11 CaMKII $\alpha$  redistribution is partially reversed after 5 min but shows a tendency to stay slightly enhanced up to 1 h.** Hippocampal cultures (18-21 DIV) were vehicle treated (ctl) or stimulated for the indicated time points with 100  $\mu$ M glutamate/10  $\mu$ M glycine. For the chase experiments the glutamate containing medium was removed, the cells shortly washed and chased for the indicated times. **(A-F)** Example pictures of vehicle treated control and glutamate stimulated cultures stained for CaMKII $\alpha$  (in green) and Shank (in red). **(G)** Analysis of CaMKII $\alpha$  fluorescence intensity in Shank positive areas after glutamate stimulation. **(H)** Analysis of CaMKII $\alpha$  fluorescence intensity of the stimulated and time chased cultures. Data represent mean  $\pm$  SEM. Statistical significance compared to ctl: one-way ANOVA with Tukey post test, \*\*\* $p$ <0.001.

### 3.2.6 Brief Stimulation with Glutamate is Sufficient to Induce CaMKII $\alpha$ Translocation

As translocation of CaMKII $\alpha$  was already observed after 2 min of glutamate stimulation followed by a 2 min chase period (Fig. 3.11 H), it was of interest to test whether a shorter application of glutamate is sufficient to

induce translocation during a subsequent chase. Straight stimulation with glutamate for 3 min resulted in a complete CaMKII translocation measured as a saturated increase of CaMKII fluorescence intensity at Shank positive puncta (Fig. 3.10 G). Accordingly, stimulation, washing and a 2.5 min chase period should give enough time for maximal redistribution.

Hippocampal cultures were stimulated with 100  $\mu$ M glutamate/10  $\mu$ M glycine, followed by immediate removal of the glutamate (1-5 s stimulation) or removal after 20-25 s (20-25 s stimulation), washing and a 2.5 min chase period before fixation. The brief stimulation for 1-5 s with glutamate was sufficient to induce the activity-dependent translocation of CaMKII to the PSD during a 2.5 min chase period. The redistribution was apparent as a change in the immunostaining of CaMKII $\alpha$  from a smoother and more dendritic staining under control conditions (Fig. 3.12 A-C) to a more clustered and synaptic (Shank overlapping) staining after stimulation (Fig. 3.12 D-I). Quantification of CaMKII $\alpha$  fluorescence intensity over the Shank mask showed a statistically significant increase of intensity after glutamate stimulation compared to control (vehicle treatment) conditions (Fig. 3.12 J).

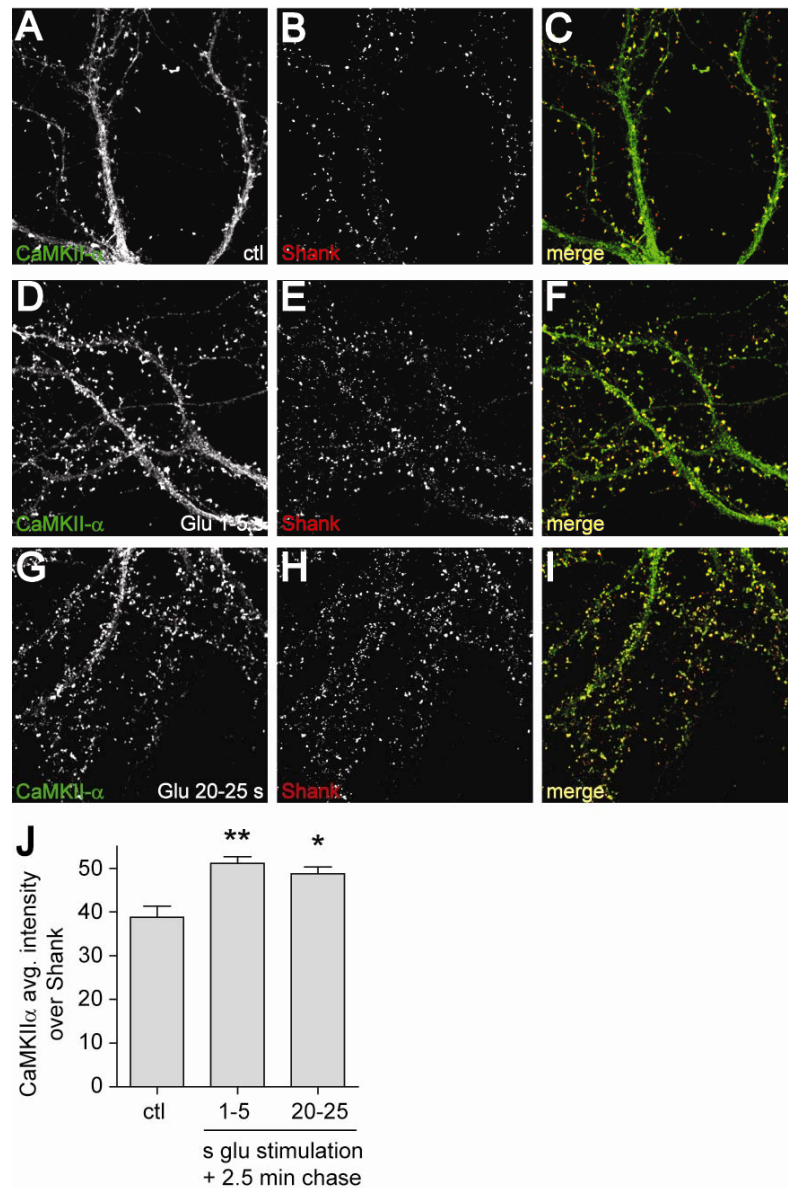


**Figure 3.12 Brief stimulation with glutamate is sufficient to induce CaMKII $\alpha$  translocation.** Hippocampal cultures were vehicle treated or stimulated with 100  $\mu$ M glutamate/10  $\mu$ M glycine by short application for 1-5 or 20-25 s, followed by a 2.5 min chase. **(A-I)** Depicted are example pictures of CaMKII $\alpha$  (green) and Shank (red) immunostained cultures for the different treatments. **(J)** Analysis of the CaMKII $\alpha$  fluorescence intensity in Shank positive puncta. Data represent mean  $\pm$  SEM. Statistical significance compared to control: one-way ANOVA with Tukey post test, \* $p$ <0.05, \*\* $p$ <0.01.

### 3.2.7 The Role of Neurogranin in the Activation and Translocation of CaMKII

Calcium influx through the NMDAR and the subsequent binding of CaM leads to the activation of CaMKII. The binding of Ca<sup>2+</sup>/CaM results in a conformational change that displaces the pseudosubstrate segment and the

T286 segment from the S- and T-site, respectively. This conformational change renders the kinase active and exposes the region around T286 to phosphorylation by the neighboring subunit and enables protein/protein interaction over the T-site, including the previously stated interaction with GluN2B (Hudmon and Schulman, 2002; Lisman et al., 2002; Merrill et al., 2005).

CaM is a ubiquitous and abundant  $\text{Ca}^{2+}$ -binding protein that mediates the calcium signal to numerous effectors including CaMKII. The consequences and downstream effects of the calcium signal are dependent on the localization and amount of the calcium influx, as well as the local availability of CaM.

Neurogranin (Ng) is a small neuron-specific apo-calmodulin-binding protein, enriched in the cortex and hippocampus (Baudier et al., 1991; Gerendasy and Sutcliffe, 1997; Represa et al., 1990). Ng is localized to the somatodendritic compartment and highly concentrated in dendritic spines (Neuner-Jehle et al., 1996; Watson et al., 1992). Binding to Ng and several other apo-CaM binding proteins such as the mainly presynaptic GAP43/neuromodulin keeps the level of free CaM low under resting conditions (Persechini and Stemmer, 2002; Tran et al., 2003). The binding of apo-CaM to Ng is mediated through an IQ motif in a calcium- and phosphorylation-dependent manner. An increase in the local calcium concentration as well as phosphorylation of S36 within the IQ motif results in dissociation of CaM (Baudier et al., 1991; Gerendasy et al., 1995; Huang et al., 2000). *In vivo* phosphorylation of S36 is mediated by  $\text{PKC}\gamma$  (Ramakers et al., 1999).

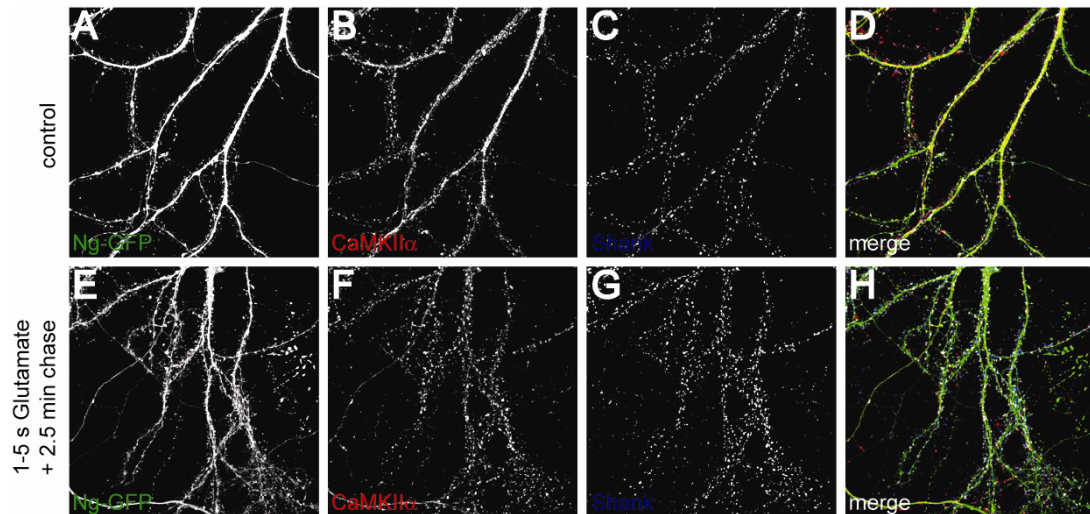
Ng mediated binding and sequestration of CaM in dendritic spines controls local CaM availability and  $\text{Ca}^{2+}$ /CaM signaling, which is important for synaptic plasticity. Based on this model, increased Ng fosters synaptic potentiation through elevated levels of bound apo-CaM, supplying more  $\text{Ca}^{2+}$ /CaM for postsynaptic signaling, with CaMKII being a central  $\text{Ca}^{2+}$ /CaM effector. Reduced Ng levels and subsequent lower CaM levels favor LTD inducing pathways that depend on PP2B. PP2B possesses a higher affinity for  $\text{Ca}^{2+}$ /CaM than CaMKII and is preferentially activated under CaM limiting

conditions (Diez-Guerra, 2010). Ng overexpression increases synaptic transmission and this potentiation is NMDAR and CaMKII dependent. Inactive Ng mutants fail to potentiate synaptic transmission and loss of postsynaptic CaM through Ng knock down prevents LTP induction (Zhabotinsky et al., 2006; Zhong et al., 2009). The Ng mutant null mice are deficient in spatial learning and display reduced levels of autophosphorylated autonomous active CaMKII (Miyakawa et al., 2001; Pak et al., 2000).

To assess the effect of Ng and thereby the local availability of CaM on the activity-induced translocation of CaMKII to synaptic sites, hippocampal cultures were transfected with various Ng constructs. The transfected cultures were vehicle treated or stimulated briefly with 100  $\mu$ M glutamate/10  $\mu$ M glycine, followed by immediate removal of the glutamate containing medium, washing and a 2.5 min chase period before fixation. The cultures were immunostained for CaMKII $\alpha$  and Shank and confocal images analyzed for glutamate induced changes in CaMKII $\alpha$  immunofluorescence intensity in Shank and GFP positive areas of transfected neurons. Untransfected cells were monitored as control for normal levels of activity-dependent CaMKII $\alpha$  redistribution. Example pictures of cultures transfected with WT Ng GFP-fusion protein (GFP is placed at the N-terminus) with and without (vehicle treated) glutamate stimulation are shown in Fig. 3.13 A-H. Besides WT Ng, hippocampal cultures were also transfected with various Ng mutants and Ng shRNA. The Ng-S/A mutant contains a S36 to A mutation, which still results in Ca<sup>2+</sup>-dependent dissociation of CaM, but the loss of inhibition of apo-CaM rebinding through PKC $\gamma$ . The Ng-S/D and Ng-SF/AW mutants function as dominant negative constructs due to their inability to bind or release CaM, respectively. The S36 to D mutation, mimics PKC $\gamma$  phosphorylation and is incapable of binding to CaM, while the F37 to W mutation renders Ng unable to release CaM with increasing calcium concentrations (Zhong et al., 2009). The F37W mutation was paired with the S36A in the SF/AW construct to further enhance apo-CaM binding by simultaneously preventing S36 phosphorylation. To silence Ng expression via RNA interference, a shRNA targeted against an intron in the mRNA sequence of Ng was transfected. Ng expression could be rescued by co-transfection of the Ng GFP-fusion protein

that lacks this intron. The Ng constructs were a generous gift from Dr. Nashaat Z. Gerges and have been described earlier (Zhong et al., 2009; Zhong et al., 2011).

The activity-induced changes in CaMKII $\alpha$  immunofluorescence intensity for each condition are expressed in % increase compared to the corresponding control/vehicle treated condition (Fig. 3.13 I). Brief stimulation of untransfected cells ( $32.00 \pm 3.53\%$ ), as well as stimulation of Ng-GFP ( $109.90 \pm 35.95\%$ ) and shRNA + Ng transfected cells ( $58.84 \pm 14.32\%$ ), the latter potentially both causing Ng overexpression, resulted in an increase of CaMKII $\alpha$  intensity. Knock down of Ng via shRNA ( $-7.69 \pm 10.00\%$ ) or expression of the dominant negative Ng-S/D ( $6.11 \pm 12.27\%$ ) and Ng-SF/AW ( $6.15 \pm 6.15\%$ ) constructs blocked the glutamate induced increase in intensity. Accordingly, Ng and with it the local activity-induced CaM availability are required for the activation-dependent translocation of CaMKII.



Glutamate-induced Change in CaMKII $\alpha$  avg. intensity in GFP and Shank pos. area

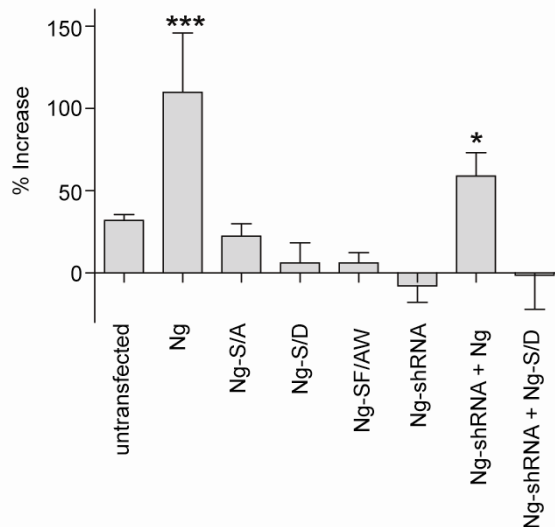


**Figure 3.13 The activation and activity-dependent translocation of CaMKII is dependent on neurogranin.** Hippocampal cultures were transfected with various Ng constructs, vehicle treated or briefly stimulated with 100  $\mu$ M glutamate/10  $\mu$ M glycine, followed by a 2.5 min chase. **(A-H)** Example pictures of CaMKII $\alpha$  (red) and Shank (blue) immunostained cultures transfected with WT Ng-GFP (green) with and without stimulation. **(I)** Analysis of the CaMKII $\alpha$  fluorescence intensity in the Shank positive puncta in the transfected cells (Shank and GFP positive) is depicted as % increase in CaMKII $\alpha$  immunofluorescence intensity compared to the corresponding vehicle treatment. Data represent mean  $\pm$  SEM. Statistical significance: one-way ANOVA with Tukey post test, \* $p$ <0.05, \*\*\* $p$ <0.001.

### 3.2.8 The Translocation of CaMKII is Independent of GluN1

CaMKII binds not only to GluN2B, but also GluN1 (Leonard et al., 2002; Leonard et al., 1999; Merrill et al., 2007; Strack and Colbran, 1998; Strack et al., 2000a). Binding to GluN2A also has been reported (Gardoni et

al., 1998; Gardoni et al., 1999), but appears to be rather weak and often undetectable (Leonard et al., 2002; Leonard et al., 1999; Strack et al., 2000a). Peptide binding studies identified residues 845-861 in the C0 region in the C-terminus of GluN1 as a CaMKII $\alpha$  binding site of good affinity (Leonard et al., 2002; Merrill et al., 2007). Modeling of this binding site on GluN1 showed that residues Q849 and N856 are part of a putative  $\alpha$ -helix with their side chains reaching in the same directions. Introduction of point mutations and further peptide binding and displacement studies revealed that the association of CaMKII with the GluN1 subunit is abrogated by the two point mutations Q849E and N856E, while binding of CaM and  $\alpha$ -actinin, which interact with the same segment (Akyol et al., 2004; Leonard et al., 2002; Merrill et al., 2007), was unaffected (Leonard and Hell unpublished data).

Based on this information GluN1 KI mice were generated in collaboration with Dr. Nils Brose introducing 3 base pair mutations resulting in the Q849E and N856E mutations, as well as deletion of a PvuII restriction site for diagnostic purposes. The GluN1 KI mice do not show any obvious phenotype with regard to appearance, LTP or learning and memory (Dallapiazza and Hell unpublished data). Hippocampal cultures from these mice were stained for pre- and postsynaptic marker proteins to establish a normal synaptic morphology. Staining for the presynaptic marker Synapsin and the postsynaptic scaffolding protein PSD-95 showed no difference between WT and GluN1 KI hippocampal cultures (Fig. 3.14 A-F) and displayed the same degree of co-localization (Fig. 3.14 M), measured as the correlation of the intensity distribution between the channels (Pearson's coefficient). Furthermore the staining for the presynaptic vesicular glutamate transporter 1 (VGLUT1) and the presynaptic cytomatrix protein Bassoon revealed no difference between the genotypes (Fig. 3.14 G-L). Analysis of the Pearson's coefficient indicated the expected high correlation between the two presynaptic proteins (Fig. 3.14 M).

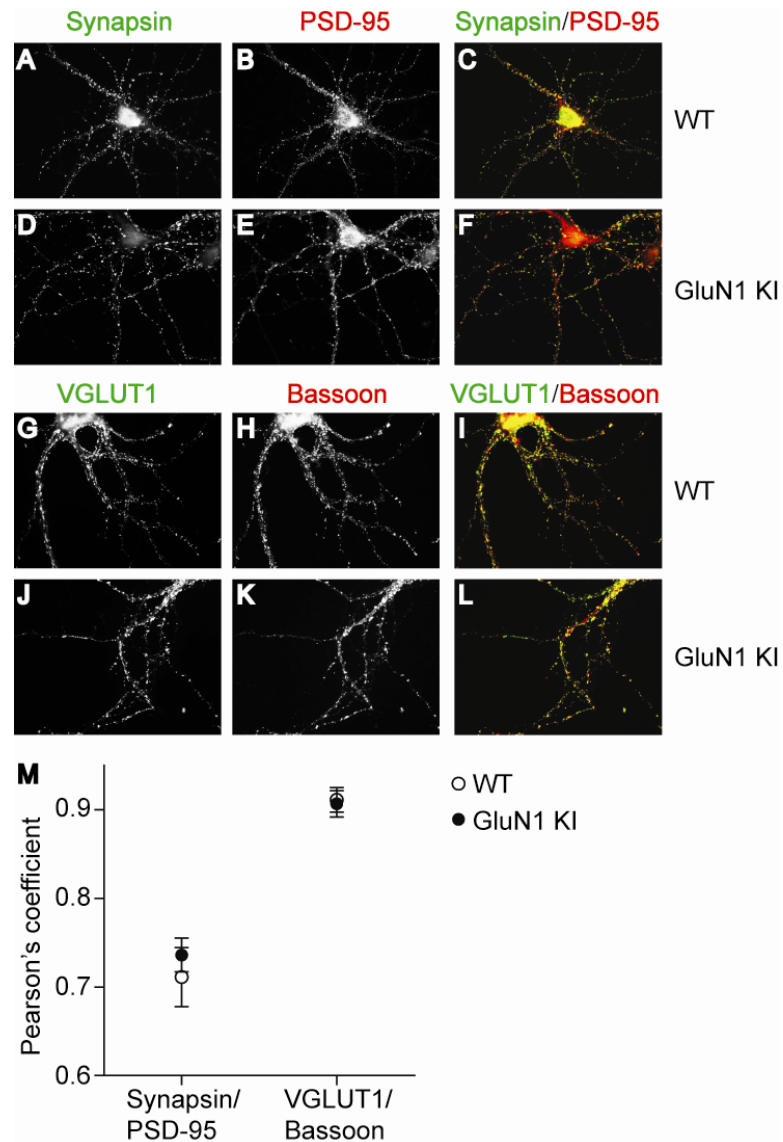


**Figure 3.14 Hippocampal cultures from GluN1 KI show a similar distribution of pre- and postsynaptic markers.** (A-F) Hippocampal cultures (DIV18-21) from WT and GluN1 KI P0 pups were stained with anti-Synapsin (green in overlay) and anti-PSD-95 (red in overlay) antibodies and labeled with Alexa fluor-coupled secondary antibodies. (G-L) WT and GluN1 KI hippocampal cultures (DIV 18-21) were immunostained for VGLUT1 and Bassoon and labeled with Alexa fluor-coupled secondary antibodies. (M) The Pearson's coefficient shows correlation of the intensity distribution between the channels of the presynaptic marker Synapsin and the postsynaptic marker PSD-95 and the expected higher degree of correlation for the two presynaptic markers VGLUT1 and Bassoon.

After a normal synaptic morphology was established, the activity-dependent redistribution of endogenous CaMKII $\alpha$  was investigated. The hippocampal cultures were vehicle treated or stimulated for 5 min with 100  $\mu$ M glutamate/10  $\mu$ M glycine. CaMKII $\alpha$  showed for both WT and GluN1 KI a smooth distribution under control/vehicle treated conditions (Fig. 3.15 A-F)

and was shifted to a clustered more punctate distribution after glutamate stimulation (Fig. 3.15 G-L). Analysis of the Pearson's coefficient revealed an increase in the correlation between the CaMKII $\alpha$  and the Synapsin signal after glutamate stimulation (Fig. 3.15 M;  $p < 0.001$ , two-way ANOVA), highlighting the redistribution of CaMKII $\alpha$  to synaptic sites, but no difference between the two genotypes ( $p = 0.9282$ ).

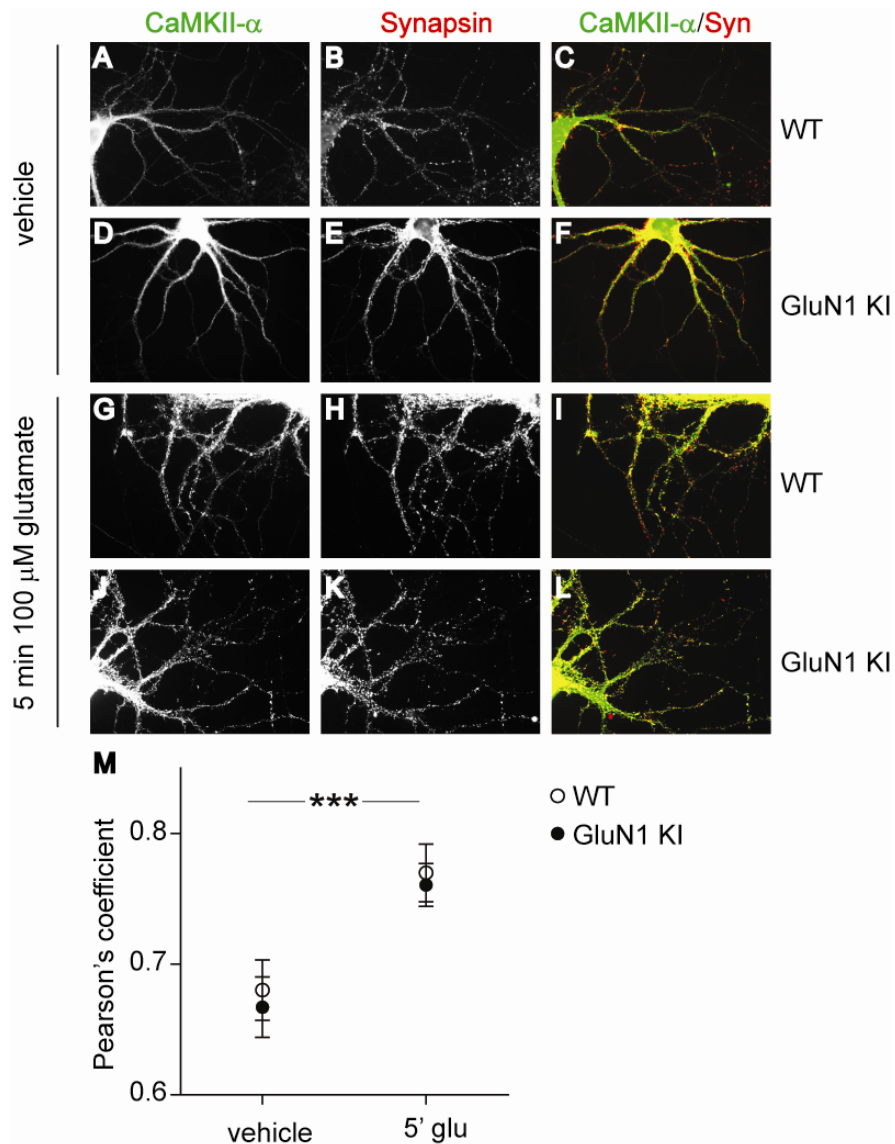


**Figure 3.15 Normal activity-dependent redistribution of CaMKII $\alpha$  in hippocampal cultures from GluN1 KI mice.** Hippocampal cultures (DIV18-21) from WT and GluN1 KI P0 pups were stained for CaMKII $\alpha$  (green in overlay) and Synapsin (red in overlay) with anti-CaMKII $\alpha$  and anti-Synapsin antibodies and Alexa fluor-labeled secondary antibodies. The cultures were vehicle treated (A-F) or stimulated for 5 min with 100  $\mu$ M glutamate/10  $\mu$ M glycine (G-L). (M) The Pearson's coefficient showed a significant increase of correlation between the CaMKII $\alpha$  and Synapsin signal after glutamate (glu) stimulation ( $p < 0.001$ , two-way ANOVA with Bonferroni post-test), but no difference between the genotypes.

### 3.3 PKA-dependent Regulation of the NMDAR

Calcium influx through the NMDAR is not only essential for synaptic plasticity, the amount and dynamics of calcium influx also determines whether LTP or LTD will be induced. Therefore the activity-dependent modulation of calcium signaling through the NMDAR is a fast and effective way for bi-directional modification of synaptic plasticity. It has been shown that phosphatase inhibitors as well as direct activation of PKA can increase NMDAR currents (Wang et al., 1994; Westphal et al., 1999) and Zukin and colleagues demonstrated that PKA specifically regulates the calcium permeability of the NMDAR and thereby the induction of LTP (Skeberdis et al., 2006). Stimulating PKA activity through  $\beta$ -adrenergic receptors or the D<sub>1</sub>/D<sub>5</sub> dopamine receptors increased NMDAR currents and facilitated the induction of LTP (Otmakhova and Lisman, 1996; Raman et al., 1996; Thomas et al., 1996).

The exact phosphorylation site of PKA on the GluN2B subunit was recently identified as serine 1166 by Suzanne Zukin and Jessica Murphy. It was shown that mutation of this serine residue to an alanine completely abrogated the PKA-dependent increase in NMDAR current and calcium permeability (Murphy and Zukin unpublished data). The results presented here characterize a custom made phospho-specific S1166 antibody and describe the regulation of this new phosphorylation site using the phospho-specific S1166 antibody.

#### 3.3.1 PKA Induces phosphorylation of GluN2B S1166 *In Vitro*

The GST-tagged GluN2B C-terminus was expressed in *E. coli*, purified on glutathione Sepharose, and phosphorylated by PKA. The *in vitro* phosphorylation resulted in strong phospho-S1166 probing, which is completely absent in the vehicle treated control (Fig. 3.16 A). GluN2B IPs from brain lysate revealed basal phosphorylation of S1166 in the CNS. Treatment of the GluN2B IPs with calf intestinal phosphatase (CIP) or homogenization of the brain lysate without the presence of phosphatase inhibitors caused dephosphorylation of S1166. *In vitro* phosphorylation with

PKA on the other hand strongly increased S1166 phosphorylation levels. The total (phosphorylation independent) GluN2B probings showed equal amounts of GluN2B over the different conditions (Fig. 3.16 B). Incubation with the primary phospho-S1166 antibody in the presence of the phospho-peptide, the antibody was derived against, demonstrated the specificity of the phospho-specific S1166 antibody (Fig. 3.16 B). The quantification of three independent experiments of *in vitro* treated GluN2B IPs from brain lysates is shown in Fig. 3.16 C. PKA phosphorylation resulted in a 5 fold increase of the phospho-S1166 signal, normalized against total GluN2B levels and compared to control. Dephosphorylation either *in vitro* or by the endogenous phosphatases after homogenization completely removed S1166 phosphorylation.

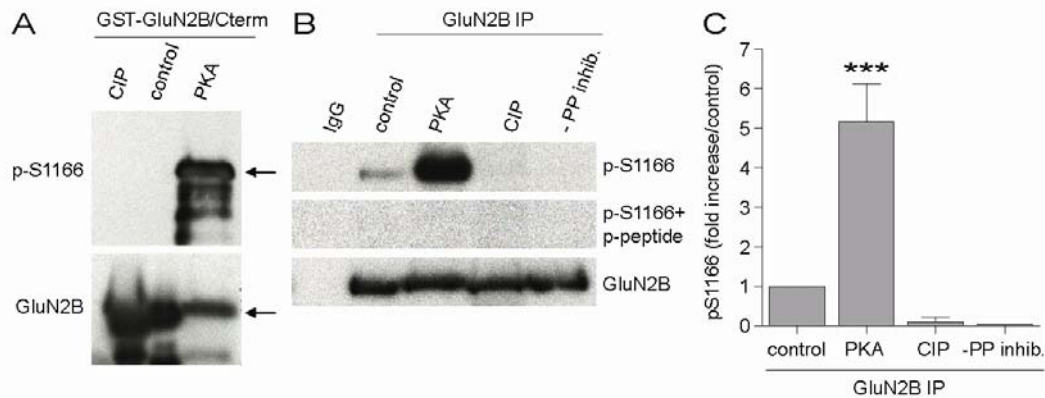


**Figure 3.16 Characterization of the phospho-specific antibody against GluN2B phosphoS1166 and PKA induced phosphorylation of S1166.** (A) PKA *in vitro* phosphorylation of a purified GST-GluN2B C-terminal fusion protein on S1166. (B) GluN2B IPs from brain lysates showed basal phosphorylation of S1166 *in vivo*. PKA *in vitro* phosphorylation increased the S1166 phosphorylation and CIP treatment or the absence of phosphatase inhibitors resulted in dephosphorylation of S1166. Incubation of the p-S1166 antibody with the phospho-peptide used to generate the antibody blocked the signal and illustrates the specificity of the antibody. (C) Quantification of the phosphorylation levels (of 3 independent experiments of the example shown in B) revealed a ~5 fold increase in S1166 phosphorylation after treatment with PKA and the complete absence of any signal after dephosphorylation. Data represent mean  $\pm$  SEM. Statistical significance: one-way ANOVA with Tukey post test, \*\*\* $p < 0.001$ .

### 3.3.2 Phosphorylation of S1166 is Enriched in the PSD

To evaluate whether GluN2B undergoes phosphorylation at postsynaptic sites, PSDs were prepared by differential centrifugation and sucrose density centrifugation. The postsynaptic scaffolding protein PSD-95

and Synaptophysin, a small integral protein of synaptic vesicles and a presynaptic marker, confirmed the purity of the PSD preparation. PSD-95, along with the NMDAR and the phospho-S1166 signal, showed a clear enrichment in the PSD over the total input (Lys), the synaptic membrane enriched (P2) pellet and the synaptosome enriched (Syn) fraction, whereas Synaptophysin was absent in the PSD (Fig. 3.17). The high phosphorylation levels of S1166 in the PSD along with the enriched NMDAR argue for a functional role of this phosphorylation in the bidirectional modification of the NMDAR.

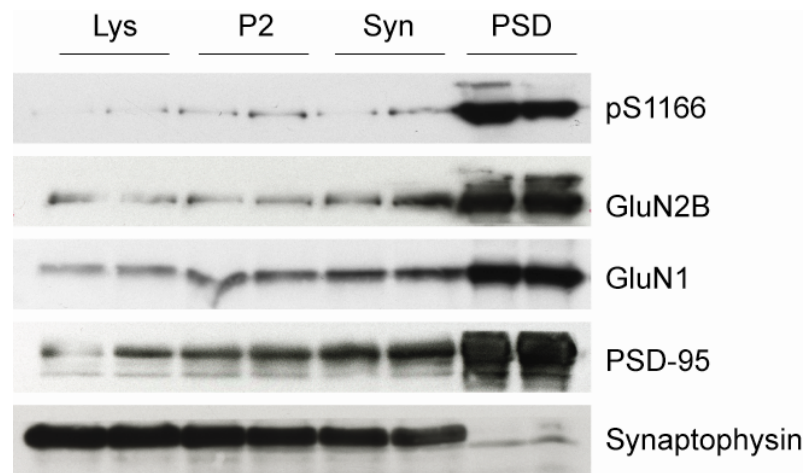


**Figure 3.17 S1166 phosphorylation is enriched in the PSD.** Postsynaptic densities were purified out of brain, separated by SDS-PAGE and immunoprobed for phospho-S1166, GluN2B, GluN1, PSD-95 and Synaptophysin. The phospho-S1166 signal as well as GluN2B, GluN1 and PSD-95 were enriched in the PSD. The presynaptic protein Synaptophysin was completely absent in the PSD and illustrates the purity of the PSD fraction (Lys: Lysate/Input, P2: membrane fraction, Syn: synaptosome enriched fraction, PSD: postsynaptic density).

### 3.3.3 $\beta$ -Adrenergic-Receptor Stimulation of Acute Forebrain Slices Increases S1166 Phosphorylation

To elucidate how S1166 phosphorylation is regulated, potential pathways involved in the modulation of PKA activity and NMDAR function were next investigated. Activation of the  $\beta$ -adrenergic receptor ( $\beta$ AR) has been previously shown to enhance NMDAR currents, lower the threshold for LTP induction and upregulate PKA phosphorylation of S845 on the GluA1 subunit during emotional stress (Hu et al., 2007; Raman et al., 1996; Thomas et al., 1996). Treatment of acute forebrain slices with isoproterenol, a  $\beta$ AR

agonist resulted not only in phosphorylation of S845 on the GluA1 subunit, but also of S897 on the GluN1 subunit as well as S1166 on GluN2B (Fig. 3.18 A). S897 is a PKA phosphorylation site on GluN1 important for suppression of ER retention and forward trafficking of the NMDAR (Scott et al., 2003). The isoproterenol induced PKA phosphorylation was in all cases (S845, S1166 and S897) significantly increased (one-way ANOVA with Tukey post test,  $p < 0.001$ ), and blocked by co application of the  $\beta$ AR antagonist propranolol (Fig. 3.18 B).

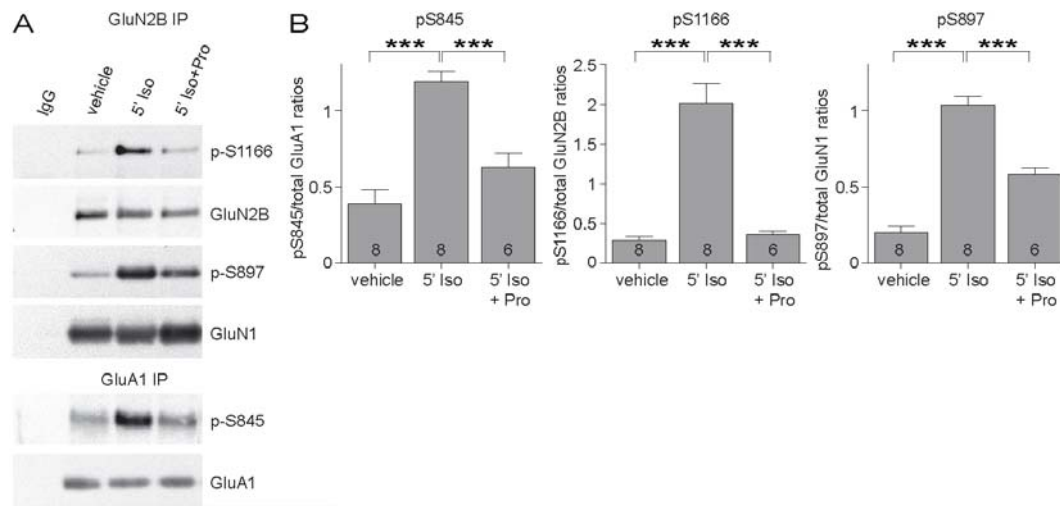


**Figure 3.18 Isoproterenol/ $\beta$ AR stimulation increases S1166 phosphorylation. (A)** Acute forebrain slices were vehicle treated and stimulated with 1  $\mu$ M isoproterenol for 5 min in the absence and in the presence of the  $\beta$ AR antagonist propranolol (1  $\mu$ M). The treated slices were solubilized with 1% deoxycholate, cleared by ultracentrifugation and GluN2B and subsequently GluA1 immunoprecipitated. The IPs were probed for phospho-S1166, GluN2B, phospho-S897, GluN1, phospho-S845 and GluA1. **(B)** Quantification of the isoproterenol induced increase in S845, S1166 and S897 phosphorylation, corrected against total receptor subunit levels and expressed as increase over vehicle treatment. Co-application of the  $\beta$ AR antagonist propranolol (1  $\mu$ M) prevented the isoproterenol induced phosphorylation. Data represent mean  $\pm$  SEM. Statistical significance: one-way ANOVA with Tukey post test, \*\*\* $p < 0.001$ .

### 3.3.4 $\beta$ -Adrenergic-Receptor Stimulation-induced Increase of S1166 Phosphorylation is Independent of AKAP150

PKA is targeted to specific compartments by A-kinase anchoring proteins (AKAPs). AKAPs tether the inactive PKA holoenzyme in proximity to their substrates, where PKA activity is regulated by local changes in cAMP levels. The NMDAR is linked to PKA activity through two different AKAPs,

Yotiao and AKAP150. Yotiao directly interacts with the C-terminus of GluN1, while AKAP150 (AKAP5) is indirectly linked to the GluN2 subunits via PSD-95 (Colledge et al., 2000; Sanderson and Dell'Acqua, 2011; Wong and Scott, 2004). To investigate whether AKAP5 anchored PKA is important for the regulation of S1166, we utilized AKAP5 knock-out and AKAP5 mutant mice (D36). D36 mice lack only the PKA anchoring site through deletion of the last 36 amino acid residues. This truncation does not interfere with AKAP5 anchoring of PP2B and PKC and should avoid potential indirect compensatory mechanisms due to the complete loss of AKAP5 in the KO. Acute forebrain slices from AKAP5 KO, D36 and WT mice were prepared and stimulated with isoproterenol. As before,  $\beta$ AR activation with isoproterenol resulted in a propranolol-sensitive increase in phosphorylation of S1166 observed with the phospho-specific S1166 antibody after GluN2B IP (Fig. 3.19 A). The isoproterenol induced increase in S1166 phosphorylation was quantified by densitometric measurements of the phospho-S1166 intensity, normalized to total GluN2B and expressed as increase over vehicle treatment (Fig. 3.19 B). Analysis revealed a ~6 fold increase in S1166 phosphorylation with isoproterenol stimulation and no difference in the phosphorylation levels between AKAP5 KO, D36 and WT (Fig. 3.19 B). Based on these findings AKAP5 is not absolutely essential if at all contributing to the isoproterenol induced phosphorylation of S1166 and targeting PKA to the NMDAR.

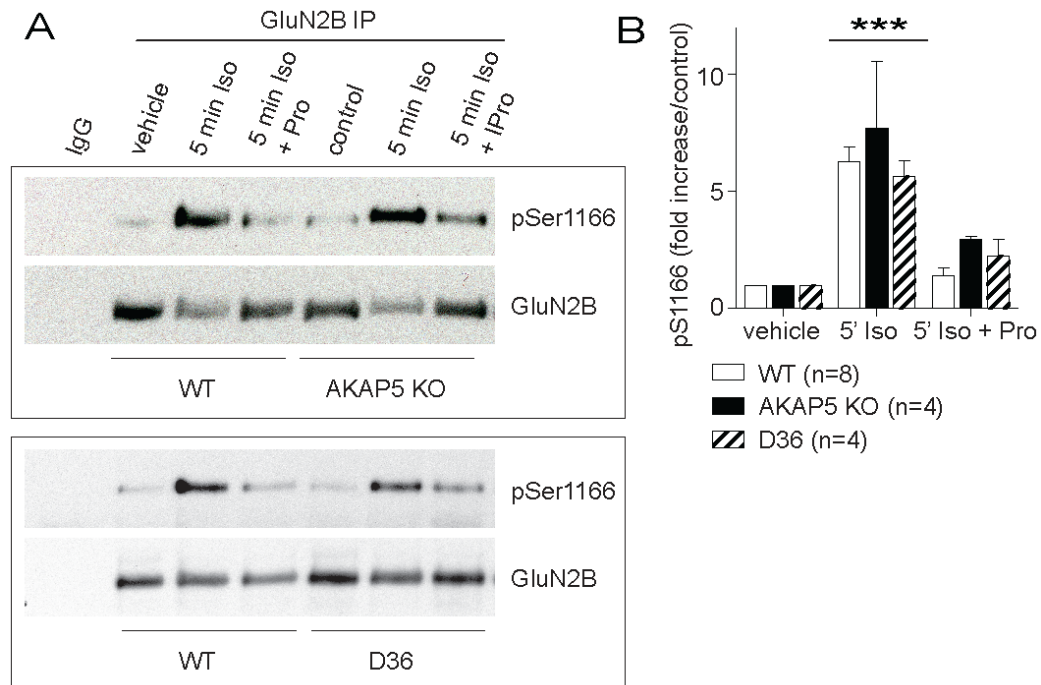


**Figure 3.19 Isoproterenol induced S1166 phosphorylation is independent of AKAP150.** (A) Acute forebrain slices from WT, AKAP5 KO and D36 mice were stimulated with vehicle, 1  $\mu$ M isoproterenol or isoproterenol + 1  $\mu$ M propranolol for 5 min. Stimulation with isoproterenol showed increased S1166 phosphorylation after a GluN2B IP for all genotypes, which can be blocked by co application of propranolol. (B) Quantification of the phospho-S1166 signal corrected for total GluN2B levels showed a significant increase in S1166 phosphorylation levels upon isoproterenol stimulation compared to vehicle treatment, but no difference between the genotypes. Data represent mean  $\pm$  SEM. Statistical significance: one-way ANOVA with Tukey post test,  $p < 0.001$ .

### 3.3.5 Forced Swim Stress Induces S1166 Phosphorylation *In Vivo*

To demonstrate PKA modulation of the NMDAR *in vivo*, stress-dependent S1166 phosphorylation in the hippocampus was investigated. Phosphorylation of S845 of the GluA1 subunit of the AMPAR is enhanced by emotional stress elicited by exposure to fox urine (Hu et al., 2007). For analysis of S1166 phosphorylation the forced swim-induced stress model was used. This stress should cause a strong and reliable response, far beyond the stress due to handling and exposure to a new environment. The forced swim was conducted with rats (male Sprague Dawley rats, age  $\sim$ P30) for 5 min in water at a temperature of 18-19  $^{\circ}$ C. After forced swim animals were sacrificed, hippocampi isolated and shock frozen for later biochemical analysis. The forced swim and hippocampal isolation were conducted by Jessica Murphy in Suzanne Zukin's laboratory and the biochemical and data

analysis of the receptor phosphorylation was performed by Sebastian Ivar Stein.

Forced swim-induced stress increased the phosphorylation of S1166, S897 and S845 in the hippocampus compared to control treated animals. The NMDARs and AMPARs were extracted with 1% deoxycholate, the homogenate cleared by ultracentrifugation and after GluN2B IP and subsequent GluA1 IP analyzed for phosphorylation by PKA with the phospho-specific antibodies (Fig. 3.20 A). Densitometric measurements and correction for total receptor levels revealed a significant increase in forced-swim induced phosphorylation, compared to control treated animals, for S1166, S845 and S897 (Fig. 3.20 B).

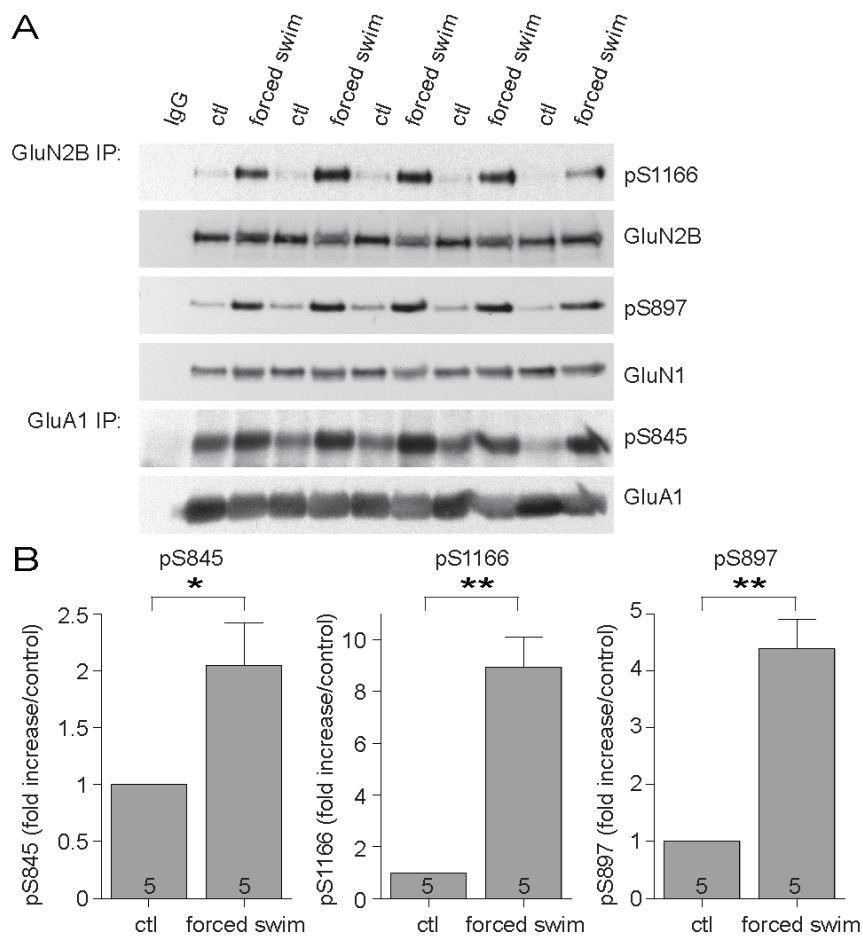


**Figure 3.20 Forced swim-induced stress increases S1166 phosphorylation.** Isolated hippocampi from control or forced swim stressed animals were solubilized with 1% deoxycholate, cleared by ultracentrifugation and GluN2B and subsequently GluA1 immunoprecipitated. **(A)** WB analysis of the hippocampal phosphorylation levels of S1166, S897 and S845 with the phosphospecific antibodies as well as total receptor probings. (continued on next page)

(Figure 3.20 continued) **(B)** Quantification of the phospho signals normalized to the total amount of receptor subunit and expressed as forced swim induced increase over control. Data represent mean  $\pm$  SEM. Statistical significance: two-tailed paired t-test, \* $p < 0.05$ , \*\* $p < 0.01$ .

### 3.3.6 I.P. Injection of Propranolol Reduces Forced Swim-induced Phosphorylation of S845 but not S1166

The  $\beta$ AR antagonist propranolol counteracted in acute slices the isoproterenol induced increase in phosphorylation of S1166, S897 and S845 (Fig. 3.18), and reduced *in vivo* the increase in S845 phosphorylation due to emotional stress (Hu et al., 2007). To investigate whether propranolol is also able to counteract the forced swim-induced S845 (as well as S897) and, most interestingly, the S1166 phosphorylation rats were injected intraperitoneal (i.p.) with propranolol 30 min before conducting the forced swim (as before, the forced swim treatment was carried out by Jessica Murphy and the analysis of the hippocampal phosphorylation levels as well as data analysis was conducted by Sebastian Ivar Stein). WB analysis revealed an increase in phosphorylation for all three PKA phosphorylation sites under forced swim conditions. Propranolol inhibited overall phosphorylation levels of S845 with no effect on S1166 and intermediate effects on S897 (Fig. 3.21 A). Notably, analysis of the phospho-signal intensities showed the same degree of forced swim-induced increase in phosphorylation after propranolol injection, even for S845 (Fig. 3.21 C). Comparison of only the ratios of phospho signal/total receptor signal illustrated that this effect is due to a decrease in basal phosphorylation of S845 after propranolol injection (compared to saline injection). The forced swim induced S845 phosphorylation after propranolol injection was not higher than basal phosphorylation levels in saline injected control animals (Fig. 3.21 B). The reduction in basal phosphorylation after propranolol injection masked this effect if only the levels of increase in phosphorylation are compared (Fig. 3.21 C). In other words: propranolol decreased basal S845 phosphorylation levels as well as forced swim-induced absolute increases in S845 phosphorylation by 50%. For S1166 phosphorylation, neither the overall increase of phosphorylation, nor the raw ratios of phospho signal/total receptor signal were affected. S897 showed a tendency towards reduced phosphorylation under basal and forced swim

conditions, as seen for S845, but the results were not clear and the difference not statistically significant.

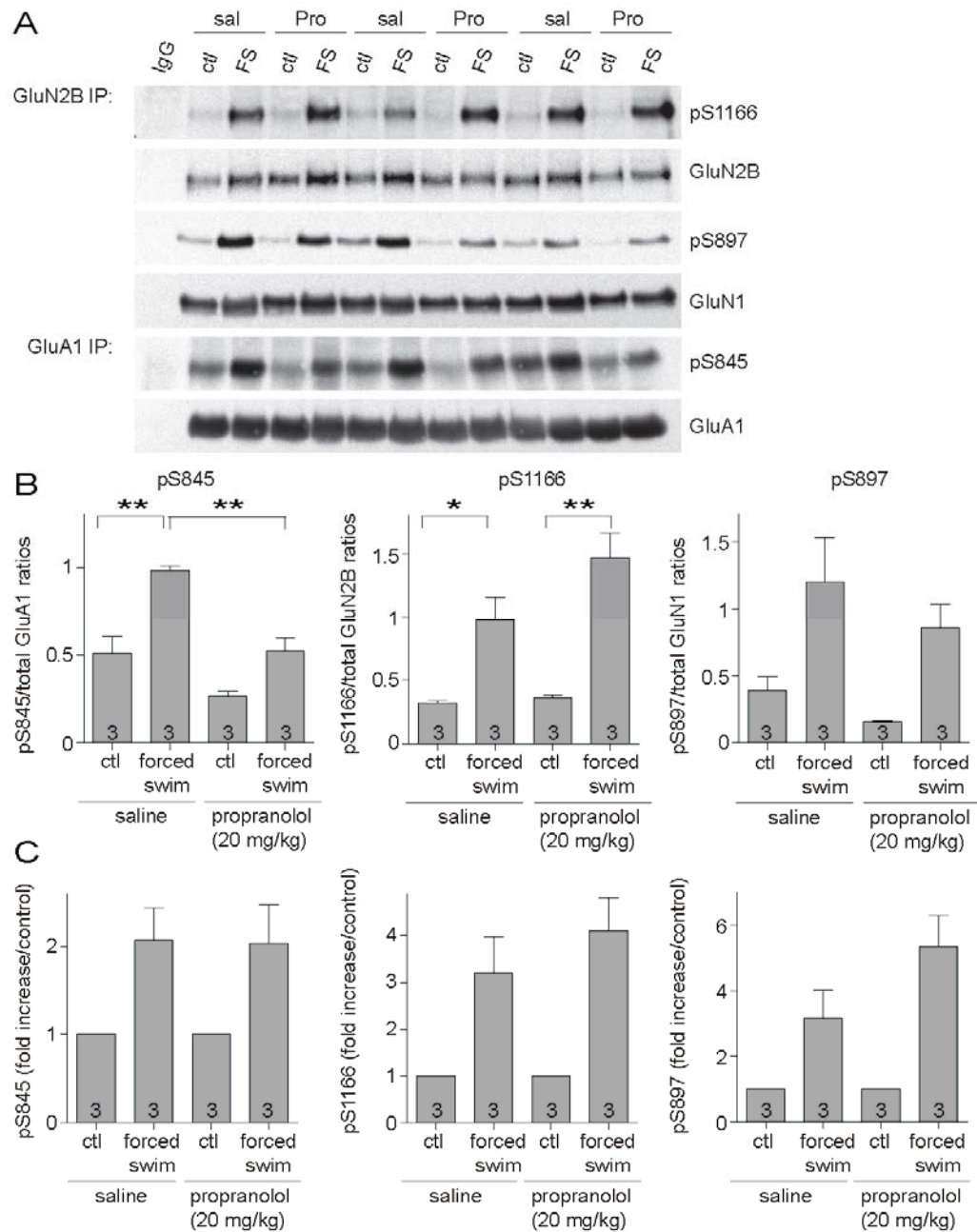


**Figure 3.21 I.p. injection of propranolol inhibits forced swim induced phosphorylation of S845, but not S1166. (A)** WB analysis of the hippocampal phosphorylation levels of controls and forced swim stressed animals. The GluN2B IPs were probed for phospho-S1166, GluN2B, phospho-S897 and GluN1 and the GluA1 IPs for phospho-S845 and GluA1. **(B)** Quantification of the overall phosphorylation levels. The changes in phosphorylation levels over the different conditions were expressed as phospho-signal ratios, corrected for differences in total receptor levels. Propranolol injection only reduced phosphorylation of S845 under basal (ctl) and forced swim (FS) conditions. (continued on next page)

(Figure 3.21 continued) **(C)** Quantification of the phospho signals normalized to the total amount of receptor subunit and expressed as forced swim induced increase over control. Data represent mean  $\pm$  SEM. Statistical significance: one-way ANOVA with Tukey post test, \* $p < 0.05$ , \*\* $p < 0.01$ .

### 3.3.7 D<sub>1</sub>/D<sub>5</sub> Receptor Stimulation of Acute Forebrain Slice Induces S1166 Phosphorylation

The fact that propranolol only blocked the forced swim induced increase in S845 phosphorylation and not S1166 could be due to the fact that this phosphorylation site is regulated by multiple G<sub>s</sub> protein coupled receptors (GPCRs) under stressful conditions. Blocking only one of them might not be sufficient to cause detectable differences in S1166 phosphorylation; even S845 phosphorylation levels in the presence of propranolol were still increased by forced swim-induced stress compared to the reduced basal levels (Fig. 3.21).

Stress results in a series of changes in neurotransmitter levels including norepinephrine, dopamine and serotonin (Hayley et al., 2001). Because D<sub>1</sub>/D<sub>5</sub> dopamine receptor stimulation enhanced early LTP (Otmakhova and Lisman, 1996), as well as the S845 phosphorylation in nucleus accumbens cultures and the GluA1 surface expression in hippocampal cultures (Chao et al., 2002; Gao et al., 2006), the effect of dopamine on S1166 phosphorylation was investigated.

Acute forebrain slices were stimulated with the D<sub>1</sub>/D<sub>5</sub> agonist SKF81297 (SKF) for different time points (0.5, 2, 5 and 15 min) and the amount of S845, S897 and S1166 phosphorylation after a GluN2B and GluA1 IP was investigated. Treatment with SKF resulted in a significant increase in S845 and S1166 phosphorylation after 15 min with a tendency to enhanced phosphorylation levels after 5 min. This increase was blocked by the D<sub>1</sub>/D<sub>5</sub> receptor antagonist SCH23390 (SCH) (Fig. 3.22 A). Quantification of the WB signals (phospho signals normalized to total receptor subunit) revealed a 2-3 fold increase in S845 phosphorylation compared to control and a 2 fold increase in S1166 (Fig. 3.22 B, C). S897 showed a tendency to increased phosphorylation after D<sub>1</sub>/D<sub>5</sub> receptor stimulation, but did not reach statistical significance (Fig. 3.22 B, C).

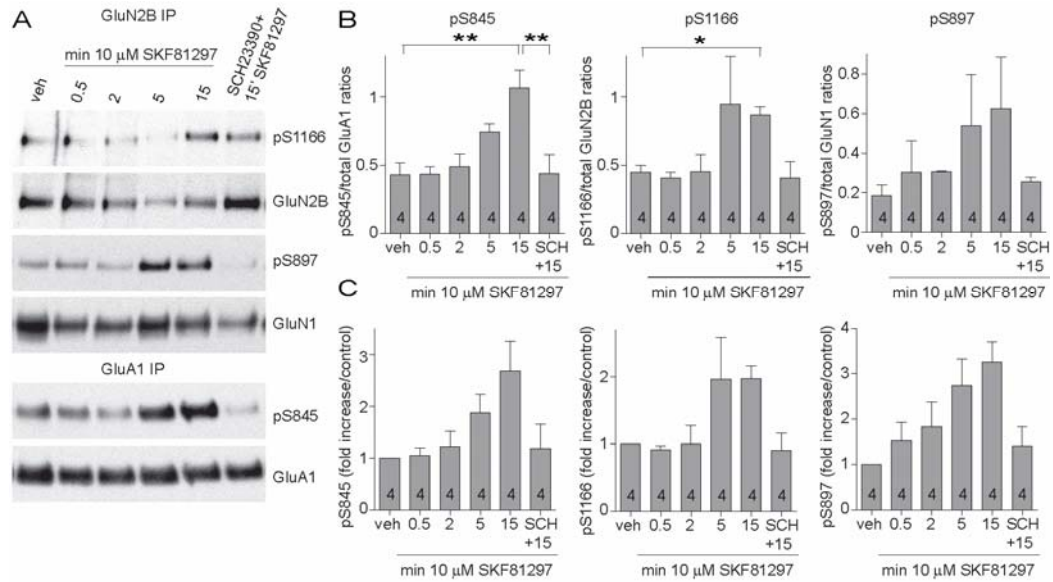


**Figure 3.22 D<sub>1</sub>/D<sub>5</sub> receptor stimulation increases S1166 phosphorylation.** (A) Acute forebrain slices were treated with vehicle, 10  $\mu$ M SKF81297 or a combination of 10  $\mu$ M SKF81297 and 5  $\mu$ M SCH23390 for the indicated time points. The treated slices were solubilized with 1% deoxycholate, cleared by ultracentrifugation and GluN2B as well as GluA1 subsequently immunoprecipitated. The representative example blots show an increase in S845 and S1166 phosphorylation detected with the phospho-specific antibodies. (B, C) Quantification of the immunosignals of the phospho-S845, S1166 and S897, corrected for variations in total receptor levels (B) and expressed as fold increase over vehicle treatment (C). Data represent mean  $\pm$  SEM. Statistical significance: one-way ANOVA with Tukey post test, \* $p$ <0.05, \*\* $p$ <0.01.

### 3.3.8 I.P. Injection of the D<sub>1</sub>/D<sub>5</sub> Receptor Antagonist SCH23390 does not Reduce Forced Swim-induced Phosphorylation

The D<sub>1</sub>/D<sub>5</sub> receptor antagonist SCH23390 was injected i.p. 30 min before forced swim. The SCH injection neither reduced any of the monitored basal phosphorylation levels in the control animals nor any of the forced swim induced increases in phosphorylation. WB probing for the phospho-specific antibodies against S845, S1166 and S897 showed no difference between saline and SCH injection in the hippocampus of either the control or forced swim stressed rats (Fig. 3.23 A). Quantification of the signal intensities with correction for variations in total receptor levels showed a significant increase in phosphorylation of S845, S1166 and S897 after forced swim-induced stress, but no effect of drug injection (Fig. 3.23 B, C).

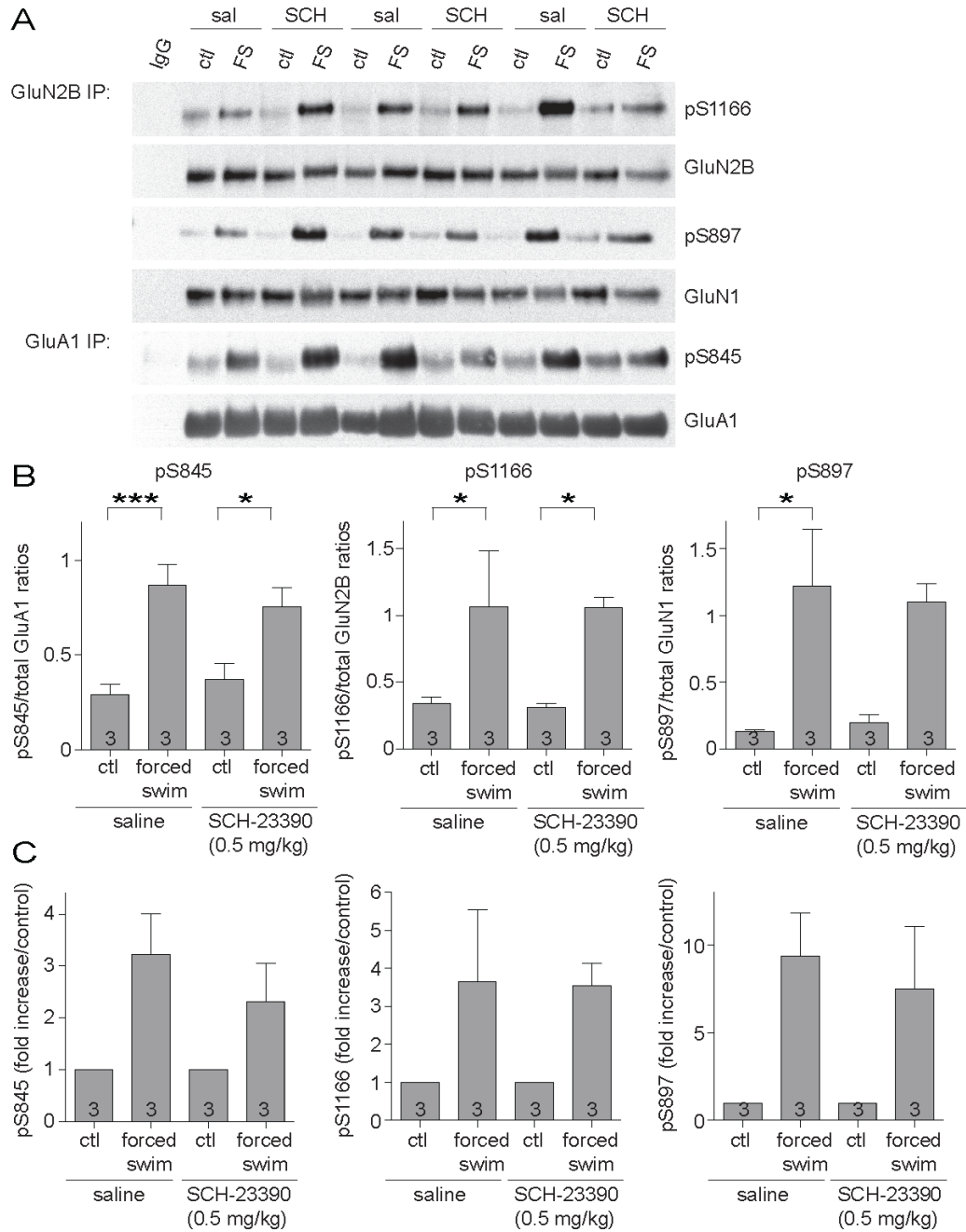


**Figure 3.23 I.p. injection of SCH23390 has no effect on forced swim-induced phosphorylation. (A)** WB analysis of the saline and SCH injected control and forced swim stressed rat hippocampi with phospho-specific antibodies for S1166, S897 and S845. **(B, C)** Quantification of the phospho-signal intensities corrected for differences in total receptor subunit levels (B), and expressed as increase in phosphorylation after forced swim stress compared to control (C). Data represent mean  $\pm$  SEM. Statistical significance: one-way ANOVA with Tukey post test, \* $p < 0.05$ , \*\*\* $p < 0.001$ .

### 3.3.9 A Combination of the Antagonists Propranolol and SCH23390 Reduces Basal Phosphorylation Levels of S1166 *In Vivo*

Since the  $\beta$ AR antagonist propranolol and the  $D_1/D_5$  receptor antagonist SCH23390 alone did not have any effect on S1166 phosphorylation *in vivo*, a combination of both drugs was injected i.p. WB analysis of the GluN2B IPs, from the isolated hippocampi, with the phospho-specific S1166 antibody showed a reduction in basal phosphorylation (Fig. 3.24 A). Densitometric analysis of the signal intensities, corrected for variations in the amount of total receptor, revealed a significant (two-tailed paired t-test,  $p=0.01$ ) decrease in S1166 basal phosphorylation levels (Fig. 3.24 B).

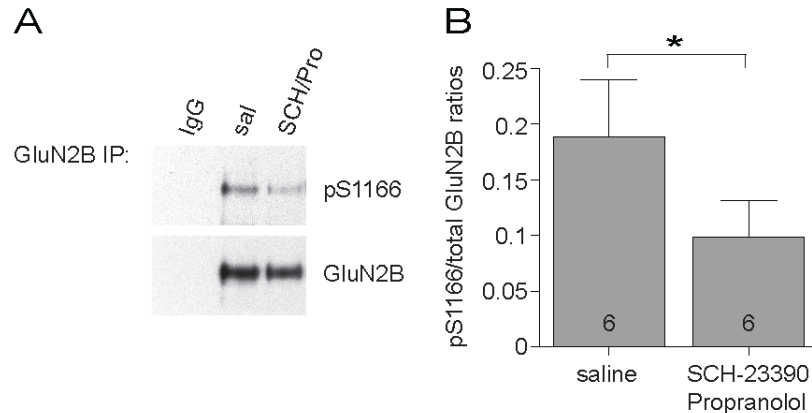


**Figure 3.24 Combined i.p. injection of propranolol and SCH23390 reduces basal S1166 phosphorylation.** (A) Propranolol (Pro, 20 mg/kg) and SCH23390 (SCH, 0.5 mg/kg) were injected i.p. Animals were euthanized after 1 h. After a GluN2B IP the S1166 phosphorylation was analyzed via immunoblotting with the phospho-S1166 antibody. (B) Bar graph represents the quantified immunosignals, corrected for variations in total GluN2B levels. Data represent mean  $\pm$  SEM. Statistical significance: two-tailed paired t-test,  $p=0.01$ .

### 3.3.10 I.P. Injection of a Combination of Propranolol and SCH23390 has no Effect on the Forced Swim-induced Increase in Phosphorylation of S1166

Combined injection of propranolol and SCH23390 30 min before the forced swim and the subsequent WB analysis of the isolated hippocampi showed no effect on the forced swim-induced increase of S1166 phosphorylation. Probing for phospho-S845 and phospho-S897 revealed a tendency for reduction in basal phosphorylation of the control animals and a reduction in the forced swim-induced phosphorylation compared to saline

injected control animals (Fig. 3.25 A), similar to the single propranolol injection (Fig. 3.21). Unlike basal phosphorylation, the stress-induced phosphorylation of S1166 is not decreased by the combination of the  $\beta$ AR and D<sub>1</sub>/D<sub>5</sub> receptor antagonists (Fig. 3.25 A). Quantification of the phospho signals is presented, after correction for changes in total receptor levels (Fig. 3.25 B), and expressed as the level of increase in phosphorylation after forced swim-induced stress compared to control animals (Fig. 3.25 C).

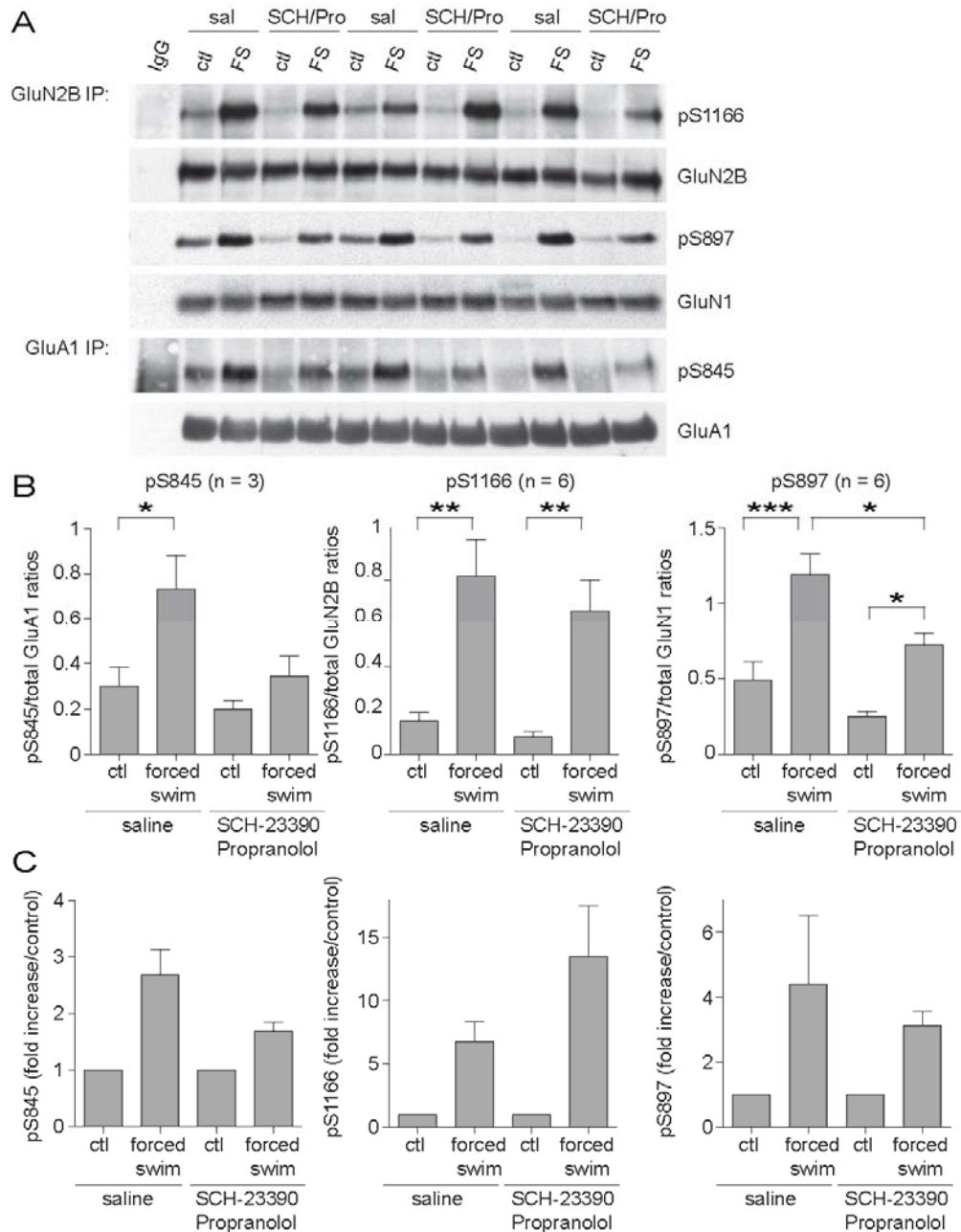


**Figure 3.25 I.p. injection of a combination of propranolol and SCH23990 does not block forced swim-induced S1166 phosphorylation.** (continued on next page)

(Figure 3.25 continued) **(A)** Propranolol (Pro, 20 mg/kg) and SCH23390 (SCH, 0.5 mg/kg) were injected i.p. 30 min before forced swim. Differences in phosphorylation levels between drug and saline injected rat hippocampi, from control and forced swim stressed rats, were immunoblotted for pS845, pS1166 and pS897 after a GluN2B and GluA1 IP. Quantification of the signal intensity is graphed as the phospho-signal ratios, corrected for total receptor levels **(B)** or as the forced swim-induced increase in phosphorylation compared to control animals **(C)**. Data represent mean  $\pm$  SEM. Statistical significance: one-way ANOVA with Tukey post test, \* $p < 0.05$ , \*\* $p < 0.01$ , \*\*\* $p < 0.001$ .

### 3.3.11 I.P. Injection of the Adenosine $A_{2A}$ Receptor does not Affect Stress-induced Regulation of S1166

The 2A-type adenosine receptor ( $A_{2A}R$ ) is also positively coupled to cAMP production via  $G_{\alpha s}$  and upregulates calcium influx through the NMDAR in a PKA dependent manner in the striatum (Higley and Sabatini, 2010). To test whether the  $A_{2A}R$  might be involved in the forced swim induced upregulation of S1166 phosphorylation in the hippocampus, the  $A_{2A}R$  antagonist SCH58261 was injected 30 min before forced swim. Forced swim-induced stress again resulted in enhanced phosphorylation of the PKA phosphorylation sites S1166, S897 and S845. Intraperitoneal injection of SCH58261 neither reduced any basal phosphorylation levels nor the stress induced increase. WB analysis (Fig. 3.26 A) and quantification of the signal intensity showed no difference between the saline and SCH58261 injected groups Fig. 3.26 B, C). To see if the forced swim-induced stress resulted in the upregulation of other serine and threonine kinases, known to phosphorylate NMDARs and AMPARs, the GluA1 IPs were also probed with a phospho-specific S831 antibody. S831 on the GluA1 subunit is phosphorylated by CaMKII and PKC (Barria et al., 1997; Mammen et al., 1997; Roche et al., 1996). Together with S845, S831 is important for the expression of LTD and LTP (Lee et al., 2003). Quantification of the phospho-S831 signal also revealed a stress induced upregulation of S831 phosphorylation (Fig. 3.26 D) that was not affected by i.p. injection of SCH58261.

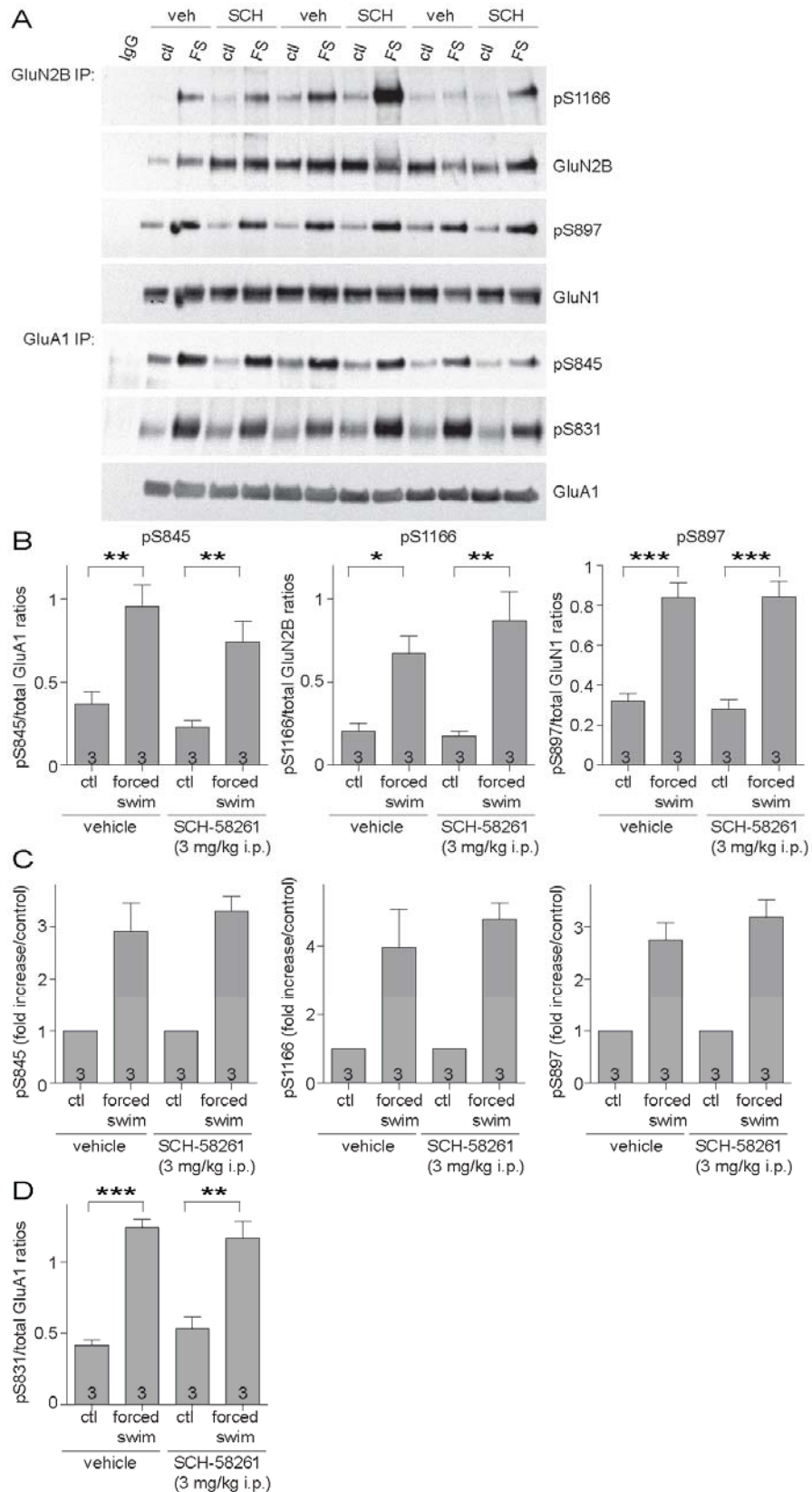


**Figure 3.26** I.p. injection of the  $A_{2A}R$  antagonist SCH58261 does not effect forced swim-induced phosphorylation. (A) Saline or SCH58261 were injected 30 min before forced swim (FS). (continued on next page)

(Figure 3.26 continued) The isolated hippocampi of the control and forced swim animals were lysed, cleared by ultracentrifugation and immunoblotted after a GluN2B and GluA1 IP for phospho-S1166, -S897, -S845 and -S831. **(B, C)** Quantified immunosignals were corrected for changes in total receptor levels and graphed as the corrected ratios (B) or as the stress induced increase in phosphorylation over control animals (C). **(D)** Quantification of the phospho-S831 signal, corrected for total GluA1 levels. Data represent mean  $\pm$  SEM. Statistical significance: one-way ANOVA with Tukey post test, \* $p < 0.05$ , \*\* $p < 0.01$ , \*\*\* $p < 0.001$ .

### 3.3.12 Reduced Forced Swim Stress Results in Reduced Receptor Phosphorylation Levels

Thus far the tested GPCR antagonists were not successful to block stress induced S1166 phosphorylation. Therefore a milder forced swim paradigm was used to see if lower stress levels might allow for better drug interference. The forced swim was conducted for 3 min instead of 5 min and the water temperature was increased from 18-19 °C to 23-25 °C. At the same time the  $A_{2A}R$  antagonist SCH58261 was tested again. The shorter swim period together with the higher water temperature resulted in reduced and more variable stress levels with an overall smaller increase in the forced swim induced phosphorylation of S1166, S897 and S845 (Fig. 3.27 A). The higher variation in the stress levels of the animals and the resulting less clear defined increase in phosphorylation had not the hypothesized effect on possible assessment of drug interference. The reduced output in phosphorylation made the evaluation of successfully induced stress more difficult. Instead of a 3-5 fold increase of phospho-signal intensity the less stressful forced swim barely increased S1166, S897 and S845 phosphorylation by 2-fold (Fig. 3.27 C). The raw data of the corrected phospho-signal intensities are shown in Fig. 3.27 B. The  $A_{2A}R$  antagonist SCH58261 again had no effect on the basal and forced swim induced phosphorylation.

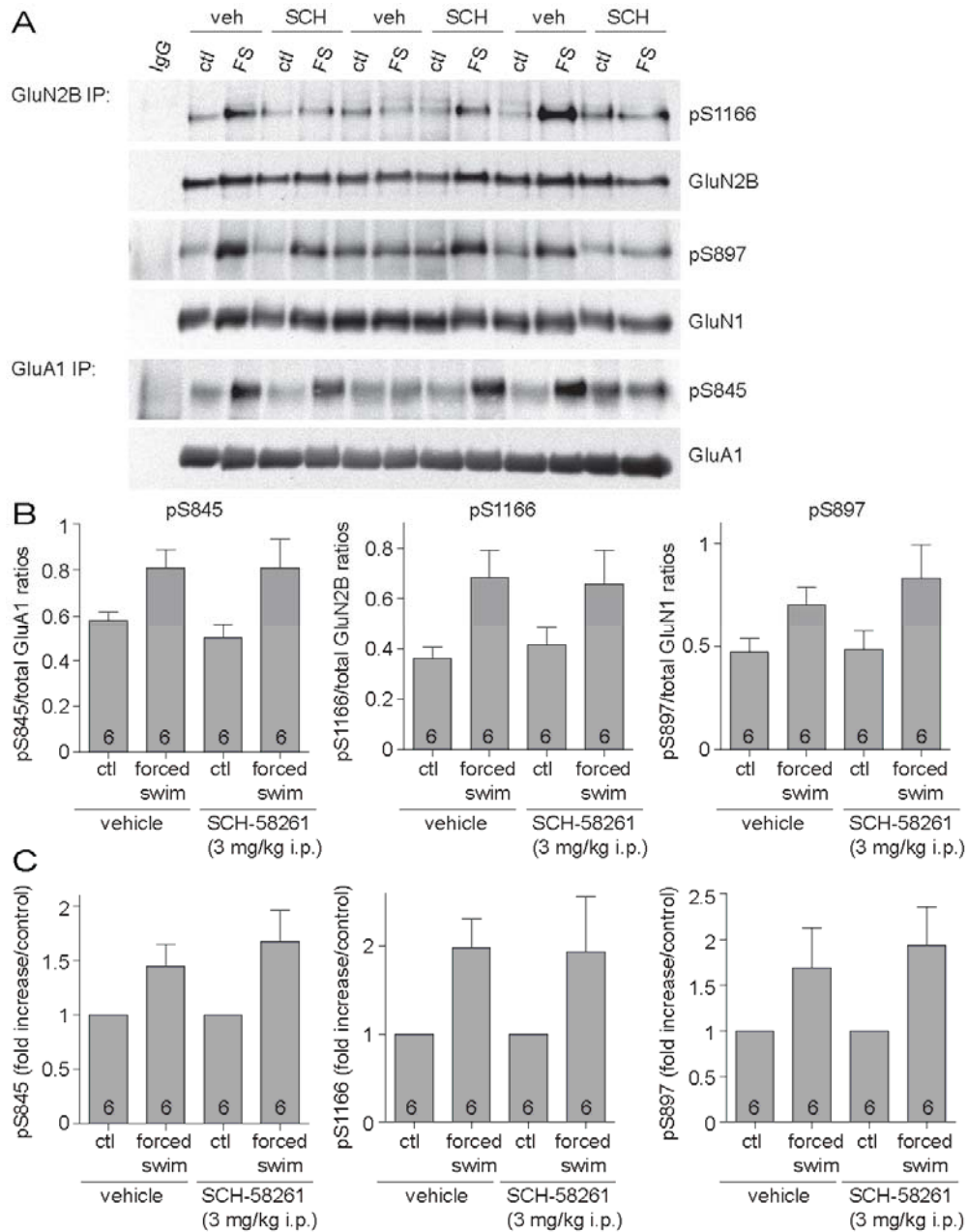


**Figure 3.27 Milder forced swim stress results in reduced phosphorylation levels. (A)** Again saline or SCH58261 were injected 30 min before the, this time, shorter (3 min) and at a higher water temperature (23-25 °C) conducted forced swim. The phosphorylation levels in the isolated hippocampi of the untreated and forced swim animals were again analyzed with phospho-specific antibodies against S845, S1166 and S897 after a GluA1 and GluN2B IP. **(B)** Quantification of the phospho-signal intensity corrected against total receptor levels. **(C)** Quantification of the phospho-signal intensity expressed as the forced swim-induced phosphorylation compared to control animals. Data represent mean  $\pm$  SEM.

### **3.3.13 Hippocampal Injection of PKA Antagonist Rp-8-Br-cAMPs Reduces Basal and Forced Swim-induced S1166 Phosphorylation**

Forced swim-induced stress results, as previously stated, in a change of a series of neurotransmitters. In addition forced swim activates other Ser/Thr-kinases at least including PKC and CaMKII, as shown by the increase in S831 phosphorylation (Fig. 3.26). To confirm that the stress-induced phosphorylation of S1166 is mediated by PKA as expected and could not be substituted by other kinases, localized to the vicinity of the NMDAR under stress conditions, the selective PKA antagonist 8-Br-Rp-cAMPs was injected directly in the hippocampus before forced swim. Injection of 8-Br-Rp-cAMPs reduced basal phosphorylation levels of S1166, S897 and S845, as well as the forced swim induced phosphorylation of these sites (Fig. 3.28 A). Quantification of the phospho-signal intensities corrected for total receptor levels, showed a clear tendency for decreased PKA phosphorylation levels under control conditions as well as forced swim-induced stress (Fig. 3.28 B). The data have not yet reached statistical significance and require repetition, particularly with regard to the difficult direct hippocampal injections.

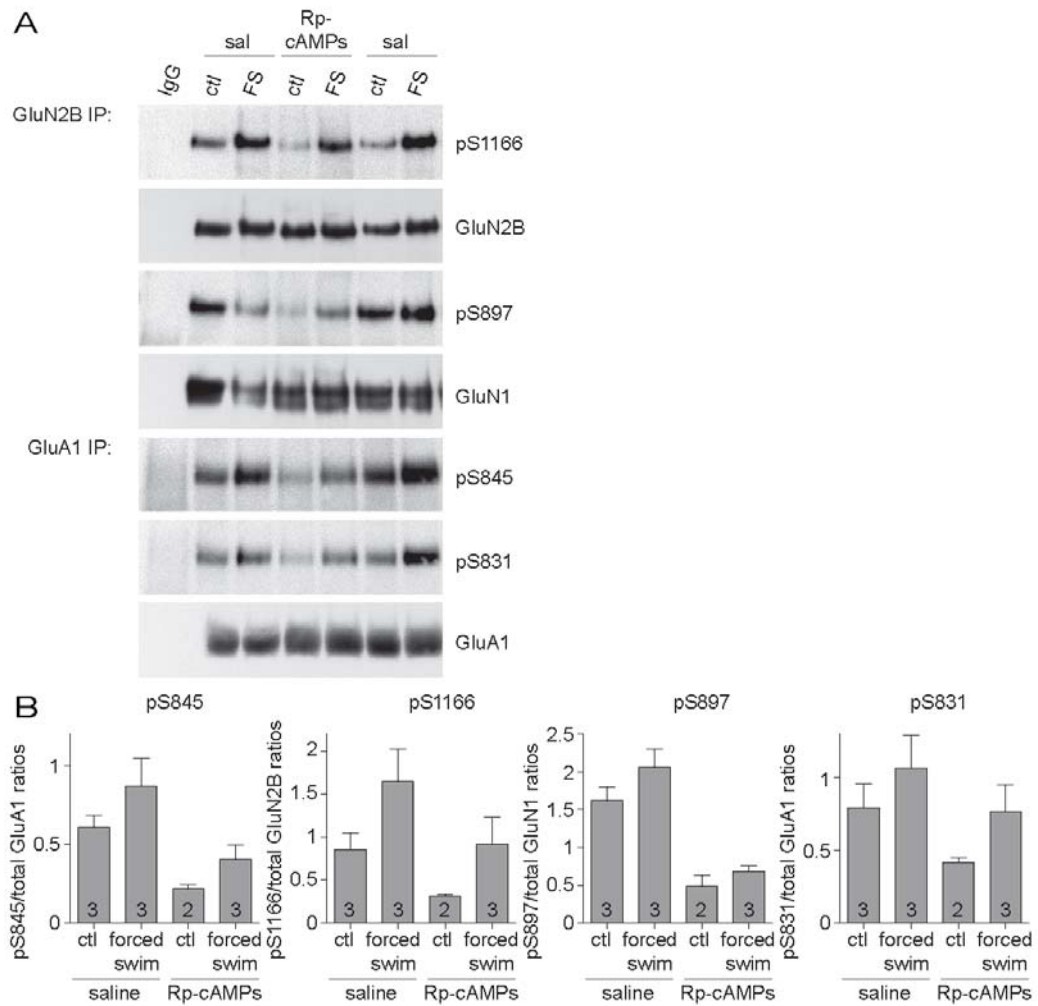


**Figure 3.28 Hippocampal injection of Rp-cAMPs blocks stress-induced phosphorylation of S1166. (A)** WB analysis of hippocampal (CA1 + DG area around injection site dissected) phosphorylation levels of S1166, S897, S845 and S831 of control and forced swim stressed (FS) animals after saline or 8-Br-Rp-cAMPs (25 nmol in 4  $\mu$ l, 1 h before FS) injection. **(B)** Bar graphs show quantification of the phospho-signal intensity corrected against total receptor levels. Data represent mean  $\pm$  SEM.

### 3.4 Side Effects of Cell Penetrating Peptides (CPP)

In order to dissect the importance of the different CaMKII interaction sites on the NMDAR and determine the role of this interaction under ischemic conditions, membrane permeable peptides derived from the binding sites on GluN1 and GluN2B were planned to be utilized. The individual peptides contained the CaMKII binding sites on the GluN2B (aa 1290-1306) and GluN1 C-terminus (aa 846-863) preceded at their N-terminus by 11 R. Arginine rich strings are cell-penetrating peptide sequences derived from the Tat sequence. The Tat sequence refers to the active 11 amino acid sequence important for the penetration of cells by the transactivator of transcription (TAT) protein of the Human Immunodeficiency Virus (Vives et al., 1997). Further research on the polybasic Tat sequence revealed that particularly the arginine residues with their guanidinium groups are important for uptake, and arginine multimers turned out to be superior compared to the original Tat sequence. Cell uptake varies with the length of the arginine oligomer and was observed for oligomers of 6-20 arginine residues, with maximum internalization around a length of 15 (Wender et al., 2008).

Application of these cell permeable peptides might have allowed us to acutely disrupt the CaMKII interactions and investigate their role not only during physiological glutamate stimuli, but also during ischemic conditions and glutamate overload. Inhibition of stimulated and autonomous CaMKII activity through the previously mentioned Tat-CN21 peptide actually attenuated glutamate induced neuronal cell death in cultures as well as in a mouse model of stroke (Coultrap et al., 2011). During the initial experiments, the 11R tagged peptides however revealed unexpected side effects on cytotoxicity and kinase activity which are described here.

### 3.4.1 The 11R Cell Penetrating Peptide Induces Cytotoxicity in a Concentration-dependent Manner

The cell penetrating NMDAR peptides were applied to mature hippocampal cultures and vehicle treated or stimulated with 100  $\mu\text{M}$  glutamate for up to 35 h and the level of excitotoxicity was determined via PI staining or the lactate dehydrogenase (LDH) cytotoxicity Kit. Treatment with 100  $\mu\text{M}$  glutamate for these long periods of time slightly induced excitotoxicity compared to vehicle treated control cells, apparent through an increased number of PI (propidium iodide) positive cells (Fig. 3.29 A; after 24 h) and a higher LDH enzyme activity (Fig. 3.29 B). LDH is released from the cytoplasm of damaged cells and its activity in the medium supernatant after 11, 24 and 35 h was measured in a colorimetric assay as a change of absorption. Unexpectedly all tested 11R-NMDAR peptides themselves were highly cytotoxic at a concentration of 10  $\mu\text{M}$ , but not 1  $\mu\text{M}$  (only the data for the 11R-GluN1 C0 peptide are shown). The increased cytotoxicity was again observed through PI intercalation of DNA in damaged cells (Fig. 3.29 A) and LDH activity (Fig. 3.29 B).

Hoechst 33342 is a cell-permeant counterstain used to label all cells and determine the percentage of PI positive cells. The glial fibrillary acidic protein (GFAP) stain was used to mark astrocytes.

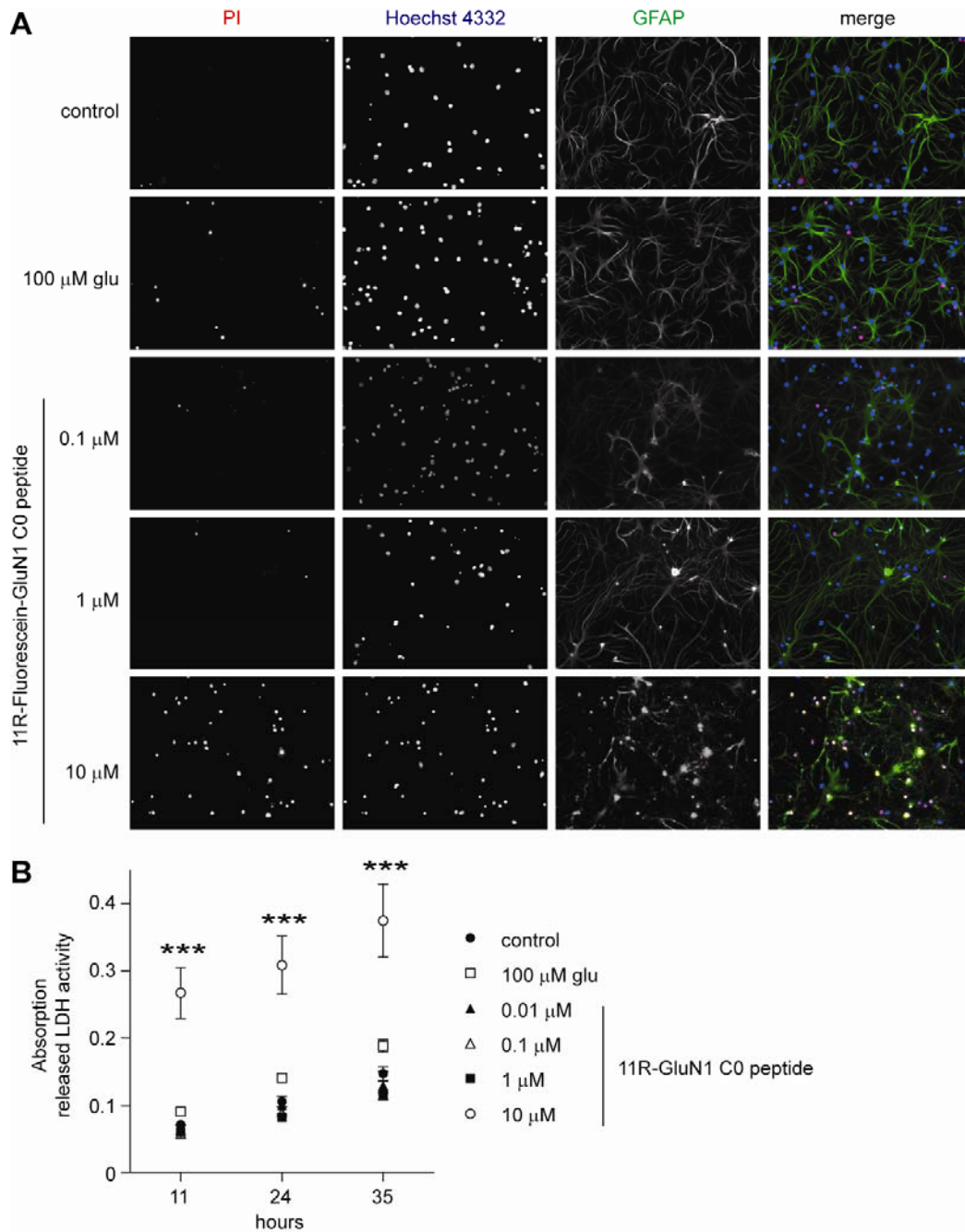


**Figure 3.29 The 11R cell penetrating peptide is cytotoxic at a concentration of 10  $\mu\text{M}$ , but not 1  $\mu\text{M}$ .** Hippocampal cultures were vehicle treated, stimulated with 100  $\mu\text{M}$  glutamate or incubated with different amounts of the 11R-Fluorescein-GluN1 C0 peptide for up to 35 h. The PI staining was performed after the indicated treatments for 24 h. For the LDH assay tissue culture (TC) supernatant taken after 11, 24 and 35 h was analyzed. **(A)** Representative pictures of the treated cultures stained for PI (red), Hoechst4332 (blue) and GFAP (green) are depicted. **(B)** Analysis of the LDH activity in the TC supernatant collected after the indicated times of treatment and measured as a change in absorption. Data represent mean  $\pm$  SEM. Statistical significance: two-way ANOVA with Bonferroni post-test, \*\*\* $p < 0.001$ .

### 3.4.2 The 11R Cell Penetrating Peptide Inhibits CaMKII Activity in a Concentration-dependent Manner

The CaMKII binding site of GluN2B displays a high degree of sequence similarity to the T286 segment (Fig. 1.3) and interacts in a similar manner with the T-site of CaMKII. Like T286 autophosphorylation of CaMKII through the neighboring subunit, the interaction with GluN2B also seems to require initial binding to the S-site before transition to a persistent interaction with the T-site (Bayer et al., 2006). The interaction with the GluN1 subunit was shown to be activity dependent as well, even though in this case T286 autophosphorylation is required and binding of  $\text{Ca}^{2+}$ /CaM alone was not sufficient (Leonard et al., 2002).

Due to the activity-dependent nature of these interactions and the fact that GluN2B binding to the S-site has been shown, we tested whether the various cell-penetrating NMDAR peptides affect CaMKII kinase activity *in vitro*.

Purified CaMKII (a generous gift from Dr. Andy Hudmon) was incubated with increasing amounts of peptide and the phosphorylation of the substrate, a GST fusion protein of the GluA1 C-terminus, monitored. The kinase activity was determined using a phospho-specific antibody against S831 on the GluA1 C-terminus, a physiological substrate of CaMKII. For quantification, the level of phosphorylation was corrected for differences in total amount of the GST-GluA1 C-terminal fusion protein. Initially, the effect of the 11R-GluN1 C0, the 11R-GluN2B/C and the 11R-GluN2B/C-LRR/ARQ peptides were tested. The LRR/ARQ peptide includes the same CaMKII binding site (aa 1290-1306) as the GluN2B/C peptide, but also carries the two point mutations (L1298A and R1300Q), which as stated previously disrupt the interaction with the T-site of CaMKII (Halt et al., 2012; Strack et al., 2000a).

All three peptides blocked CaMKII kinase activity in a concentration dependent manner. The 11R-GluN2B/C and 11R-2B/C-LRR-ARQ peptide already blocked kinase activity by over 50% compared to the positive control (no peptide addition) at a concentration of 1  $\mu\text{M}$ . The 11R-GluN1C0 peptide only showed reduced activity at a concentration 3.3  $\mu\text{M}$  (Fig. 3.30 A, B). Based on the fact that also the LRR-ARQ mutant peptide, which should not interact with CaMKII, also strongly inhibited *in vitro* kinase activity, a different peptide sequence was tested. The readily available N2ACT peptide,

containing the very end of the GluN2A C-terminus, not known to interact with CaMKII, was used. Differently tagged versions of this peptide, with or without the 11R sequence as well as a myristoylated form were applied to determine possible unspecific side effects of the 11R sequence. Incubation of the CaMKII reaction mix with increasing concentrations of the untagged and myristoylated GluN2ACT peptide had no effect at all on GST-GluA1-C-terminal S831 phosphorylation, while the 11R-GluN2ACT peptide significantly blocked phosphorylation by 25% at a concentration of 1  $\mu$ M and by roughly 50% at a concentration of 3.3 and 10  $\mu$ M (Fig. 3.30 C, D). To confirm that the 11R sequence also reduces kinase activity of endogenous CaMKII, CaMKII $\alpha$  and  $\beta$  were immunoprecipitated from brain lysate and incubated with the reaction mix containing no peptide (positive control), no ATP (negative control) or 10  $\mu$ M of the GluN2ACT peptide with or without the 11R sequence. WB analysis of S831 phosphorylation again demonstrated inhibition of CaMKII activity by the 11R sequence (Fig. 3.30 E).

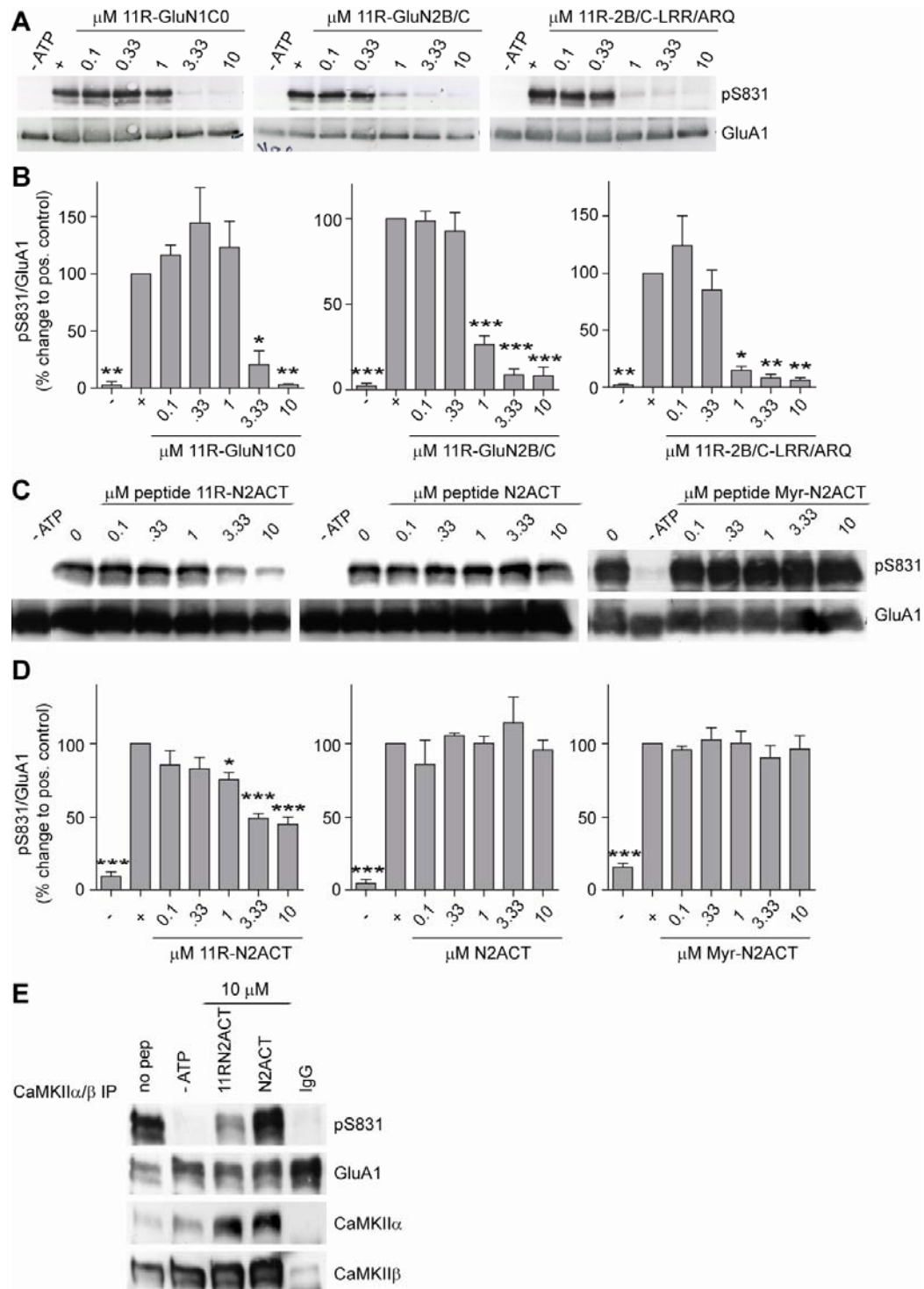


**Figure 3.30 The 11R cell penetrating peptide, but not myristoylation, inhibits CaMKII kinase activity.** (A) Representative examples of western blots probed for phospho-S831 and total levels of the GST-GluA1 C-terminal substrate are depicted. Purified CaMKII was incubated without ATP (-, negative control), without peptide (+, positive control) or increasing concentrations of the indicated peptide. (B) Quantification of the S831 phosphorylation, corrected against total GluA1 substrate levels, and expressed as % change compared to the positive control. (C) Examples of immunoblots analyzed for S831 phosphorylation after incubation of CaMKII with the shown differently tagged GluN2ACT peptide versions and concentrations. (continued on next page)

(Figure 3.30 continued) **(D)** Quantification of the changes in CaMKII activity were measured and are represented as % change of S831 phosphorylation compared to control, after correction for the total amount of GluA1 substrate. **(E)** A mix of CaMKII $\alpha$  and  $\beta$  was immunoprecipitated from brain lysate and incubated with 10  $\mu$ M GluN2ACT peptide with or without the 11R sequence. Kinase activity was determined by WB analysis with the phospho-specific S831 antibody. Data represent mean  $\pm$  SEM. Statistical significance: one-way ANOVA with Tukey post test, \* $p$ <0.05, \*\* $p$ <0.01, \*\*\* $p$ <0.001.

### 3.4.3 The 11R Cell Penetrating Peptide Inhibits PKA Activity in a Concentration-dependent Manner, with no Effect of the Tat Sequence or Myristoylation

For CaMKII the presence of an arginine residue N-terminal of the phosphorylatable serine or threonine residue was found to be essential for substrate recognition. Many of the CaMKII substrates contain the minimal motif of R-X-X-S/T (with X representing any amino acid), but additional determinants also seem to be important and a few CaMKII substrates without an arginine at the -3 position have been identified (White et al., 1998).

PKA (protein kinase A or cAMP-dependent protein kinase) also requires the presence of N-terminal basic residues, particularly arginine. At least one arginine in -2 or -3 position of the phosphorylatable serine or threonine is required and the optimal substrate sequence was determined as: R-R-X-S/T (Kennelly and Krebs, 1991).

These requirements for arginine residues in the recognition of substrates for CaMKII as well as PKA could explain the observed side effects of the 11R sequence on CaMKII kinase activity. To investigate whether PKA is blocked as well, kinase activity of purified PKA (Sigma) was monitored *in vitro* in the presence of increasing concentrations of the differently tagged versions of the previously described GluN2ACT peptide. The GST fusion protein of the GluA1 C-terminus served again as substrate and the phospho-specific antibody against S845 on the GluA1 C-terminus, a physiological PKA substrate important for LTP and emotional learning (Hu et al., 2007; Lee et al., 2000), was used to determine kinase activity.

The 11R-GluN2ACT peptide significantly blocked S845 phosphorylation by ~40% at a concentration of just 0.33  $\mu$ M. The inhibition of PKA was concentration dependent and at a peptide concentration of 10  $\mu$ M kinase activity was blocked by more than 90%. The untagged version of the

GluN2ACT peptide only impaired activity by ~30% at the maximal concentration of 10  $\mu$ M, while myristoylation had no effect. If anything, Myr-GluN2ACT showed a slight tendency towards increased activity with a higher inter-experiment variability (Fig. 3.31 A, B).

To confirm the concentration dependent inhibition of PKA activity by the 11R sequence, the 11R-DAPA peptide (Joiner et al., 2010) was tested. The 11R-DAPA peptide was derived from the C-terminus of the  $\beta$ 2 adrenergic receptor, and like the GluN2ACT peptide sequence, not known to interact with PKA. Again, the presence of the 11R sequence inhibited PKA activity in a concentration dependent manner and to nearly the same extent as the 11R-GluN2ACT, starting at a concentration of 0.33  $\mu$ M (Fig. 3.31 C, D left side).

The 11R sequence was originally designed from the Tat sequence which is a polybasic region including multiple lysine and arginine residues (Tat 48-60: GRKKRRQRRRPPQ). The differences compared to the 11R sequence are an overall lower charge, less and shorter R stretches, as well as a missing N-terminal arginine residue. All the tested concentrations of the Tat-SCR peptide (described earlier, 3.2.2) did not significantly prevent PKA activity, even though there was a tendency of a slight reduction at all measured concentrations (Fig. 3.31 C, D right side).

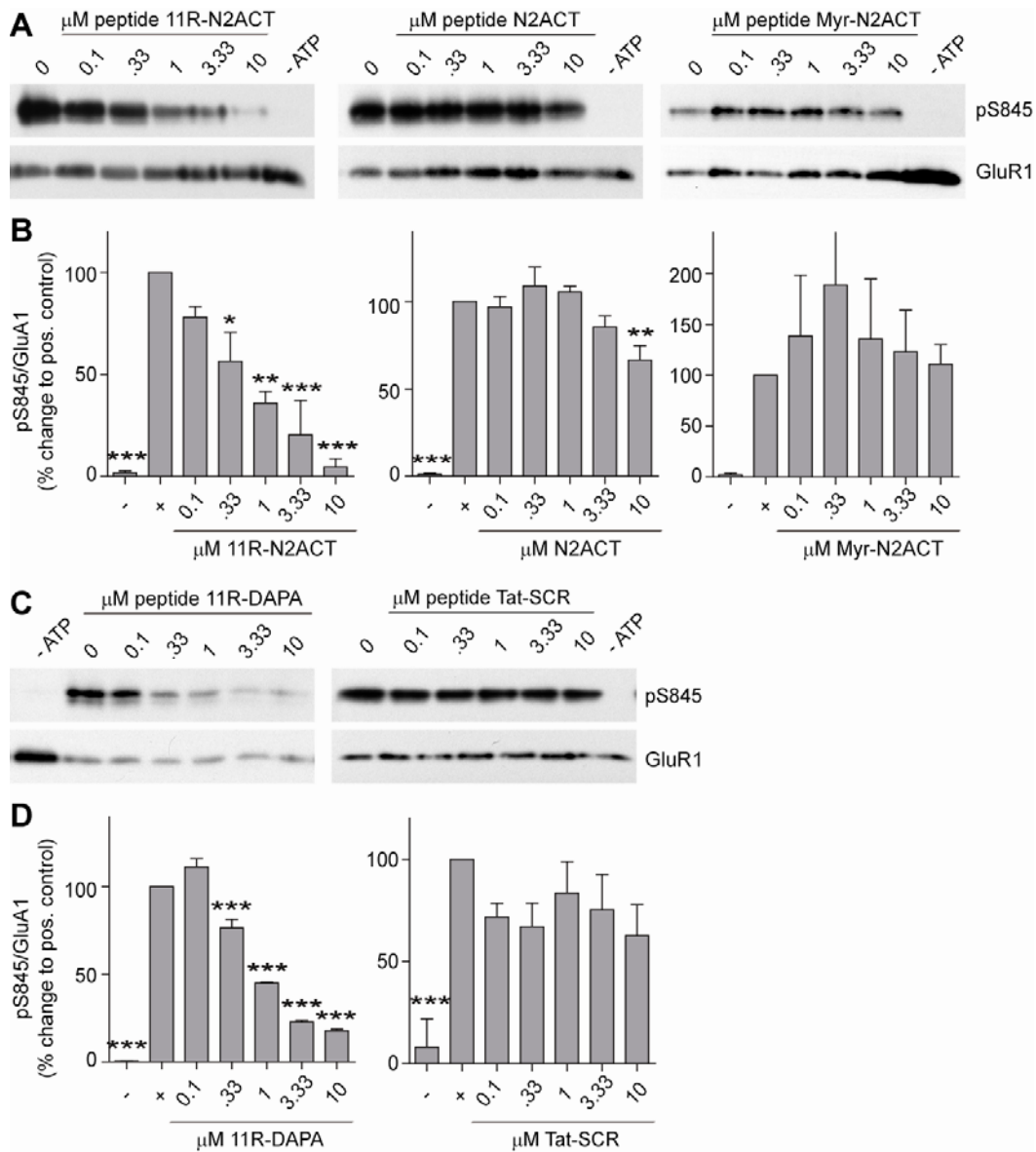


**Figure 3.31 The 11R cell penetrating peptide, but neither myristoylation nor the Tat Sequence, inhibits PKA kinase activity. (A)** Purified PKA was incubated with the indicated increasing concentrations of differently tagged (11R vs. no tag vs. myristoylation) versions of the GluN2ACT peptide, no peptide (positive control) or no ATP (negative control). Representative blots probed for phospho-S845 and total GluA1 are depicted. **(B)** Quantification of PKA activity. S845 phosphorylation was normalized for total GluA1 substrate levels, and expressed as % change compared to the positive control. **(C)** WB analysis of phospho-S845 and total GluA1 C-term levels after in vitro PKA phosphorylation in the presence of different concentrations of the 11R-DAPA (left side) and the Tat-SCR peptide (right side). **(D)** S845 phosphorylation as a measure of PKA activity was quantified, normalized for total GluA1 substrate levels, and expressed as % change compared to positive control. Data represent mean  $\pm$  SEM. Statistical significance: one-way ANOVA with Tukey post test, \* $p < 0.05$ , \*\* $p < 0.01$ , \*\*\* $p < 0.001$ .

## 4 Discussion

### 4.1 The Role of the CaMKII/GluN2B Interaction in Learning and Memory

CaMKII and the NMDAR are crucial not only for hippocampal LTP, but also for hippocampus-dependent spatial learning and memory formation (Elgersma et al., 2004; Malenka et al., 1989; Malinow et al., 1989; Morris et al., 1986). In a number of studies CaMKII $\alpha$  KO and mutant mice displayed learning deficits, primarily in aversively motivated tasks (Elgersma et al., 2002; Giese et al., 1998; Irvine et al., 2005; Silva et al., 1992a), while appetitive learning was unaffected (Carvalho et al., 2001).

Moreover, regulation of CaMKII $\alpha$  expression or activity seems to have an emotional component and especially impact emotional and anxiety-like behavior and learning. CaMKII $\alpha$  heterozygous KO mice show decreased freezing in fear conditioning induced by an electric foot shock and are more active in the open field suggesting decreased anxiety-related behaviors (Chen et al., 1994). On the contrary, transgenic mice overexpressing CaMKII $\alpha$  exhibit an increase in anxiety-like behaviors in the open field, light-dark transition, and the elevated zero maze (Hasegawa et al., 2009). CaMKII $\alpha$  T286A mutant mice spend more time in, and entered more often, the open arm in the elevated plus maze and generally react with hyperactivity to novel stimuli that could be perceived as potentially threatening (Easton et al., 2011). However, behavior in the non-threatening neutral environment of the home cage is normal (Easton et al., 2011), in accordance with impaired learning in MWM and fear conditioning (Giese et al., 1998; Irvine et al., 2005) but normal appetitive instrumental conditioning (Carvalho et al., 2001). The results obtained from our GluN2B KI mice argue for a specific requirement of CaMKII binding to GluN2B in aversive and more demanding spatial learning.

Learning during massed training sessions, i.e., when training trials are given in short order on a single day, generally results in lower levels of

learning than spaced training over a period of several days. For instance, in the MWM rats showed faster and better acquisition during spaced (16 trials over 4 days) than massed training (16 trials in 1 day) as well as better memory formation (Commins et al., 2003). During contextual fear conditioning 1 h spaced training also results in better memory formation than massed training, while cued fear conditioning is unaffected (Scharf et al., 2002). Likely because of the more demanding nature of massed training the GluN2B KI mice showed reduced learning in the one-day paradigm (Fig. 3.2 A) when they did not in the six-day MWM training protocol compared to WT mice (Halt et al., 2012). The learning deficit in the one-day paradigm suggests that the learning capacity over a more limited time period is reduced in GluN2B KI mice.

This phenotype is similar to alpha and delta CREB knock-out mice, which are impaired in massed but not spaced MWM learning and contextual fear conditioning (Kogan et al., 1997). The improvement in memory after spaced learning is also mimicked in acute hippocampal slices where successive spaced theta burst stimulation resulted in enhanced previously saturated LTP (Kramar et al., 2012). In this study by Kramer et al. the induction of LTP in a subset of synapses during the first theta burst train primed the initially unresponsive neighbors (probably in a translation dependent manner, since the two stimulations have to be spaced 1 h apart; see also (Scharf et al., 2002)), resulting in potentiation after stimulation with the second theta burst train. This mechanism will probably be especially important in cases of impaired LTP induction or expression like in our GluN2B KI mice where LTP by two 100Hz tetani that are 1 min apart is reduced by 50% (Halt et al., 2012).

Whether the observed deficit in recall of the MWM task 1 and 7 days after single day training (Fig. 3.2 B, C) reflects reduced learning, reduced memory consolidation, or both cannot be answered at this point. In order to draw a definitive conclusion and dissociate the effects of learning and memory, the mice would need to be trained to reach a certain performance criterion. The achievement of similar escape latencies during MWM learning, independent of a presumably different number of required learning trials, would expose differences in memory formation.

The Barnes maze is a fairly demanding spatial task using visual cues in the room for navigation, comparable to the MWM, but without the same level of stress during learning trials because the environment is far less aversive. The finding that GluN2B KI mice acquire (Fig. 3.1 A) and maintain (Fig. 3.1 B, C) the Barnes maze task comparable to WT mice suggests that CaMKII binding to GluN2B is less important for spatial learning in environments where general stress levels are fairly low. Exposure to light and open space during the Barnes maze causes a much smaller increase in plasma corticosterone levels than swim stress (Harrison et al., 2009; Sternberg et al., 1992). The effect of different stress levels and glucocorticoids on learning and memory is biphasic. Optimal levels of corticosterone enhance memory, while memory is impaired by levels that are too high. In the object recognition task, administration of different corticosterone doses after learning affected 24 h retention in an inverted U-shaped dose-response curve (Okuda et al., 2004). Chronic stress was also reported to affect spatial memory. Rats treated for 3 months with stress-equivalent corticosterone levels showed impaired performance in the Barnes maze (McLay et al., 1998). Therefore, testing of corticosterone treated WT and GluN2B KI mice in the Barnes maze could potentially reveal the learning deficits seen during the MWM 1 day massed training (Fig. 3.2) or the consolidation deficit observed after the six-day MWM training protocol (Halt et al., 2012).

On the other hand, fear conditioning creates a high level of anxiety but only for a short time period. The contextual conditioning only requires memorization of a far less complex environment, in which memorization of the context is associated with the shock and does not require navigation and localization of a certain target. Additionally, at the beginning of the conditioning the mice have time to explore their environment and form a spatial map without being stressed or being more anxious than during the normal exposure to a novel environment. The first shock is only delivered at the end of the third minute. During the milder conditioning paradigm (Fig. 3.5) the mice were pre-exposed to the shocking chamber one day prior to conditioning, which allowed the formation of an even better spatial

representation (Fanselow, 2000; Frankland et al., 2004; Hu et al., 2007). This lack of a demanding spatial learning requirement and possible formation of contextual memory during still low stress levels, explains why conditioning as well as memory were not affected in the GluN2B KI (Fig. 3.4 and 3.5). In addition, it was shown that spatial and contextual LTM formation is differently regulated. Not only are there different regional requirements within the hippocampus, but the control of gene transcription also varies between spatial and contextual LTM formation (Mizuno and Giese, 2005). These differences provide another possible explanation for normal contextual learning and memory. Regional differences were also observed in CaMKII $\alpha$  heterozygous null mice with impaired cortical, but normal hippocampal LTP (Frankland et al., 2001).

Contrasting CaMKII $\alpha$  heterozygous KO, T286A KI mice, or transgenic mice overexpressing CaMKII $\alpha$ , the GluN2B KI mice display no change in basal anxiety levels or anxiety-like behaviors. They show avoidance of the open arms in the EPM (Fig. 3.3), normal behavior in the open field (Halt et al., 2012), and reaction to TMT (the anxiogenic compound in fox urine), a measure of innate fear, that is comparable to WT mice (Halt et al., 2012).

These findings provide a specific requirement for the activity-dependent interaction of CaMKII with the NMDAR during the acquisition of more elaborate spatial learning tasks under aversive, stressful conditions. This learning impairment can be rescued by spaced training, but results in a subsequent consolidation deficit (Halt et al., 2012). The presented results argue for a role of CaMKII binding to GluN2B during both learning in emotional situations and also consolidation that becomes obvious under the more demanding MWM conditions but not the less stressful Barnes maze. Contextual fear conditioning is a strong and aversive associative learning paradigm and is not affected in the GluN2B KI mice. This discrepancy between spatial and contextual learning might be due to an unaffected formation of a spatial representation before shock delivery and increased

stress levels or slight regional and signaling differences between the two forms of learning.

## 4.2 The Activity-dependent Translocation of CaMKII

Neuronal activity and the  $\text{Ca}^{2+}$  influx through the NMDAR lead to activation of CaMKII and recruitment to the PSD (Dosemeci et al., 2001; Otmakhov et al., 2004; Strack et al., 1997b). The synaptic translocation of CaMKII (Bayer et al., 2001; Bayer et al., 2006; Hudmon et al., 2005; Lee et al., 2009; Otmakhov et al., 2004; Shen and Meyer, 1999; Shen et al., 2000; Zhang et al., 2008) depends on activation of its cytoplasmic pool, including mobilization of the F-actin bound fraction, for diffusion to its synaptic binding partners.

To date multiple binding partners for CaMKII have been identified. A lot of them were initially identified by  $^{32}\text{P}$ -T286 CaMKII $\alpha$  overlay and autoradiography, as presented in Fig. 3.6. The presented overlay indicates that CaMKII binds strongly to bands that correspond in their molecular weight to GluN2B, densin-180 and  $\alpha$ -actinin, as worked out more definitively in previous published work (Robison et al., 2005a; Strack and Colbran, 1998; Strack et al., 2000b). The NMDAR is an important binding partner in the PSD. Not only does this interaction allow anchoring of CaMKII in the PSD, it also brings the NMDAR together with CaMKII, both of which both have been shown to be essential for LTP and learning and memory. CaMKII and the NMDAR interact under basal conditions, but strong synaptic activation leads to an increased complex formation (Leonard et al., 1999). Interactions with the GluN2B, GluN1 and GluN2A subunit of the NMDAR were initially reported (Gardoni et al., 1998; Leonard et al., 1999; Strack and Colbran, 1998), but it was later shown that specific disruption of the GluN2B interaction abrogates activity-driven NMDAR/CaMKII complex formation and reduces LTP induction as well as spatial learning and memory consolidation (Barria and Malinow, 2005; Halt et al., 2012; Zhou et al., 2007).

The importance of CaMKII and its kinase activity for LTP induction was observed using other CaMKII inhibitors and manipulations, but thus far no

inhibitor that specifically inhibited CaMKII activity was able to reverse LTP (Buard et al., 2010; Chen et al., 2001; Malinow et al., 1989; Otmakhov et al., 1997; Wang et al., 2008). In addition in dendritic spines of organotypic hippocampal slice culture, the majority of CaMKII was only active for about one minute after LTP induction (Lee et al., 2009). This brief window of CaMKII activity as well as the lack of LTP reversal left the role of CaMKII during the late-phase of LTP and the processes that maintain synaptic strength uncertain. On the other hand, autonomous CaMKII activity due to T286 autophosphorylation always argued against an only transient role during LTP induction. This was supported by the observations that high frequency stimulation in the hippocampus resulted in a long lasting increase of this autonomous activity (Fukunaga et al., 1993), and that chemical LTP induced a persistent accumulation of CaMKII $\alpha$  at the PSD.

A possible explanation for this discrepancy is a potential structural role for the CaMKII/NMDAR complex. CaMKII is a dodecamer capable of simultaneously binding multiple PSD proteins, allowing the formation of macromolecular complexes (Colbran, 2004; Robison et al., 2005b; Walikonis et al., 2001). Moreover, CaMKII plays a structural role in the activity-dependent recruitment of the proteasome to spines, independent of its kinase activity and on a time scale exceeding the initial phase of LTP induction (Bingol et al., 2010). The ubiquitin-proteasome system is important for the functional reorganization of the synapse due to synaptic activity and experience-dependent remodeling (Ehlers, 2003).

The new CaMKII inhibitor CN21 was used to address the role of the CaMKII/NMDAR complex in the maintenance of synaptic strength (Sanhueza et al., 2011). CN21 is derived from the endogenous specific CaMKII inhibitor CaMKIIN (Chang et al., 1998, 2001). It binds not only to the S-site, but also to the T-site of CaMKII, where it interferes with GluN2B binding (Vest et al., 2007).

Application of the membrane permeable Tat-CN21 peptide resulted in a concentration-dependent disruption of the CaMKII/NMDAR complex (Fig. 3.7). A concentration of 5  $\mu$ M which blocks CaMKII activity and the induction of LTP, but does not reverse LTP (Buard et al., 2010), was not sufficient to

displace CaMKII from the NMDAR (Fig. 3.7 A, B). On the other hand 20  $\mu$ M CN21 reduced the CaMKII/NMDAR complex by 50% (Fig. 3.7 C, D). The activity-independent interaction of CaMKII with  $\alpha$ -actinin, which is not mediated by the T-site (Jalan-Sakrikar et al., 2012; Robison et al., 2005a), was not affected at either concentration. A scrambled version of the CN21 peptide (Tat-SCR) had no effect on the co-immunoprecipitation of the CaMKII/NMDAR complex at both concentrations (Fig. 3.7). In addition, it was shown that transient application of 20  $\mu$ M Tat-CN21, the concentration sufficient to disrupt the activity-induced complex, was able to reduce basal synaptic transmission and reverse saturated LTP (Sanhueza et al., 2011). These results indicate that CaMKII is also important for the maintenance of synaptic strength. In contrast to its activity-dependent function during LTP induction, the role of CaMKII during late-phase LTP and the maintenance of synaptic strength is structural and dependent on the interaction with the NMDAR.

There are multiple known binding partners of CaMKII in the PSD (Colbran, 2004; Colbran and Brown, 2004; Merrill et al., 2005), which could potentially be affected by CN21. Particularly, those involving activity-dependent interactions with the T-site. Regardless of these potential side effects of CN21, the CaMKII/NMDAR interaction and specifically the binding to the GluN2B subunit is clearly important for synaptic strength and LTP. This was not only demonstrated by CN21 inhibition, but also through multiple independent specific disruptions of this interaction, even *in vivo* (Barria and Malinow, 2005; Halt et al., 2012; Sanhueza et al., 2011; Zhou et al., 2007).

The activity-driven clustering of CaMKII to synaptic sites contributes to the synapse specificity of LTP (Lee et al., 2009; Rose et al., 2009; Zhang et al., 2008) and anchors the active kinase close to its substrates important for LTP induction (Lisman et al., 2012). The activity-induced relocation of CaMKII was investigated in dissociated hippocampal cultures. Given that ectopically expressed GFP-tagged CaMKII has a tendency to accumulate in large intracellular clusters in the somata (Chen and Hell, 2004), it might not properly reflect the behavior of endogenous CaMKII. In contrast to earlier imaging

studies relying on GFP-tagged CaMKII, the redistribution of endogenous CaMKII was for the first time systematically analyzed.

Using GFP-CaMKII expression in hippocampal cultures it was shown that the translocation time is controlled by the relative expression of CaMKII $\alpha$  to  $\beta$ . The time for half-maximal translocation was determined as 20, 80 and 280 s for  $\alpha$ ,  $\alpha/\beta$  and  $\beta$  oligomers respectively (Shen and Meyer, 1999). The faster recruitment of  $\alpha$  homomers compared to  $\alpha/\beta$  or  $\beta$  oligomers is attributed to the interaction of CaMKII $\beta$  with F-actin under basal, non stimulated conditions, which adds a dissociation step during the translocation process. Here, the conversion from a smooth to mainly clustered CaMKII $\alpha$  (Fig. 3.8) and  $\beta$  (Fig. 3.9) immunostaining started at ~90 s and was complete after ~3 min of glutamate stimulation, similar to the 80 s half-maximal translocation of  $\alpha/\beta$  oligomers (Shen and Meyer, 1999). Analysis of CaMKII $\beta$  fluorescence intensity at synaptic sites (Shank positive areas) revealed a slight increase in CaMKII $\beta$  avg. intensity after 120 s of glutamate stimulation, which became significant after 150 s and saturated after 180 s of stimulation (Fig. 3.10). CaMKII $\alpha$  (Fig. 3.8) and CaMKII $\beta$  (Fig. 3.9) display similar translocation kinetics, indicating that the majority of CaMKII holoenzymes exist as heteromers. These observations are consistent with the essential activity-independent structural role of CaMKII $\beta$  through targeting CaMKII holoenzymes to the F-actin cytoskeleton in spines (Borgesius et al., 2011).

The duration of the translocation of GFP-CaMKII is dependent on the CaMKII autophosphorylation state as well as phosphatase activity. Translocation of WT GFP-CaMKII was already reversed after ~3 min (Shen et al., 2000). The T286A mutant displayed an even faster dissociation with a nearly complete reversal after just 1 min. On the contrary, the T286D and the TT305/306AA GFP-CaMKII mutants dissociated more slowly (Shen et al., 2000).

The, compared to WT GFP-CaMKII, faster reversal of translocation for T286A and the slower reversal of T286D suggests an involvement of T286 phosphorylation in activity-induced postsynaptic CaMKII anchoring. Indeed, the activity-induced clustering of CaMKII was prolonged by phosphatase inhibitors (Shen et al., 2000), consistent with PP1 dependent

dephosphorylation of PSD associated CaMKII (Strack et al., 1997a; Strack et al., 1997b). The prolonged translocation of TT305/306AA GFP-CaMKII is in agreement with data from non-phosphorylatable TT305/306VA KI mice, which exhibited increased PSD associated CaMKII levels (Elgersma et al., 2002).

The fast reversal of WT GFP-CaMKII was also observed in a later study. The glutamate stimulation-induced postsynaptic translocation was reversed within 2 min, however, ~20% of kinase peak translocation remained localized even after a 30 min wash (Bayer et al., 2006). A persistent clustering of CaMKII $\alpha$  was attributed to a change from a reversible S-site interaction to a stable T-site interaction after prolonged periods of glutamate stimulation. This switch was only demonstrated in HEK cells, where the already long glutamate stimulation (compare to Fig. 3.12) for 2 min was reversed after a 10 min wash, whereas a stimulation for 6 min still resulted in residual clustering after a 45 min wash (Bayer et al., 2006).

Endogenous CaMKII $\alpha$  translocation was still increased after a 2 min chase period and reversed after a 5 min chase (Fig. 3.11 H). Even though not significant, the reversal after 5 min was only partial (~20-30% of initial CaMKII $\alpha$  fluorescence intensity increase) and stayed elevated even for the longer 20 and 60 min chase periods (with no difference between stimulation for 2 min and 5 min). This tendency to maintain a small (~20-30% of initial increase), stable translocated pool of CaMKII $\alpha$  was observed in two independent experiments, but needs further validation to establish statistical significance.

The fast reversal is possibly due to a removal of the majority of loosely anchored CaMKII (not bound to the NMDAR) by PP1 sensitive dephosphorylation of T286 (Shen et al., 2000; Strack et al., 1997a; Strack et al., 1997b). The remaining NMDAR bound CaMKII pool could be placed in a unique environment where T286 is protected from dephosphorylation (Mullasseril et al., 2007) and firmly anchored at the PSD for prolonged time periods. In organotypic hippocampal slices chemical LTP resulted in a persistent increase (for at least 1 h after stimulation) of endogenous CaMKII $\alpha$  associated with the PSD (Otmakhov et al., 2004).

Activation of CaMKII and its subsequent translocation is mediated by calcium influx through the NMDAR. A brief stimulation with glutamate (100  $\mu$ M glutamate/10  $\mu$ M glycine for 1-5 s) is sufficient to induce the activation and translocation, which is detectable after an additional 2.5 min chase period (without the presence of glutamate) as an increase in postsynaptic (Shank positive area) CaMKII $\alpha$  fluorescence intensity (Fig. 3.12).

Using this short and more physiological stimulation paradigm, the role of CaM availability and localization of CaM to spines by Ng, for the activity-induced postsynaptic targeting was investigated. Ng is highly concentrated in dendritic spines (Neuner-Jehle et al., 1996; Watson et al., 1992) and controls the level of free CaM (Persechini and Stemmer, 2002; Tran et al., 2003). Ng and the local availability of CaM are important for synaptic plasticity. Overexpression of Ng enhances synaptic AMPAR mediated currents in an activity-dependent fashion, relying on the NMDAR and CaMKII activation. Ng mutants showed that CaM binding is required for the potentiation, and knock-down of Ng prevented LTP induction (Zhong et al., 2009). In addition, Ng mutant null mice are deficient in spatial learning and display reduced levels of autophosphorylated autonomous active CaMKII (Miyakawa et al., 2001; Pak et al., 2000). The interaction of CaM with the IQ motif is modulated by activity and activity-induced phosphorylation. An increase in the local calcium concentration as well as phosphorylation of S36 within the IQ motif results in dissociation of CaM (Baudier et al., 1991; Gerendasy et al., 1995; Huang et al., 2000). *In vivo* phosphorylation of S36 is mediated by PKC $\gamma$  (Ramakers et al., 1999) and was shown to be important for fine tuning LTP (Zhong et al., 2011). Expression of phosphorylation deficient Ng mutants leads to expression of submaximal LTP. This is probably due to the faster rebinding of CaM to Ng (normally prevented by S36 phosphorylation), resulting in a faster termination of the intracellular calcium signal leading to submaximal LTP induction (Zhong et al., 2011). Accordingly, increased PKC dependent Ng phosphorylation was observed after LTP (Chen, 1994; Ramakers et al., 2000). Activation of PKC $\gamma$  is mediated through stimulation of mGluRs and the downstream phospholipase C/diacylglycerol/protein kinase C pathway. The

PKC $\gamma$  dependent phosphorylation of S36 on Ng thereby provides potential crosstalk between NMDAR and mGluR signaling important for LTP.

Brief stimulation with glutamate resulted in postsynaptic translocation of CaMKII observed as a 32% increase of CaMKII $\alpha$  fluorescence intensity. For comparison over all different transfection conditions the change in postsynaptic (Shank positive area) CaMKII $\alpha$  fluorescence intensity after glutamate stimulation was expressed as % increase compared to the corresponding vehicle treated condition. Transfection of the Ng-S/D and Ng-SF/AW dominant negative mutants as well as knock-down of Ng results in a nearly complete lack of the activity-induced translocation. Rescue of the knock-down by expression of the resistant Ng-GFP fusion protein again enables the activity-dependent redistribution, which is not rescued by co expression of the resistant, dominant negative Ng-S/D mutant (Fig. 3.13).

These data show that Ng anchored CaM is required for NMDAR mediated activation of CaMKII and the subsequent translocation to the PSD, and explain how the Ng overexpression dependent potentiation of synaptic AMPAR transmission is dependent on NMDAR and CaMKII (Zhong et al., 2009).

It would be interesting to investigate whether manipulation of Ng phosphorylation would affect CaMKII translocation or LTP induced by weak stimulation paradigms. Transfection of the Ng-SA mutant might reduce or block CaMKII translocation as well as LTP induction under these circumstances. Using the specific group I mGluR antagonist 4-CPG, it was shown that the involvement of the G $_q$  (PLC/DAG/PKC pathway) coupled group I mGluR in hippocampal LTP and spatial learning depends on the specific stimulation paradigm. Notably, 4-CPG application blocked LTP induced by weak, but not strong tetanization (Balschun et al., 1999). This argues for a role of PKC in fine-tuning synaptic plasticity and learning.

One of the multiple identified binding partners of CaMKII in the PSD is the GluN1 subunit, common to all NMDAR subtypes (Leonard et al., 2002; Leonard et al., 1999). Of the initially identified interactions with the GluN2B, GluN1 and GluN2A subunit of the NMDAR (Gardoni et al., 1998; Leonard et

al., 2002; Leonard et al., 1999; Strack and Colbran, 1998), only the importance of the GluN2B interaction for postsynaptic CaMKII function and LTP has so far been tested and established (Barria and Malinow, 2005; Halt et al., 2012; Strack et al., 2000a; Zhou et al., 2007).

CaMKII $\alpha$  binds to residues 845-861 in the membrane proximal C0 domain, common to all splice variants of the GluN1 subunit (Leonard et al., 2002). Further peptide binding and displacement studies showed that the interaction is abrogated by the two point mutations, Q849E and N856E, while CaM and  $\alpha$ -actinin binding was unaffected (Leonard and Hell unpublished data). CaM and  $\alpha$ -actinin bind to the same distal segment of the GluN1 C0 region (Leonard et al., 2002). GluN1 KI mice carrying these two point mutations, Q849E and N856E, were generated (Dallapiazza, Brose and Hell, unpublished data) and hippocampal cultures from these mice were investigated for differences in activity-induced CaMKII $\alpha$  translocation. Immunostaining for pre- and postsynaptic markers displayed normal synaptic morphology (Fig. 3.14), and glutamate stimulation showed a normal activity-induced translocation to synaptic sites with no detectable difference between WT and GluN1 KI (Fig. 3.15).

These data indicate that either the GluN1 interaction is not important for CaMKII $\alpha$  binding to the NMDAR and anchoring at the PSD *in vivo*, or that these two point mutations defined in an *in vitro* peptide binding assay are not sufficient to disrupt this interaction *in vivo*. The normal CaMKII $\alpha$  immunostaining and the unaffected activity-dependent translocation are consistent with other data, showing no obvious phenotype of GluN1 KI mice with regard to appearance, LTP or learning and memory (Dallapiazza and Hell unpublished data). In addition, the co immunoprecipitation (co IP) of GluN1 with CaMKII $\alpha$  or vice versa the CaMKII $\alpha$  co IP with GluN1 is not affected (Dallapiazza, Ulrich and Hell unpublished data). The fact that no interaction at ~130 kDa, the molecular weight of GluN1, was identified during the  $^{32}\text{P}$ -T286 labeled CaMKII $\alpha$  overlay (Fig. 3.6) indicates that this interaction is not prevalent and perhaps not important *in vivo*. The complete absence of activity-induced CaMKII translocation and increased complex formation in the GluN2B KI also argues against an important role of GluN1 anchoring, even

though under basal conditions the NMDAR co-IP in the GluN2B KI mice is only reduced by 30% (Halt et al., 2012). This remaining partial co-IP, as well as no difference in the co-IP from GluN1KI, does not exclude a role for GluN1 in CaMKII anchoring under basal condition, but is probably of minor if any role with regard to the multitude of other unaffected protein interactions in the PSD.

### 4.3 PKA-dependent Regulation of the NMDAR

The dynamic modulation of the NMDAR-mediated calcium influx is a fast and effective way for bi-directional modification of NMDAR-dependent synaptic plasticity, which is expressed as a change in AMPAR mediated transmission. PKA phosphorylation of the NMDAR specifically regulates the calcium permeability (Skeberdis et al., 2006). Modulation of the cAMP/PKA pathway should therefore influence the NMDAR-mediated calcium influx and control the induction of LTP. Indeed, direct modulation of G-protein coupled receptors like the  $\beta$ -adrenergic receptor, the D<sub>1</sub>/D<sub>5</sub> dopamine receptor or the A<sub>2A</sub> adenosine receptor, all coupled to G<sub>αs</sub>, enhance NMDAR current and calcium-influx as well as facilitate the induction of LTP (Higley and Sabatini, 2010; Otmakhova and Lisman, 1996; Raman et al., 1996; Thomas et al., 1996). On the other hand activation of G<sub>αi</sub> coupled receptors lower intracellular cAMP levels and subsequent PKA activity. Loss of PKA activity or activation of phosphatases reduce the NMDAR dependent Ca<sup>2+</sup>-influx, as shown for the NMDAR-mediated Ca<sup>2+</sup>-influx in the striatum. There, calcium influx through the NMDAR is bidirectionally modulated by the A<sub>2A</sub> adenosine receptor and the G<sub>αi</sub> coupled D<sub>2</sub> dopamine receptor (Higley and Sabatini, 2010).

PKA substrate recognition requires the presence of N-terminal basic residues, particularly arginine. The presence of at least one arginine in the -2 or -3 position of the phosphorylatable serine or threonine is a key determinant of PKA substrate recognition. A survey of 93 known phosphorylation sites showed that 88 of those possess at least one arginine at one of these positions (Kennelly and Krebs, 1991).

Follow up work from Suzanne Zukin's lab on PKA regulation of the NMDAR calcium permeability (Skeberdis et al., 2006) identified PKA consensus motifs in the GluN2B C-terminus. GluN2B containing receptors are differentially regulated by PKA than GluN2A containing NMDARs. In both cases PKA enhances the  $\text{Ca}^{2+}$ -influx, but differentially regulates the NMDAR-mediated total currents. Inhibition of PKA more profoundly reduced currents mediated by GluN2B containing receptors (Skeberdis et al., 2006). This effect could be due to a substantially greater fractional calcium current of GluN2B containing receptors (Sobczyk et al., 2005) or additional effects of PKA on permeation of also monovalent cations through GluN2B containing NMDARs.

Introduction of the S1166A mutation in the putative PKA phosphorylation site (K-R-D-S1166) in the GluN2B C-terminus completely abrogated the PKA-dependent increase in calcium permeability of recombinant NMDARs, expressed in HEK293 cells (Murphy and Zukin, unpublished data).

Characterization of the custom-made phospho-specific S1166 antibody (Fig. 3.16) revealed a specific phosphorylation-dependent signal. Investigation of GluN2B IPs demonstrated basal phosphorylation of S1166. This basal level of phosphorylation was removed by phosphatase treatment and upregulated by *in vitro* PKA phosphorylation (Fig. 3.16). S1166 phosphorylation was, along with the GluN2B subunit itself, enriched in purified postsynaptic density fractions (Fig. 3.17).

Emotional stress leads to activation of the locus coeruleus and the subsequent release of norepinephrine (noradrenaline) throughout the brain. The locus coeruleus sends adrenergic projections to different brain regions including the hippocampus (Tully and Bolshakov, 2010). Activation of  $\beta$ -adrenergic receptors with norepinephrine or through emotional stress resulted in GluA1 S845 phosphorylation in the hippocampus. Norepinephrine application also allowed LTP induction after mild electrical stimulation (10 Hz), which is normally not sufficient to induce LTP (Hu et al., 2007).

Stimulation of PKA activity in acute forebrain slices through activation of the  $G_{\alpha_s}$  coupled  $\beta$ -adrenergic receptor with isoproterenol not only increased

(as expected) S845 phosphorylation, but resulted in an even bigger increase of S1166 phosphorylation (Fig. 3.18). To show that modulation of S1166 phosphorylation is also important *in vivo* under emotionally charged conditions, hippocampal phosphorylation levels of forced swim stressed animals were investigated. Emotional arousal and subsequent  $\beta$ -adrenergic receptor stimulation not only facilitate LTP, but also learning and memory (Hu et al., 2007; McGaugh, 2004; Richter-Levin and Akirav, 2003). The forced swim-induced stress resulted in a strong upregulation of S845 as well as S1166 phosphorylation (Fig. 3.20). Surprisingly, injection of the  $\beta$ -adrenergic receptor antagonist propranolol only inhibited stress-induced S845 phosphorylation (Hu et al., 2007), but not S1166 phosphorylation (Fig. 3.21). Propranolol reduced basal, as well as forced swim-induced S845 phosphorylation (Fig. 3.21 B). Notably, the concurrent reduction in both basal and forced swim-induced phosphorylation still yielded in the same stress-dependent 2-fold increase of S845 phosphorylation (Fig. 3.21 C).

Stress results in a series of changes in neurotransmitter levels including norepinephrine, dopamine and serotonin (Hayley et al., 2001). Dopamine is another catecholamine neurotransmitter and activation of D<sub>1</sub>/D<sub>5</sub> dopamine receptors is important for the induction, expression and maintenance of hippocampal LTP (Huang and Kandel, 1995; Navakkode et al., 2007; Otmakhova and Lisman, 1996). In addition, in cultured neurons D<sub>1</sub>/D<sub>5</sub> receptor stimulation increases S845 phosphorylation as well as GluA1 surface expression (Chao et al., 2002; Gao et al., 2006). These effects seem to be primarily mediated by activation of D<sub>1</sub> receptors, because the impaired hippocampal LTP in D<sub>1</sub> knock-out mice can not be further reduced by a D<sub>1</sub>/D<sub>5</sub> receptor antagonist (Granado et al., 2008). The primary dopaminergic input to the hippocampus is provided by fibers from the midbrain dopaminergic neurons of the ventral tegmental area (Lisman and Grace, 2005).

Stimulation of PKA activity in acute forebrain slices through activation of the G<sub>αs</sub> coupled D<sub>1</sub>/D<sub>5</sub> dopamine receptor increased S845 and S1166 phosphorylation (Fig. 3.22). Injection of the D<sub>1</sub>/D<sub>5</sub> receptor antagonist SCH23390 neither reduced basal, nor the forced swim-induced increase of S845 or S1166 phosphorylation (Fig. 3.23). Activation of the D<sub>1</sub>/D<sub>5</sub> receptor as

well as the  $\beta$  adrenergic receptor clearly upregulated S1166 phosphorylation in acute slices. Potentially, activation of only one of these pathways under forced swim-induced stress is already sufficient to saturate S1166 phosphorylation. Support for a possible simultaneous stimulation of  $D_1$  and  $\beta$  adrenergic receptors also comes from a recent study, which reported both norepinephrine and dopamine release from locus coeruleus terminals in the hippocampus (Smith and Greene, 2012).

Combined injection of the  $\beta$ AR antagonist propranolol and the  $D_1/D_5$  receptor antagonist SCH23390 reduced basal S1166 phosphorylation levels (Fig. 3.24), but did not affect the forced swim-induced total increase in S1166 phosphorylation (Fig. 3.25). S845 phosphorylation displayed reduced basal and stress induced phosphorylation levels, similar to those observed during single propranolol injection.

In the striatum NMDAR mediated  $Ca^{2+}$ -influx is inhibited by the  $D_2$  dopamine receptor and enhanced by activation of the  $A_{2A}$  adenosine receptor in a PKA-dependent manner (Higley and Sabatini, 2010). Injection of the  $A_{2A}$ AR antagonist SCH58261 did not have any effect on basal or forced swim-induced phosphorylation of S845 or S1166 (Fig. 3.26).

There are multiple explanations as to why the inhibitors tested thus far have failed to show any effect on the stress induced increase in S1166 phosphorylation. One possibility would be the activation of a different Ser/Thr kinase, which is able to phosphorylate S1166 under the stress-induced conditions. On the other hand phosphorylation under basal conditions might be mainly mediated by PKA and regulated by a combination of the  $\beta$ AR  $D_1/D_5$  antagonist (Fig. 3.24). S831, just upstream of S845, on the GluA1 subunit is phosphorylated by CaMKII and PKC (Barria et al., 1997; Mammen et al., 1997; Roche et al., 1996). Forced swim-elicited stress also results in a strong upregulation of S831 phosphorylation (Fig. 3.26 D). Even though CaMKII and PKC activity is also upregulated during forced swim, preliminary data of direct hippocampal injection of the PKA selective inhibitor 8-Br-Rp-cAMPs support a PKA dependent phosphorylation of S1166. Direct hippocampal injection of the

PKA antagonist prevented the forced swim induced increase of S1166 phosphorylation (Fig. 3.28).

Another explanation centers on the problem of the efficiency of drug delivery. For example intracerebroventricular (ICV) injection of membrane permeant Rp-cAMPs and myristoylated PKI, another potent PKA inhibitor, did not block any of the monitored PKA dependent phosphorylations in the hippocampus (data not shown). Even though the ICV injection of the drugs did not require crossing of the blood brain barrier, delivery to the hippocampus was not sufficient to block PKA activity. This is probably due to the slow rate of drug diffusion together with the rapid flow rate of cerebrospinal fluid through the ventricular compartments before it is rapidly absorbed into the peripheral blood stream at the superior saggital sinus (Pardridge, 2005). Direct injection of Rp-cAMPs into the hippocampus, however, was sufficient in even reducing the forced swim induced increase of S1166 as well as S845 (Fig. 3.28). The tested antagonists of the G-protein coupled receptors ( $\beta$ AR, D<sub>1</sub>/D<sub>5</sub>R and A<sub>2A</sub>R) were injected intraperitoneal (i.p.). The observed effects on S845 phosphorylation after propranolol ( $\beta$ AR antagonist) injection demonstrate successful delivery (Fig. 3.24, Fig. 3.25). The combined effect of propranolol and SCH23390 (D<sub>1</sub>/D<sub>5</sub> antagonist) on basal phosphorylation of S1166 also suggests at least partial delivery of SCH23390 (Fig. 3.24). Since the simultaneous injection affected basal GluN2B S1166 phosphorylation, the effect after combined direct hippocampal injection will be tested. This experiment will address remaining concerns about efficient drug delivery and again test whether the forced swim-induced increase in S1166 phosphorylation can be inhibited by a combination of  $\beta$ AR and D<sub>1</sub>/D<sub>5</sub> receptor antagonists.

In an attempt to rule out effects of over-activation and saturation of the system, a milder swim stress protocol (shorter duration and higher water temperature) was performed. Originally designed to better evaluate the effect of drug injections on the stress-induced PKA phosphorylations, the milder forced swim actually impaired analysis of differences in the phosphorylation levels. The milder swim stress enhanced the variation in the stress level of the

individual animals. This resulted in an overall reduced increase in PKA phosphorylation (Fig. 3.27), but not in an overall similar medium stress level with consistently reduced PKA phosphorylation levels of S845 and S1166, compared to the more aversive forced swim conditions.

S845 phosphorylation of GluA1 and S1166 phosphorylation of GluN2B seem to be differentially regulated, while propranolol reduced both basal and forced swim-induced S845 phosphorylation, it did not exhibit any effect on S1166 phosphorylation levels (Fig. 3.21). This differential regulation might be due to the formation of different signaling complexes. In fact the NMDAR is indirectly coupled to PKA over two different A-kinase anchoring proteins (AKAPs). More precisely, the AKAP Yotiao, which is directly interacting with the C-terminus (C1 region) of GluN1 links NMDARs to PKA and PP1, while AKAP5 (AKAP150), which binds via PSD-95 to the GluN2 subunits, links them to PKA, PKC and PP2B (Colledge et al., 2000; Sanderson and Dell'Acqua, 2011; Westphal et al., 1999; Wong and Scott, 2004). GluA1 is together with the  $\beta$  adrenergic receptor in a signaling complex (Joiner et al., 2010) and is also linked indirectly through PSD-95 and SAP-97 to PKA via AKAP5 (Colledge et al., 2000; Sanderson and Dell'Acqua, 2011; Wong and Scott, 2004).

To investigate whether AKAP5 anchored PKA is important for the regulation of S1166, acute slices from WT, AKAP5 knock-out and AKAP5 mutant mice (D36) were stimulated with isoproterenol. D36 mice selectively miss the PKA anchoring site through deletion of the last 36 amino acid residues. This truncation does not interfere with AKAP5 anchoring of PP2B and PKC and should avoid other potential indirect compensatory mechanisms due to the complete loss of AKAP5 in the KO (Weisenhaus et al., 2010).  $\beta$ AR activation resulted as observed previously in increased phosphorylation of S1166, and no discernable difference between WT, AKAP5 KO and D36 genotypes (Fig. 3.19). Accordingly, AKAP5 is not important for S1166 phosphorylation even though activity-induced phosphorylation levels of S845 are reduced in D36 mice (Lu et al., 2007) and AKAP5 KO mice (Zhang and Hell, unpublished data).

The differential regulation and anchoring of PKA to the NMDAR through Yotiao is probably underlying the differential effects seen on S1166 and S845 phosphorylation. One surprising finding with this regard is the S897 phosphorylation on the GluN1 subunit, which seems to be regulated similar to S845. Be that as it may, S897 is a PKA phosphorylation site on GluN1 important for suppression of ER retention and forward trafficking of the NMDAR to the plasma membrane over a number of hours (Scott et al., 2003), and not involved in fast postsynaptic modulation of the NMDAR (Tingley et al., 1997). It is thus quite conceivable that S897 regulation differs from those for S1166. The presented results suggest that PKA anchored at different regions of the NMDAR shows preference for different target sites within the same receptor.

#### **4.4 Side Effects of Cell Penetrating Peptides (CPP)**

Cellular internalization is one of the main problems in drug design and controlled drug delivery. Besides its potential for clinical applications, the discovery of cell penetrating peptides (CPPs) also provided a valuable research tool for the fast and specific inhibition or disruption of protein interactions and signaling complexes. The application of CPPs constitutes a specific way to study acute physiological effects, without dealing with potential compensatory problems correlated with protein overexpression or knock-down.

The discovery of CPPs goes back to the unexpected observation that certain full-length proteins or protein domains (protein transduction domains) were able to cross the plasma membrane. The first described CPPs or protein transduction domains are the Tat sequence, the active 11 amino acid sequence important for the penetration of cells by the transactivator of transcription (TAT) protein of the Human Immunodeficiency Virus (Green and Loewenstein, 1988; Vives et al., 1997) and penetratin. The later discovered penetratin (Antp) consists of the 16 amino acid peptide sequence of the homeodomain of the *Drosophila melanogaster* transcription factor Antennapedia, shown to translocate across the membrane (Derossi et al.,

1994; Joliot et al., 1991). Tat, penetratin as well as oligoarginines (Wender et al., 2008), like the 11R sequence, belong to the most studied group of arginine-rich-cell-penetrating peptides.

In our hands the 11R sequence revealed cytotoxic side effects in cultured hippocampal neurons at a concentration of 10  $\mu\text{M}$  (Fig. 3.29) and inhibited CaMKII as well as PKA activity in a concentration dependent manner. Cytotoxicity at a concentration of 10  $\mu\text{M}$  and in a length-dependent manner has been reported before for Tat and Antp (Cardozo et al., 2007). The study by Cardozo et al., demonstrated that Tat conjugates are more toxic than the 10 aa Tat transporter sequence alone, which could be applied up to 100  $\mu\text{M}$ , and that the level of cytotoxicity at a certain peptide concentration depends on the length of the peptide.

The observed side effects seen on CaMKII and PKA activity were more surprising. 11R conjugated peptides blocked CaMKII activity by 50% at a concentration of 3.3  $\mu\text{M}$  (Fig. 3.30 D) and PKA activity by 50% at a concentration of just 1  $\mu\text{M}$  (Fig. 3.31 B, D). The same unconjugated or myristoylated peptide had no or minimal effects on CaMKII as well as PKA activity. A different Tat conjugated peptide also did not affect PKA activity, even not at 10  $\mu\text{M}$  (Fig. 3.31 D).

Even though the level of cytotoxicity of CPPs seems to depend on the peptide length and not on the charge (Cardozo et al., 2007), the observed effects on CaMKII and PKA kinase activity implicate a dependency on the charge or the number of present arginine residues. The 11R sequence was originally designed from the polybasic Tat sequence, which already contains multiple lysine and arginine residues (Wender et al., 2008). Based on this polybasic nature, the observation that the Tat sequence (as well as the unconjugated or myristoylated peptide) had no effect on PKA activity (Fig. 3.31 D), besides a slight insignificant and concentration independent tendency to reduction, was unexpected. It shows that the precise localization of arginine and presumably lysine residues in the Tat leader peptide is critical.

Taken together these findings suggest caution for choosing the right cell penetrating peptide sequence and recommend the use of the Tat sequence over oligoarginines, or at least oligoarginines of a length of 11 or

higher, even though they have proven superior with regard to cell permeability (Wender et al., 2008). Generally, if using CPP conjugated peptides, these should be designed with the shortest possible sequence and the highest possible affinity to allow the use of concentrations below 10 or optimally 1  $\mu\text{M}$ . Myristoylation thus appears as the more desirable modification for making peptides membrane permeant.

## 5 Summary

### 5.1 Summary

Long term potentiation (LTP) is thought to be the cellular equivalent of learning and memory. The cellular changes occurring during this long-lasting strengthening of synaptic transmission are best studied at glutamatergic synapses in the CA1 region of the hippocampus. This type of LTP is, like spatial learning and memory, dependent on the N-methyl-D-aspartate-type glutamate receptor (NMDAR) as well as the calcium/calmodulin-dependent protein kinase II (CaMKII).

Using GluN2B KI mutant mice, the importance of the CaMKII/NMDAR interaction for spatial learning and memory formation was investigated in this study. GluN2B KI mice carry two point mutations that specifically disrupt the critical interaction between CaMKII and the GluN2B subunit of the NMDAR. The findings presented here provide a specific requirement for the activity-dependent interaction of CaMKII with the NMDAR during the acquisition of elaborate spatial learning tasks under aversive, stressful conditions. Specifically, learning of the Morris Water Maze (MWM) by GluN2B KI mice is impaired in a single day massed training paradigm. This learning impairment is not observed in spaced MWM training distributed over 6 days, but this paradigm reveals a subsequent consolidation deficit (Halt et al., 2012). The presented results argue not only for a role for CaMKII binding to GluN2B during learning in emotional situations but also consolidation that becomes obvious under the more demanding MWM conditions (Halt et al., 2012) but not the less stressful Barnes maze, as presented here. Contextual fear conditioning is a strong and aversive associative learning paradigm and is not affected in the GluN2B KI mice. This discrepancy between spatial and contextual learning might be due to an unaffected formation of a spatial representation before shock delivery and increased stress levels or slight regional and signaling differences between the two forms of learning.

The activity-induced clustering of CaMKII at postsynaptic sites and the underlying interaction with the NMDAR contribute to synapse specificity of LTP. As part of this thesis it was shown in hippocampal cultures that the activation, diffusion and postsynaptic trapping of endogenous CaMKII takes about 3 min. The clustering of the bulk of the translocated kinase is, except for a small stable pool, reversed within 5 min. In addition, the activity-driven translocation of the kinase is dependent on postsynaptic anchoring of apocalmodulin under basal conditions by neurogranin, but the CaMKII interaction with the GluN1 subunit of the NMDAR is not required.

The calcium influx through the NMDAR is important for the modulation of synaptic plasticity and is regulated through PKA phosphorylation. In this thesis the novel regulatory phosphorylation site S1166 on the GluN2B subunit of the NMDAR was biochemically characterized. It was shown that S1166 phosphorylation is controlled by norepinephrine and dopamine in acute forebrain slices as well as *in vivo*, at least under basal conditions. S1166 phosphorylation is upregulated through forced swim-induced stress and might be important for plasticity and learning under emotionally charged conditions.

## 5.2 Zusammenfassung

Langzeit-Potenzierung (LTP von eng. long-term potentiation) ist die langandauernde Verstärkung der synaptischen Übertragung. Diese Form der synaptischen Plastizität wurde am besten an den sogenannten Schaffer-Kollateralen Synapsen untersucht. Für diese Form der Langzeit-Potenzierung sind, genauso wie für räumliches Lernen, der ionotrope Glutamat-aktivierte N-Methyl-D-Aspartat-Rezeptor (NMDA-Rezeptor) und die Kalzium/Calmodulin-abhängige Kinase (CaMKII) unerlässlich.

Im Rahmen dieser Arbeit wurde mit Hilfe eines Knock-in (KI) Mausmodells die Rolle der direkten Interaktion zwischen dem NMDA-Rezeptor und CaMKII im Zusammenhang mit räumlichen Lern- und Gedächtnisprozessen untersucht. Die verwendete GluN2B KI Maus besitzt in der GluN2B-Untereinheit des NMDA-Rezeptors zwei mutierte Aminosäuren, die selektiv die Interaktion mit CaMKII unterbinden. Die erhaltenen Ergebnisse zeigen, dass die Interaktion zwischen CaMKII und dem NMDA-Rezeptor besonders für schwierigeres räumliches Lernen in stressvollen Situationen wichtig ist. Speziell das Lernen im „Morris-Water-Maze“ (ein Verhaltensexperiment zur Untersuchung des räumlichen Lernens) ist in einem gehäuften ein-Tages-Training beeinträchtigt. Dieses Lerndefizit ist nicht sichtbar, wenn die Mäuse über mehrere Tage gestaffelt hinweg trainiert werden. Dafür resultiert die Unterbrechung der Interaktion zwischen dem NMDA-Rezeptor und CaMKII in diesem Fall in einem beeinträchtigten Erinnerungsvermögen (Halt et al., 2012). Die Ergebnisse zeigen das diese Interaktion für Lern- und Gedächtnisprozesse in emotionalen oder stressvollen Situation wichtig ist, während räumliches Lernen in dem weniger Stress auslösendem Barnes Trockenlabyrinth nicht beeinflusst wird. Die beschriebenen Ergebnisse zeigen auch, daß die massiv Angst-einflössende klassische kontextabhängige Angstkonditionierung (fear conditioning) in den KI Mäusen ebenfalls nicht beeinflusst ist.

Die aktivitätsabhängige Rekrutierung von CaMKII zur postsynaptischen Membran und dem NMDA-Rezeptor wurde ebenfalls auf molekularer Ebene in hippocampalen Neuronen untersucht. Diese spezifische Translokation

zur Synapse ist innerhalb von 3 Minuten nach der anfänglichen Glutamatstimulation abgeschlossen, wobei nur ein kleiner Teil der ursprünglich rekrutierten Kinase dauerhaft an der Postsynapse verankert wird und auch noch 5-60 Minuten nach Stimulation sichtbar ist. Die Verankerung von CaMKII ist dabei nicht abhängig von der Interaktion mit der GluN1 Untereinheit des NMDA-Rezeptors. Allerdings wird die Translokation durch das an der Postsynapse angereicherte Protein Neurogranin reguliert. Neurogranin kontrolliert die Verfügbarkeit von apo-Calmodulin und damit die Aktivierung von CaMKII.

Der Kalzium-Einstrom durch den NMDA-Rezeptor ist wichtig für die Aktivierung von CaMKII und die Regulation der synaptischen Plastizität. Die Menge des einströmenden Kalziums ist ein wichtiger Faktor, der entscheidet, ob es zu einer Verstärkung oder zu einer Abschwächung der Übertragung kommt. Es wurde gezeigt, dass speziell die Phosphorylierung durch die Proteinkinase A (PKA) die Leitfähigkeit für Kalzium beeinflusst. Die diesem Phänomen zu Grunde liegende neu-identifizierte Phosphorylierungsstelle S1166 auf der GluN2B Untereinheit des NMDA-Rezeptors wurde innerhalb dieser Arbeit charakterisiert. In akuten Gehirnschnitten so wie *in vivo* wurde die Phosphorylierung von S1166 nach Stimulation durch Noradrenalin oder Dopamin nachgewiesen. Die Phosphorylierung von S1166 wird durch Stress während erzwungenem Schwimmen im Hippocampus von Ratten hochreguliert und könnte eine wichtige Rolle für Lern- und Gedächtnisprozesse unter emotionalem Stress spielen.

## 6 References

Abraham, W.C., Logan, B., Greenwood, J.M., and Dragunow, M. (2002). Induction and experience-dependent consolidation of stable long-term potentiation lasting months in the hippocampus. *J Neurosci* 22, 9626-9634.

Ahmed, R., Zha, X.M., Green, S.H., and Dailey, M.E. (2006). Synaptic activity and F-actin coordinately regulate CaMKIIalpha localization to dendritic postsynaptic sites in developing hippocampal slices. *Mol Cell Neurosci* 31, 37-51.

Akyol, Z., Bartos, J.A., Merrill, M.A., Faga, L.A., Jaren, O.R., Shea, M.A., and Hell, J.W. (2004). Apo-calmodulin binds with its C-terminal domain to the N-methyl-D-aspartate receptor NR1 C0 region. *J Biol Chem* 279, 2166-2175.

Al-Hallaq, R.A., Conrads, T.P., Veenstra, T.D., and Wenthold, R.J. (2007). NMDA di-heteromeric receptor populations and associated proteins in rat hippocampus. *J Neurosci* 27, 8334-8343.

Bach, M.E., Hawkins, R.D., Osman, M., Kandel, E.R., and Mayford, M. (1995). Impairment of spatial but not contextual memory in CaMKII mutant mice with a selective loss of hippocampal LTP in the range of the theta frequency. *Cell* 81, 905-915.

Balschun, D., Manahan-Vaughan, D., Wagner, T., Behnisch, T., Reymann, K.G., and Wetzel, W. (1999). A specific role for group I mGluRs in hippocampal LTP and hippocampus-dependent spatial learning. *Learn Mem* 6, 138-152.

Bard, L., Sainlos, M., Bouchet, D., Cousins, S., Mikasova, L., Breillat, C., Stephenson, F.A., Imperiali, B., Choquet, D., and Groc, L. (2010). Dynamic and specific interaction between synaptic NR2-NMDA receptor and PDZ proteins. *Proc Natl Acad Sci U S A* 107, 19561-19566.

Barria, A., Derkach, V., and Soderling, T. (1997). Identification of the Ca<sup>2+</sup>/calmodulin-dependent protein kinase II regulatory phosphorylation site in the alpha-amino-3-hydroxyl-5-methyl-4-isoxazole-propionate-type glutamate receptor. *J Biol Chem* 272, 32727-32730.

Barria, A., and Malinow, R. (2005). NMDA receptor subunit composition controls synaptic plasticity by regulating binding to CaMKII. *Neuron* 48, 289-301.

Baudier, J., Deloulme, J.C., Van Dorsselaer, A., Black, D., and Matthes, H.W. (1991). Purification and characterization of a brain-specific protein kinase C substrate, neurogranin (p17). Identification of a consensus amino acid sequence between neurogranin and neuromodulin (GAP43) that corresponds to the protein kinase C phosphorylation site and the calmodulin-binding domain. *J Biol Chem* 266, 229-237.

Bayer, K.U., De Koninck, P., Leonard, A.S., Hell, J.W., and Schulman, H. (2001). Interaction with the NMDA receptor locks CaMKII in an active conformation. *Nature* 411, 801-805.

Bayer, K.U., LeBel, E., McDonald, G.L., O'Leary, H., Schulman, H., and De Koninck, P. (2006). Transition from reversible to persistent binding of CaMKII to postsynaptic sites and NR2B. *J Neurosci* 26, 1164-1174.

Bejar, R., Yasuda, R., Krugers, H., Hood, K., and Mayford, M. (2002). Transgenic calmodulin-dependent protein kinase II activation: dose-dependent effects on synaptic plasticity, learning, and memory. *J Neurosci* 22, 5719-5726.

Berta, S., Gert, L., Harald, H., and Sudarshan, P. (2007). Barnes maze, a useful task to assess spatial reference memory in the mice.

Bingol, B., Wang, C.F., Arnott, D., Cheng, D., Peng, J., and Sheng, M. (2010). Autophosphorylated CaMKIIalpha acts as a scaffold to recruit proteasomes to dendritic spines. *Cell* 140, 567-578.

Bliss, T.V., and Lomo, T. (1973). Long-lasting potentiation of synaptic transmission in the dentate area of the anaesthetized rabbit following stimulation of the perforant path. *J Physiol* 232, 331-356.

Borgesius, N.Z., van Woerden, G.M., Buitendijk, G.H., Keijzer, N., Jaarsma, D., Hoogenraad, C.C., and Elgersma, Y. (2011). betaCaMKII plays a nonenzymatic role in hippocampal synaptic plasticity and learning by targeting alphaCaMKII to synapses. *J Neurosci* 31, 10141-10148.

Brocke, L., Chiang, L.W., Wagner, P.D., and Schulman, H. (1999). Functional implications of the subunit composition of neuronal CaM kinase II. *J Biol Chem* 274, 22713-22722.

Brun, V.H., Ytterbo, K., Morris, R.G., Moser, M.B., and Moser, E.I. (2001). Retrograde amnesia for spatial memory induced by NMDA receptor-mediated long-term potentiation. *J Neurosci* 21, 356-362.

Buard, I., Coultrap, S.J., Freund, R.K., Lee, Y.S., Dell'Acqua, M.L., Silva, A.J., and Bayer, K.U. (2010). CaMKII "autonomy" is required for initiating but not for maintaining neuronal long-term information storage. *J Neurosci* 30, 8214-8220.

Burgin, K.E., Waxham, M.N., Rickling, S., Westgate, S.A., Mobley, W.C., and Kelly, P.T. (1990). In situ hybridization histochemistry of Ca<sup>2+</sup>/calmodulin-dependent protein kinase in developing rat brain. *J Neurosci* 10, 1788-1798.

Cardozo, A.K., Buchillier, V., Mathieu, M., Chen, J., Ortis, F., Ladriere, L., Allaman-Pillet, N., Poirot, O., Kellenberger, S., Beckmann, J.S., *et al.* (2007). Cell-permeable peptides induce dose- and length-dependent cytotoxic effects. *Biochim Biophys Acta* 1768, 2222-2234.

Carlin, R.K., Grab, D.J., Cohen, R.S., and Siekevitz, P. (1980). Isolation and characterization of postsynaptic densities from various brain regions: enrichment of different types of postsynaptic densities. *J Cell Biol* 86, 831-845.

Carvalho, M., O., SILVA, J., A., Balleine, and W., B. (2001). Evidence of selective learning deficits on tests of pavlovian and instrumental conditioning in  $\alpha$ -CaMKII T286A mutant mice, Vol 14 (New York, NY, ETATS-UNIS: Human Sciences Press).

Chang, B.H., Mukherji, S., and Soderling, T.R. (1998). Characterization of a calmodulin kinase II inhibitor protein in brain. *Proc Natl Acad Sci U S A* 95, 10890-10895.

Chang, B.H., Mukherji, S., and Soderling, T.R. (2001). Calcium/calmodulin-dependent protein kinase II inhibitor protein: localization of isoforms in rat brain. *Neuroscience* 102, 767-777.

Chao, S.Z., Lu, W., Lee, H.K., Haganir, R.L., and Wolf, M.E. (2002). D(1) dopamine receptor stimulation increases GluR1 phosphorylation in postnatal nucleus accumbens cultures. *J Neurochem* 81, 984-992.

Chen, C., Rainnie, D.G., Greene, R.W., and Tonegawa, S. (1994). Abnormal fear response and aggressive behavior in mutant mice deficient for alpha-calcium-calmodulin kinase II. *Science* 266, 291-294.

Chen, C.C. (1994). Alterations of protein kinase C isozyme and substrate proteins in mouse brain after electroconvulsive seizures. *Brain Res* 648, 65-72.

Chen, H.X., Otmakhov, N., Strack, S., Colbran, R.J., and Lisman, J.E. (2001). Is persistent activity of calcium/calmodulin-dependent kinase required for the maintenance of LTP? *J Neurophysiol* 85, 1368-1376.

Chen, Y., and Hell, J.W. (2004). Glutamate-induced endogenous CaMKII clustering in rat hippocampal neuronal cultures. *Soc Neurosci Abstr*, 969.918.

Chen, Y., Stevens, B., Chang, J., Milbrandt, J., Barres, B.A., and Hell, J.W. (2008). NS21: re-defined and modified supplement B27 for neuronal cultures. *J Neurosci Methods* 171, 239-247.

Colbran, R.J. (2004). Targeting of calcium/calmodulin-dependent protein kinase II. *Biochem J* 378, 1-16.

Colbran, R.J., and Brown, A.M. (2004). Calcium/calmodulin-dependent protein kinase II and synaptic plasticity. *Curr Opin Neurobiol* 14, 318-327.

Colledge, M., Dean, R.A., Scott, G.K., Langeberg, L.K., Haganir, R.L., and Scott, J.D. (2000). Targeting of PKA to glutamate receptors through a MAGUK-AKAP complex. *Neuron* 27, 107-119.

- Commins, S., Cunningham, L., Harvey, D., and Walsh, D. (2003). Massed but not spaced training impairs spatial memory. *Behav Brain Res* 139, 215-223.
- Coultrap, S.J., Vest, R.S., Ashpole, N.M., Hudmon, A., and Bayer, K.U. (2011). CaMKII in cerebral ischemia. *Acta Pharmacol Sin* 32, 861-872.
- Cull-Candy, S.G., and Leszkiewicz, D.N. (2004). Role of distinct NMDA receptor subtypes at central synapses. *Sci STKE* 2004, re16.
- Curzon, P., Rustay, N.R., and Browman, K.E. (2009). Cued and Contextual Fear Conditioning for Rodents. In *Methods of Behavior Analysis in Neuroscience*, J.J. Buccafusco, ed. (Boca Raton (FL)).
- Dalby, B., Cates, S., Harris, A., Ohki, E.C., Tilkins, M.L., Price, P.J., and Ciccarone, V.C. (2004). Advanced transfection with Lipofectamine 2000 reagent: primary neurons, siRNA, and high-throughput applications. *Methods* 33, 95-103.
- Derossi, D., Joliot, A.H., Chassaing, G., and Prochiantz, A. (1994). The third helix of the Antennapedia homeodomain translocates through biological membranes. *J Biol Chem* 269, 10444-10450.
- Deshayes, S., Morris, M.C., Divita, G., and Heitz, F. (2005). Cell-penetrating peptides: tools for intracellular delivery of therapeutics. *Cell Mol Life Sci* 62, 1839-1849.
- Diez-Guerra, F.J. (2010). Neurogranin, a link between calcium/calmodulin and protein kinase C signaling in synaptic plasticity. *IUBMB Life* 62, 597-606.
- Dosemeci, A., Tao-Cheng, J.H., Vinade, L., Winters, C.A., Pozzo-Miller, L., and Reese, T.S. (2001). Glutamate-induced transient modification of the postsynaptic density. *Proc Natl Acad Sci U S A* 98, 10428-10432.
- Easton, A.C., Lucchesi, W., Schumann, G., Giese, K.P., Muller, C.P., and Fernandes, C. (2011). alphaCaMKII autophosphorylation controls exploratory activity to threatening novel stimuli. *Neuropharmacology* 61, 1424-1431.
- Ehlers, M.D. (2003). Activity level controls postsynaptic composition and signaling via the ubiquitin-proteasome system. *Nat Neurosci* 6, 231-242.
- Elgersma, Y., Fedorov, N.B., Ikonen, S., Choi, E.S., Elgersma, M., Carvalho, O.M., Giese, K.P., and Silva, A.J. (2002). Inhibitory autophosphorylation of CaMKII controls PSD association, plasticity, and learning. *Neuron* 36, 493-505.
- Elgersma, Y., Sweatt, J.D., and Giese, K.P. (2004). Mouse genetic approaches to investigating calcium/calmodulin-dependent protein kinase II function in plasticity and cognition. *J Neurosci* 24, 8410-8415.
- Erondu, N.E., and Kennedy, M.B. (1985). Regional distribution of type II Ca<sup>2+</sup>/calmodulin-dependent protein kinase in rat brain. *J Neurosci* 5, 3270-3277.

Fanselow, M.S. (2000). Contextual fear, gestalt memories, and the hippocampus. *Behav Brain Res* 110, 73-81.

Fetterolf, F., and Foster, K.A. (2011). Regulation of long-term plasticity induction by the channel and C-terminal domains of GluN2 subunits. *Mol Neurobiol* 44, 71-82.

Flint, A.C., Maisch, U.S., Weishaupt, J.H., Kriegstein, A.R., and Monyer, H. (1997). NR2A subunit expression shortens NMDA receptor synaptic currents in developing neocortex. *J Neurosci* 17, 2469-2476.

Frankland, P.W., Josselyn, S.A., Anagnostaras, S.G., Kogan, J.H., Takahashi, E., and Silva, A.J. (2004). Consolidation of CS and US representations in associative fear conditioning. *Hippocampus* 14, 557-569.

Frankland, P.W., O'Brien, C., Ohno, M., Kirkwood, A., and Silva, A.J. (2001). Alpha-CaMKII-dependent plasticity in the cortex is required for permanent memory. *Nature* 411, 309-313.

Fukaya, M., Kato, A., Lovett, C., Tonegawa, S., and Watanabe, M. (2003). Retention of NMDA receptor NR2 subunits in the lumen of endoplasmic reticulum in targeted NR1 knockout mice. *Proc Natl Acad Sci U S A* 100, 4855-4860.

Fukunaga, K., Stoppini, L., Miyamoto, E., and Muller, D. (1993). Long-term potentiation is associated with an increased activity of Ca<sup>2+</sup>/calmodulin-dependent protein kinase II. *J Biol Chem* 268, 7863-7867.

Gao, C., Sun, X., and Wolf, M.E. (2006). Activation of D1 dopamine receptors increases surface expression of AMPA receptors and facilitates their synaptic incorporation in cultured hippocampal neurons. *J Neurochem* 98, 1664-1677.

Gardoni, F., Caputi, A., Cimino, M., Pastorino, L., Cattabeni, F., and Di Luca, M. (1998). Calcium/calmodulin-dependent protein kinase II is associated with NR2A/B subunits of NMDA receptor in postsynaptic densities. *J Neurochem* 71, 1733-1741.

Gardoni, F., Schrama, L.H., van Dalen, J.J., Gispen, W.H., Cattabeni, F., and Di Luca, M. (1999). AlphaCaMKII binding to the C-terminal tail of NMDA receptor subunit NR2A and its modulation by autophosphorylation. *FEBS Lett* 456, 394-398.

Gerendasy, D.D., Herron, S.R., Jennings, P.A., and Sutcliffe, J.G. (1995). Calmodulin stabilizes an amphiphilic alpha-helix within RC3/neurogranin and GAP-43/neuromodulin only when Ca<sup>2+</sup> is absent. *J Biol Chem* 270, 6741-6750.

Gerendasy, D.D., and Sutcliffe, J.G. (1997). RC3/neurogranin, a postsynaptic calpacitin for setting the response threshold to calcium influxes. *Mol Neurobiol* 15, 131-163.

- Giese, K.P., Fedorov, N.B., Filipkowski, R.K., and Silva, A.J. (1998). Autophosphorylation at Thr286 of the alpha calcium-calmodulin kinase II in LTP and learning. *Science* 279, 870-873.
- Granado, N., Ortiz, O., Suarez, L.M., Martin, E.D., Cena, V., Solis, J.M., and Moratalla, R. (2008). D1 but not D5 dopamine receptors are critical for LTP, spatial learning, and LTP-Induced arc and zif268 expression in the hippocampus. *Cereb Cortex* 18, 1-12.
- Green, M., and Loewenstein, P.M. (1988). Autonomous functional domains of chemically synthesized human immunodeficiency virus tat trans-activator protein. *Cell* 55, 1179-1188.
- Griffith, L.C. (2004). Regulation of calcium/calmodulin-dependent protein kinase II activation by intramolecular and intermolecular interactions. *J Neurosci* 24, 8394-8398.
- Halt, A.R., Dallapiazza, R.F., Zhou, Y., Stein, I.S., Qian, H., Juntti, S., Wojcik, S., Brose, N., Silva, A.J., and Hell, J.W. (2012). CaMKII binding to GluN2B is critical during memory consolidation. *EMBO J* 31, 1203-1216.
- Harrison, F.E., Hosseini, A.H., and McDonald, M.P. (2009). Endogenous anxiety and stress responses in water maze and Barnes maze spatial memory tasks. *Behav Brain Res* 198, 247-251.
- Hasegawa, S., Furuichi, T., Yoshida, T., Endoh, K., Kato, K., Sado, M., Maeda, R., Kitamoto, A., Miyao, T., Suzuki, R., *et al.* (2009). Transgenic up-regulation of alpha-CaMKII in forebrain leads to increased anxiety-like behaviors and aggression. *Mol Brain* 2, 6.
- Hayley, S., Borowski, T., Merali, Z., and Anisman, H. (2001). Central monoamine activity in genetically distinct strains of mice following a psychogenic stressor: effects of predator exposure. *Brain Res* 892, 293-300.
- Hebb, D.O. (1949). *The organization of behavior; a neuropsychological theory* (New York,: Wiley).
- Higley, M.J., and Sabatini, B.L. (2010). Competitive regulation of synaptic Ca<sup>2+</sup> influx by D2 dopamine and A2A adenosine receptors. *Nat Neurosci* 13, 958-966.
- Hu, H., Real, E., Takamiya, K., Kang, M.G., Ledoux, J., Huganir, R.L., and Malinow, R. (2007). Emotion enhances learning via norepinephrine regulation of AMPA-receptor trafficking. *Cell* 131, 160-173.
- Huang, K.P., Huang, F.L., Li, J., Schuck, P., and McPhie, P. (2000). Calcium-sensitive interaction between calmodulin and modified forms of rat brain neurogranin/RC3. *Biochemistry* 39, 7291-7299.
- Huang, Y.Y., and Kandel, E.R. (1995). D1/D5 receptor agonists induce a protein synthesis-dependent late potentiation in the CA1 region of the hippocampus. *Proc Natl Acad Sci U S A* 92, 2446-2450.

Hudmon, A., Lebel, E., Roy, H., Sik, A., Schulman, H., Waxham, M.N., and De Koninck, P. (2005). A mechanism for Ca<sup>2+</sup>/calmodulin-dependent protein kinase II clustering at synaptic and nonsynaptic sites based on self-association. *J Neurosci* 25, 6971-6983.

Hudmon, A., and Schulman, H. (2002). Neuronal CA<sup>2+</sup>/calmodulin-dependent protein kinase II: the role of structure and autoregulation in cellular function. *Annu Rev Biochem* 71, 473-510.

Irvine, E.E., Danhiez, A., Radwanska, K., Nassim, C., Lucchesi, W., Godaux, E., Ris, L., and Giese, K.P. (2011). Properties of contextual memory formed in the absence of alphaCaMKII autophosphorylation. *Mol Brain* 4, 8.

Irvine, E.E., Vernon, J., and Giese, K.P. (2005). AlphaCaMKII autophosphorylation contributes to rapid learning but is not necessary for memory. *Nat Neurosci* 8, 411-412.

Jalan-Sakrikar, N., Bartlett, R.K., Baucum, A.J., and Colbran, R.J. (2012). Substrate-selective and calcium-independent activation of CaMKII by alpha-actinin. *J Biol Chem*.

Jama, A.M., Fenton, J., Robertson, S.D., and Torok, K. (2009). Time-dependent autoinactivation of phospho-Thr286-alphaCa<sup>2+</sup>/calmodulin-dependent protein kinase II. *J Biol Chem* 284, 28146-28155.

Jiao, Y., Jalan-Sakrikar, N., Robison, A.J., Baucum, A.J., 2nd, Bass, M.A., and Colbran, R.J. (2011). Characterization of a central Ca<sup>2+</sup>/calmodulin-dependent protein kinase II alpha/beta binding domain in densin that selectively modulates glutamate receptor subunit phosphorylation. *J Biol Chem* 286, 24806-24818.

Jiao, Y., Robison, A.J., Bass, M.A., and Colbran, R.J. (2008). Developmentally regulated alternative splicing of densin modulates protein-protein interaction and subcellular localization. *J Neurochem* 105, 1746-1760.

Joiner, M.L., Lise, M.F., Yuen, E.Y., Kam, A.Y., Zhang, M., Hall, D.D., Malik, Z.A., Qian, H., Chen, Y., Ulrich, J.D., *et al.* (2010). Assembly of a beta2-adrenergic receptor--GluR1 signalling complex for localized cAMP signalling. *EMBO J* 29, 482-495.

Joliot, A., Pernelle, C., Deagostini-Bazin, H., and Prochiantz, A. (1991). Antennapedia homeobox peptide regulates neural morphogenesis. *Proc Natl Acad Sci U S A* 88, 1864-1868.

Kennelly, P.J., and Krebs, E.G. (1991). Consensus sequences as substrate specificity determinants for protein kinases and protein phosphatases. *J Biol Chem* 266, 15555-15558.

Kogan, J.H., Frankland, P.W., Blendy, J.A., Coblenz, J., Marowitz, Z., Schutz, G., and Silva, A.J. (1997). Spaced training induces normal long-term memory in CREB mutant mice. *Curr Biol* 7, 1-11.

Kramar, E.A., Babayan, A.H., Gavin, C.F., Cox, C.D., Jafari, M., Gall, C.M., Rumbaugh, G., and Lynch, G. (2012). Synaptic evidence for the efficacy of spaced learning. *Proc Natl Acad Sci U S A* 109, 5121-5126.

Kristensen, A.S., Jenkins, M.A., Banke, T.G., Schousboe, A., Makino, Y., Johnson, R.C., Huganir, R., and Traynelis, S.F. (2011). Mechanism of Ca<sup>2+</sup>/calmodulin-dependent kinase II regulation of AMPA receptor gating. *Nat Neurosci* 14, 727-735.

Lau, C.G., Takeuchi, K., Rodenas-Ruano, A., Takayasu, Y., Murphy, J., Bennett, M.V., and Zukin, R.S. (2009). Regulation of NMDA receptor Ca<sup>2+</sup> signalling and synaptic plasticity. *Biochem Soc Trans* 37, 1369-1374.

Lau, C.G., and Zukin, R.S. (2007). NMDA receptor trafficking in synaptic plasticity and neuropsychiatric disorders. *Nat Rev Neurosci* 8, 413-426.

Lee, H.K., Barbarosie, M., Kameyama, K., Bear, M.F., and Huganir, R.L. (2000). Regulation of distinct AMPA receptor phosphorylation sites during bidirectional synaptic plasticity. *Nature* 405, 955-959.

Lee, H.K., Takamiya, K., Han, J.S., Man, H., Kim, C.H., Rumbaugh, G., Yu, S., Ding, L., He, C., Petralia, R.S., *et al.* (2003). Phosphorylation of the AMPA receptor GluR1 subunit is required for synaptic plasticity and retention of spatial memory. *Cell* 112, 631-643.

Lee, S.J., Escobedo-Lozoya, Y., Szatmari, E.M., and Yasuda, R. (2009). Activation of CaMKII in single dendritic spines during long-term potentiation. *Nature* 458, 299-304.

Lee, Y.S., and Silva, A.J. (2009). The molecular and cellular biology of enhanced cognition. *Nat Rev Neurosci* 10, 126-140.

Lengyel, I., Voss, K., Cammarota, M., Bradshaw, K., Brent, V., Murphy, K.P., Giese, K.P., Rostas, J.A., and Bliss, T.V. (2004). Autonomous activity of CaMKII is only transiently increased following the induction of long-term potentiation in the rat hippocampus. *Eur J Neurosci* 20, 3063-3072.

Leonard, A.S., Bayer, K.U., Merrill, M.A., Lim, I.A., Shea, M.A., Schulman, H., and Hell, J.W. (2002). Regulation of calcium/calmodulin-dependent protein kinase II docking to N-methyl-D-aspartate receptors by calcium/calmodulin and alpha-actinin. *J Biol Chem* 277, 48441-48448.

Leonard, A.S., Davare, M.A., Horne, M.C., Garner, C.C., and Hell, J.W. (1998). SAP97 is associated with the alpha-amino-3-hydroxy-5-methylisoxazole-4-propionic acid receptor GluR1 subunit. *J Biol Chem* 273, 19518-19524.

Leonard, A.S., and Hell, J.W. (1997). Cyclic AMP-dependent protein kinase and protein kinase C phosphorylate N-methyl-D-aspartate receptors at different sites. *J Biol Chem* 272, 12107-12115.

- Leonard, A.S., Lim, I.A., Hemsworth, D.E., Horne, M.C., and Hell, J.W. (1999). Calcium/calmodulin-dependent protein kinase II is associated with the N-methyl-D-aspartate receptor. *Proc Natl Acad Sci U S A* 96, 3239-3244.
- Lisman, J., and Raghavachari, S. (2006). A unified model of the presynaptic and postsynaptic changes during LTP at CA1 synapses. *Sci STKE* 2006, re11.
- Lisman, J., Schulman, H., and Cline, H. (2002). The molecular basis of CaMKII function in synaptic and behavioural memory. *Nat Rev Neurosci* 3, 175-190.
- Lisman, J., Yasuda, R., and Raghavachari, S. (2012). Mechanisms of CaMKII action in long-term potentiation. *Nat Rev Neurosci* 13, 169-182.
- Lisman, J.E., and Grace, A.A. (2005). The hippocampal-VTA loop: controlling the entry of information into long-term memory. *Neuron* 46, 703-713.
- Lou, L.L., and Schulman, H. (1989). Distinct autophosphorylation sites sequentially produce autonomy and inhibition of the multifunctional Ca<sup>2+</sup>/calmodulin-dependent protein kinase. *J Neurosci* 9, 2020-2032.
- Lu, Y., Allen, M., Halt, A.R., Weisenhaus, M., Dallapiazza, R.F., Hall, D.D., Usachev, Y.M., McKnight, G.S., and Hell, J.W. (2007). Age-dependent requirement of AKAP150-anchored PKA and GluR2-lacking AMPA receptors in LTP. *EMBO J* 26, 4879-4890.
- Malenka, R.C., and Bear, M.F. (2004). LTP and LTD: an embarrassment of riches. *Neuron* 44, 5-21.
- Malenka, R.C., Kauer, J.A., Perkel, D.J., Mauk, M.D., Kelly, P.T., Nicoll, R.A., and Waxham, M.N. (1989). An essential role for postsynaptic calmodulin and protein kinase activity in long-term potentiation. *Nature* 340, 554-557.
- Malinow, R., Schulman, H., and Tsien, R.W. (1989). Inhibition of postsynaptic PKC or CaMKII blocks induction but not expression of LTP. *Science* 245, 862-866.
- Mammen, A.L., Kameyama, K., Roche, K.W., and Huganir, R.L. (1997). Phosphorylation of the alpha-amino-3-hydroxy-5-methylisoxazole4-propionic acid receptor GluR1 subunit by calcium/calmodulin-dependent kinase II. *J Biol Chem* 272, 32528-32533.
- Martin, S.J., Grimwood, P.D., and Morris, R.G. (2000). Synaptic plasticity and memory: an evaluation of the hypothesis. *Annu Rev Neurosci* 23, 649-711.
- Mayford, M., Bach, M.E., Huang, Y.Y., Wang, L., Hawkins, R.D., and Kandel, E.R. (1996). Control of memory formation through regulated expression of a CaMKII transgene. *Science* 274, 1678-1683.

Mayford, M., Wang, J., Kandel, E.R., and O'Dell, T.J. (1995). CaMKII regulates the frequency-response function of hippocampal synapses for the production of both LTD and LTP. *Cell* 81, 891-904.

McGaugh, J.L. (2004). The amygdala modulates the consolidation of memories of emotionally arousing experiences. *Annu Rev Neurosci* 27, 1-28.

McGuinness, T.L., Lai, Y., and Greengard, P. (1985). Ca<sup>2+</sup>/calmodulin-dependent protein kinase II. Isozymic forms from rat forebrain and cerebellum. *J Biol Chem* 260, 1696-1704.

McLay, R.N., Freeman, S.M., and Zadina, J.E. (1998). Chronic corticosterone impairs memory performance in the Barnes maze. *Physiol Behav* 63, 933-937.

Merrill, M.A., Chen, Y., Strack, S., and Hell, J.W. (2005). Activity-driven postsynaptic translocation of CaMKII. *Trends Pharmacol Sci* 26, 645-653.

Merrill, M.A., Malik, Z., Akyol, Z., Bartos, J.A., Leonard, A.S., Hudmon, A., Shea, M.A., and Hell, J.W. (2007). Displacement of alpha-actinin from the NMDA receptor NR1 C0 domain By Ca<sup>2+</sup>/calmodulin promotes CaMKII binding. *Biochemistry* 46, 8485-8497.

Meyer, T., Hanson, P.I., Stryer, L., and Schulman, H. (1992). Calmodulin trapping by calcium-calmodulin-dependent protein kinase. *Science* 256, 1199-1202.

Miller, S., Yasuda, M., Coats, J.K., Jones, Y., Martone, M.E., and Mayford, M. (2002). Disruption of dendritic translation of CaMKIIalpha impairs stabilization of synaptic plasticity and memory consolidation. *Neuron* 36, 507-519.

Miyakawa, T., Yared, E., Pak, J.H., Huang, F.L., Huang, K.P., and Crawley, J.N. (2001). Neurogranin null mutant mice display performance deficits on spatial learning tasks with anxiety related components. *Hippocampus* 11, 763-775.

Mizuno, K., and Giese, K.P. (2005). Hippocampus-dependent memory formation: do memory type-specific mechanisms exist? *J Pharmacol Sci* 98, 191-197.

Morris, R.G., Anderson, E., Lynch, G.S., and Baudry, M. (1986). Selective impairment of learning and blockade of long-term potentiation by an N-methyl-D-aspartate receptor antagonist, AP5. *Nature* 319, 774-776.

Mullasseril, P., Dosemeci, A., Lisman, J.E., and Griffith, L.C. (2007). A structural mechanism for maintaining the 'on-state' of the CaMKII memory switch in the post-synaptic density. *J Neurochem* 103, 357-364.

Navakkode, S., Sajikumar, S., and Frey, J.U. (2007). Synergistic requirements for the induction of dopaminergic D1/D5-receptor-mediated LTP in hippocampal slices of rat CA1 in vitro. *Neuropharmacology* 52, 1547-1554.

Neuner-Jehle, M., Denizot, J.P., and Mallet, J. (1996). Neurogranin is locally concentrated in rat cortical and hippocampal neurons. *Brain Res* 733, 149-154.

O'Leary, H., Lasda, E., and Bayer, K.U. (2006). CaMKII $\beta$  association with the actin cytoskeleton is regulated by alternative splicing. *Mol Biol Cell* 17, 4656-4665.

Ohki, E.C., Tilkins, M.L., Ciccarone, V.C., and Price, P.J. (2001). Improving the transfection efficiency of post-mitotic neurons. *J Neurosci Methods* 112, 95-99.

Okamoto, K., Nagai, T., Miyawaki, A., and Hayashi, Y. (2004). Rapid and persistent modulation of actin dynamics regulates postsynaptic reorganization underlying bidirectional plasticity. *Nat Neurosci* 7, 1104-1112.

Okamoto, K., Narayanan, R., Lee, S.H., Murata, K., and Hayashi, Y. (2007). The role of CaMKII as an F-actin-bundling protein crucial for maintenance of dendritic spine structure. *Proc Natl Acad Sci U S A* 104, 6418-6423.

Okuda, S., Roozendaal, B., and McGaugh, J.L. (2004). Glucocorticoid effects on object recognition memory require training-associated emotional arousal. *Proc Natl Acad Sci U S A* 101, 853-858.

Omkumar, R.V., Kiely, M.J., Rosenstein, A.J., Min, K.T., and Kennedy, M.B. (1996). Identification of a phosphorylation site for calcium/calmodulin-dependent protein kinase II in the NR2B subunit of the N-methyl-D-aspartate receptor. *J Biol Chem* 271, 31670-31678.

Opazo, P., and Choquet, D. (2011). A three-step model for the synaptic recruitment of AMPA receptors. *Mol Cell Neurosci* 46, 1-8.

Opazo, P., Labrecque, S., Tigaret, C.M., Frouin, A., Wiseman, P.W., De Koninck, P., and Choquet, D. (2010). CaMKII triggers the diffusional trapping of surface AMPARs through phosphorylation of stargazin. *Neuron* 67, 239-252.

Ostroff, L.E., Fiala, J.C., Allwardt, B., and Harris, K.M. (2002). Polyribosomes redistribute from dendritic shafts into spines with enlarged synapses during LTP in developing rat hippocampal slices. *Neuron* 35, 535-545.

Otmakhov, N., Griffith, L.C., and Lisman, J.E. (1997). Postsynaptic inhibitors of calcium/calmodulin-dependent protein kinase type II block induction but not maintenance of pairing-induced long-term potentiation. *J Neurosci* 17, 5357-5365.

Otmakhov, N., Tao-Cheng, J.H., Carpenter, S., Asrican, B., Dosemeci, A., Reese, T.S., and Lisman, J. (2004). Persistent accumulation of calcium/calmodulin-dependent protein kinase II in dendritic spines after induction of NMDA receptor-dependent chemical long-term potentiation. *J Neurosci* 24, 9324-9331.

- Otmakhova, N.A., and Lisman, J.E. (1996). D1/D5 dopamine receptor activation increases the magnitude of early long-term potentiation at CA1 hippocampal synapses. *J Neurosci* 16, 7478-7486.
- Ouyang, Y., Kantor, D., Harris, K.M., Schuman, E.M., and Kennedy, M.B. (1997). Visualization of the distribution of autophosphorylated calcium/calmodulin-dependent protein kinase II after tetanic stimulation in the CA1 area of the hippocampus. *J Neurosci* 17, 5416-5427.
- Ouyang, Y., Rosenstein, A., Kreiman, G., Schuman, E.M., and Kennedy, M.B. (1999). Tetanic stimulation leads to increased accumulation of Ca(2+)/calmodulin-dependent protein kinase II via dendritic protein synthesis in hippocampal neurons. *J Neurosci* 19, 7823-7833.
- Pak, J.H., Huang, F.L., Li, J., Balschun, D., Reymann, K.G., Chiang, C., Westphal, H., and Huang, K.P. (2000). Involvement of neurogranin in the modulation of calcium/calmodulin-dependent protein kinase II, synaptic plasticity, and spatial learning: a study with knockout mice. *Proc Natl Acad Sci U S A* 97, 11232-11237.
- Paoletti, P. (2011). Molecular basis of NMDA receptor functional diversity. *Eur J Neurosci* 33, 1351-1365.
- Pardridge, W.M. (2005). The blood-brain barrier: bottleneck in brain drug development. *NeuroRx* 2, 3-14.
- Persechini, A., and Stemmer, P.M. (2002). Calmodulin is a limiting factor in the cell. *Trends Cardiovasc Med* 12, 32-37.
- Pi, H.J., Otmakhov, N., El Gaamouch, F., Lemelin, D., De Koninck, P., and Lisman, J. (2010a). CaMKII control of spine size and synaptic strength: role of phosphorylation states and nonenzymatic action. *Proc Natl Acad Sci U S A* 107, 14437-14442.
- Pi, H.J., Otmakhov, N., Lemelin, D., De Koninck, P., and Lisman, J. (2010b). Autonomous CaMKII can promote either long-term potentiation or long-term depression, depending on the state of T305/T306 phosphorylation. *J Neurosci* 30, 8704-8709.
- Ramakers, G.M., Gerendasy, D.D., and de Graan, P.N. (1999). Substrate phosphorylation in the protein kinase Cgamma knockout mouse. *J Biol Chem* 274, 1873-1874.
- Ramakers, G.M., Pasinelli, P., van Beest, M., van der Slot, A., Gispen, W.H., and De Graan, P.N. (2000). Activation of pre- and postsynaptic protein kinase C during tetraethylammonium-induced long-term potentiation in the CA1 field of the hippocampus. *Neurosci Lett* 286, 53-56.
- Raman, I.M., Tong, G., and Jahr, C.E. (1996). Beta-adrenergic regulation of synaptic NMDA receptors by cAMP-dependent protein kinase. *Neuron* 16, 415-421.

Represa, A., Deloulme, J.C., Sensenbrenner, M., Ben-Ari, Y., and Baudier, J. (1990). Neurogranin: immunocytochemical localization of a brain-specific protein kinase C substrate. *J Neurosci* 10, 3782-3792.

Richter-Levin, G., and Akirav, I. (2003). Emotional tagging of memory formation--in the search for neural mechanisms. *Brain Res Brain Res Rev* 43, 247-256.

Robison, A.J., Bartlett, R.K., Bass, M.A., and Colbran, R.J. (2005a). Differential modulation of Ca<sup>2+</sup>/calmodulin-dependent protein kinase II activity by regulated interactions with N-methyl-D-aspartate receptor NR2B subunits and alpha-actinin. *J Biol Chem* 280, 39316-39323.

Robison, A.J., Bass, M.A., Jiao, Y., MacMillan, L.B., Carmody, L.C., Bartlett, R.K., and Colbran, R.J. (2005b). Multivalent interactions of calcium/calmodulin-dependent protein kinase II with the postsynaptic density proteins NR2B, densin-180, and alpha-actinin-2. *J Biol Chem* 280, 35329-35336.

Roche, K.W., O'Brien, R.J., Mammen, A.L., Bernhardt, J., and Huganir, R.L. (1996). Characterization of multiple phosphorylation sites on the AMPA receptor GluR1 subunit. *Neuron* 16, 1179-1188.

Rose, J., Jin, S.X., and Craig, A.M. (2009). Heterosynaptic molecular dynamics: locally induced propagating synaptic accumulation of CaM kinase II. *Neuron* 61, 351-358.

Sanabria, H., Swulius, M.T., Kolodziej, S.J., Liu, J., and Waxham, M.N. (2009).  $\beta$ CaMKII regulates actin assembly and structure. *J Biol Chem* 284, 9770-9780.

Sanderson, J.L., and Dell'Acqua, M.L. (2011). AKAP signaling complexes in regulation of excitatory synaptic plasticity. *Neuroscientist* 17, 321-336.

Sanhueza, M., Fernandez-Villalobos, G., Stein, I.S., Kasumova, G., Zhang, P., Bayer, K.U., Otmakhov, N., Hell, J.W., and Lisman, J. (2011). Role of the CaMKII/NMDA receptor complex in the maintenance of synaptic strength. *J Neurosci* 31, 9170-9178.

Sanhueza, M., McIntyre, C.C., and Lisman, J.E. (2007). Reversal of synaptic memory by Ca<sup>2+</sup>/calmodulin-dependent protein kinase II inhibitor. *J Neurosci* 27, 5190-5199.

Sanz-Clemente, A., Nicoll, R.A., and Roche, K.W. (2012). Diversity in NMDA Receptor Composition: Many Regulators, Many Consequences. *Neuroscientist*.

Scharf, M.T., Woo, N.H., Lattal, K.M., Young, J.Z., Nguyen, P.V., and Abel, T. (2002). Protein synthesis is required for the enhancement of long-term potentiation and long-term memory by spaced training. *J Neurophysiol* 87, 2770-2777.

Scott, D.B., Blanpied, T.A., and Ehlers, M.D. (2003). Coordinated PKA and PKC phosphorylation suppresses RXR-mediated ER retention and regulates the surface delivery of NMDA receptors. *Neuropharmacology* 45, 755-767.

Scoville, W.B., and Milner, B. (1957). Loss of recent memory after bilateral hippocampal lesions. *J Neurol Neurosurg Psychiatry* 20, 11-21.

Shen, K., and Meyer, T. (1999). Dynamic control of CaMKII translocation and localization in hippocampal neurons by NMDA receptor stimulation. *Science* 284, 162-166.

Shen, K., Teruel, M.N., Connor, J.H., Shenolikar, S., and Meyer, T. (2000). Molecular memory by reversible translocation of calcium/calmodulin-dependent protein kinase II. *Nat Neurosci* 3, 881-886.

Shen, K., Teruel, M.N., Subramanian, K., and Meyer, T. (1998). CaMKIIbeta functions as an F-actin targeting module that localizes CaMKIIalpha/beta heterooligomers to dendritic spines. *Neuron* 21, 593-606.

Sheng, M., Cummings, J., Roldan, L.A., Jan, Y.N., and Jan, L.Y. (1994). Changing subunit composition of heteromeric NMDA receptors during development of rat cortex. *Nature* 368, 144-147.

Silva, A.J., Paylor, R., Wehner, J.M., and Tonegawa, S. (1992a). Impaired spatial learning in alpha-calcium-calmodulin kinase II mutant mice. *Science* 257, 206-211.

Silva, A.J., Stevens, C.F., Tonegawa, S., and Wang, Y. (1992b). Deficient hippocampal long-term potentiation in alpha-calcium-calmodulin kinase II mutant mice. *Science* 257, 201-206.

Skeberdis, V.A., Chevalleyre, V., Lau, C.G., Goldberg, J.H., Pettit, D.L., Suadecani, S.O., Lin, Y., Bennett, M.V., Yuste, R., Castillo, P.E., *et al.* (2006). Protein kinase A regulates calcium permeability of NMDA receptors. *Nat Neurosci* 9, 501-510.

Smith, C.C., and Greene, R.W. (2012). CNS dopamine transmission mediated by noradrenergic innervation. *J Neurosci* 32, 6072-6080.

Sobczyk, A., Scheuss, V., and Svoboda, K. (2005). NMDA receptor subunit-dependent [Ca<sup>2+</sup>] signaling in individual hippocampal dendritic spines. *J Neurosci* 25, 6037-6046.

Squire, L.R. (1992). Memory and the hippocampus: a synthesis from findings with rats, monkeys, and humans. *Psychol Rev* 99, 195-231.

Squire, L.R. (2009). The legacy of patient H.M. for neuroscience. *Neuron* 61, 6-9.

Sternberg, E.M., Glowa, J.R., Smith, M.A., Calogero, A.E., Listwak, S.J., Aksentijevich, S., Chrousos, G.P., Wilder, R.L., and Gold, P.W. (1992).

Corticotropin releasing hormone related behavioral and neuroendocrine responses to stress in Lewis and Fischer rats. *Brain Res* 570, 54-60.

Strack, S., Barban, M.A., Wadzinski, B.E., and Colbran, R.J. (1997a). Differential inactivation of postsynaptic density-associated and soluble Ca<sup>2+</sup>/calmodulin-dependent protein kinase II by protein phosphatases 1 and 2A. *J Neurochem* 68, 2119-2128.

Strack, S., Choi, S., Lovinger, D.M., and Colbran, R.J. (1997b). Translocation of autophosphorylated calcium/calmodulin-dependent protein kinase II to the postsynaptic density. *J Biol Chem* 272, 13467-13470.

Strack, S., and Colbran, R.J. (1998). Autophosphorylation-dependent targeting of calcium/ calmodulin-dependent protein kinase II by the NR2B subunit of the N-methyl- D-aspartate receptor. *J Biol Chem* 273, 20689-20692.

Strack, S., McNeill, R.B., and Colbran, R.J. (2000a). Mechanism and regulation of calcium/calmodulin-dependent protein kinase II targeting to the NR2B subunit of the N-methyl-D-aspartate receptor. *J Biol Chem* 275, 23798-23806.

Strack, S., Robison, A.J., Bass, M.A., and Colbran, R.J. (2000b). Association of calcium/calmodulin-dependent kinase II with developmentally regulated splice variants of the postsynaptic density protein densin-180. *J Biol Chem* 275, 25061-25064.

Sumioka, A., Yan, D., and Tomita, S. (2010). TARP phosphorylation regulates synaptic AMPA receptors through lipid bilayers. *Neuron* 66, 755-767.

Swanson, L.W., Grant, G., Hokfelt, T., Jones, E.G., and Morrison, J.H. (2007). A century of neuroscience discovery: reflecting on the Nobel Prize awarded to Golgi and Cajal in 1906. *Brain Res Rev* 55, 191-192.

Tan, S.E., and Liang, K.C. (1996). Spatial learning alters hippocampal calcium/calmodulin-dependent protein kinase II activity in rats. *Brain Res* 711, 234-240.

Tang, Y.P., Shimizu, E., Dube, G.R., Rampon, C., Kerchner, G.A., Zhuo, M., Liu, G., and Tsien, J.Z. (1999). Genetic enhancement of learning and memory in mice. *Nature* 401, 63-69.

Thiagarajan, T.C., Piedras-Renteria, E.S., and Tsien, R.W. (2002). alpha- and betaCaMKII. Inverse regulation by neuronal activity and opposing effects on synaptic strength. *Neuron* 36, 1103-1114.

Thomas, M.J., Moody, T.D., Makhinson, M., and O'Dell, T.J. (1996). Activity-dependent beta-adrenergic modulation of low frequency stimulation induced LTP in the hippocampal CA1 region. *Neuron* 17, 475-482.

Tingley, W.G., Ehlers, M.D., Kameyama, K., Doherty, C., Ptak, J.B., Riley, C.T., and Huganir, R.L. (1997). Characterization of protein kinase A and

protein kinase C phosphorylation of the N-methyl-D-aspartate receptor NR1 subunit using phosphorylation site-specific antibodies. *J Biol Chem* 272, 5157-5166.

Tomita, S., Stein, V., Stocker, T.J., Nicoll, R.A., and Brecht, D.S. (2005). Bidirectional synaptic plasticity regulated by phosphorylation of stargazin-like TARPs. *Neuron* 45, 269-277.

Tran, Q.K., Black, D.J., and Persechini, A. (2003). Intracellular coupling via limiting calmodulin. *J Biol Chem* 278, 24247-24250.

Tully, K., and Bolshakov, V.Y. (2010). Emotional enhancement of memory: how norepinephrine enables synaptic plasticity. *Mol Brain* 3, 15.

Vest, R.S., Davies, K.D., O'Leary, H., Port, J.D., and Bayer, K.U. (2007). Dual mechanism of a natural CaMKII inhibitor. *Mol Biol Cell* 18, 5024-5033.

Vives, E., Brodin, P., and Lebleu, B. (1997). A truncated HIV-1 Tat protein basic domain rapidly translocates through the plasma membrane and accumulates in the cell nucleus. *J Biol Chem* 272, 16010-16017.

Walf, A.A., and Frye, C.A. (2007). The use of the elevated plus maze as an assay of anxiety-related behavior in rodents. *Nat Protoc* 2, 322-328.

Walikonis, R.S., Oguni, A., Khorosheva, E.M., Jeng, C.J., Asuncion, F.J., and Kennedy, M.B. (2001). Densin-180 forms a ternary complex with the (alpha)-subunit of Ca<sup>2+</sup>/calmodulin-dependent protein kinase II and (alpha)-actinin. *J Neurosci* 21, 423-433.

Wang, H., Feng, R., Phillip Wang, L., Li, F., Cao, X., and Tsien, J.Z. (2008). CaMKII activation state underlies synaptic labile phase of LTP and short-term memory formation. *Curr Biol* 18, 1546-1554.

Wang, L.Y., Orser, B.A., Brautigan, D.L., and MacDonald, J.F. (1994). Regulation of NMDA receptors in cultured hippocampal neurons by protein phosphatases 1 and 2A. *Nature* 369, 230-232.

Watson, J.B., Sutcliffe, J.G., and Fisher, R.S. (1992). Localization of the protein kinase C phosphorylation/calmodulin-binding substrate RC3 in dendritic spines of neostriatal neurons. *Proc Natl Acad Sci U S A* 89, 8581-8585.

Weisenhaus, M., Allen, M.L., Yang, L., Lu, Y., Nichols, C.B., Su, T., Hell, J.W., and McKnight, G.S. (2010). Mutations in AKAP5 disrupt dendritic signaling complexes and lead to electrophysiological and behavioral phenotypes in mice. *PLoS One* 5, e10325.

Wender, P.A., Galliher, W.C., Goun, E.A., Jones, L.R., and Pillow, T.H. (2008). The design of guanidinium-rich transporters and their internalization mechanisms. *Adv Drug Deliv Rev* 60, 452-472.

Westphal, R.S., Tavalin, S.J., Lin, J.W., Alto, N.M., Fraser, I.D., Langeberg, L.K., Sheng, M., and Scott, J.D. (1999). Regulation of NMDA receptors by an associated phosphatase-kinase signaling complex. *Science* 285, 93-96.

White, R.R., Kwon, Y.G., Taing, M., Lawrence, D.S., and Edelman, A.M. (1998). Definition of optimal substrate recognition motifs of Ca<sup>2+</sup>-calmodulin-dependent protein kinases IV and II reveals shared and distinctive features. *J Biol Chem* 273, 3166-3172.

Whitlock, J.R., Heynen, A.J., Shuler, M.G., and Bear, M.F. (2006). Learning induces long-term potentiation in the hippocampus. *Science* 313, 1093-1097.

Wong, W., and Scott, J.D. (2004). AKAP signalling complexes: focal points in space and time. *Nat Rev Mol Cell Biol* 5, 959-970.

Yamauchi, T. (2005). Neuronal Ca<sup>2+</sup>/calmodulin-dependent protein kinase II--discovery, progress in a quarter of a century, and perspective: implication for learning and memory. *Biol Pharm Bull* 28, 1342-1354.

Zhabotinsky, A.M., Camp, R.N., Epstein, I.R., and Lisman, J.E. (2006). Role of the neurogranin concentrated in spines in the induction of long-term potentiation. *J Neurosci* 26, 7337-7347.

Zhang, Y.P., Holbro, N., and Oertner, T.G. (2008). Optical induction of plasticity at single synapses reveals input-specific accumulation of alphaCaMKII. *Proc Natl Acad Sci U S A* 105, 12039-12044.

Zhong, L., Cherry, T., Bies, C.E., Florence, M.A., and Gerges, N.Z. (2009). Neurogranin enhances synaptic strength through its interaction with calmodulin. *EMBO J* 28, 3027-3039.

Zhong, L., Kaleka, K.S., and Gerges, N.Z. (2011). Neurogranin phosphorylation fine-tunes long-term potentiation. *Eur J Neurosci* 33, 244-250.

Zhou, Y., Takahashi, E., Li, W., Halt, A., Wiltgen, B., Ehninger, D., Li, G.D., Hell, J.W., Kennedy, M.B., and Silva, A.J. (2007). Interactions between the NR2B receptor and CaMKII modulate synaptic plasticity and spatial learning. *J Neurosci* 27, 13843-13853.

## Figures

Figure 1.1: The Role of CaMKII during early LTP.....	4
Figure 1.2: CaMKII Subunit Structure and Activation. ....	9
Figure 1.3: The CaMKII-GluN2B Interaction. ....	12
Figure 1.4: The Molecular Organization of the NMDAR. ....	16
Figure 2.1 Creation and genotyping of GluN2B KI mice.....	20
Figure 3.1 Spatial learning and memory is unaffected in the Barnes maze. ...	50
Figure 3.2 Spatial learning in the Morris water maze (MWM) is impaired in GluN2B KI mice.....	52
Figure 3.3 Basal anxiety levels in the GluN2B KI mice are normal. ....	54
Figure 3.4 Contextual fear conditioning and memory is unaffected in GluN2B KI mice.....	55
Figure 3.5 Contextual fear conditioning with milder conditioning trials/stimuli is unaffected in GluN2B KI mice. ....	57
Figure 3.6 Overlay of <sup>32</sup> P-labeled autophosphorylated CaMKII on brain lysate. .....	59
Figure 3.7 Concentration dependent displacement of the CaMKII/NMDAR complex by Tat-CN21.....	61
Figure 3.8 CaMKII $\alpha$ clustering time course.....	63
Figure 3.9 CaMKII $\beta$ clustering time course.....	65
Figure 3.10 Time-dependence of the increase in synaptic CaMKII $\beta$ intensity after glutamate stimulation. ....	67
Figure 3.11 CaMKII $\alpha$ redistribution is partially reversed after 5 min but shows a tendency to stay slightly enhanced up to 1 h. ....	69
Figure 3.12 Brief stimulation with glutamate is sufficient to induce CaMKII $\alpha$ translocation. ....	71
Figure 3.13 The activation and activity-dependent translocation of CaMKII is dependent on neurogranin. ....	75
Figure 3.14 Hippocampal cultures from GluN1 KI show a similar distribution of pre- and postsynaptic markers.....	77
Figure 3.15 Normal activity-dependent redistribution of CaMKII $\alpha$ in hippocampal cultures from GluN1 KI mice.....	78

Figure 3.16 Characterization of the phospho-specific antibody against GluN2B phosphoS1166 and PKA induced phosphorylation of S1166. ....	80
Figure 3.17 S1166 phosphorylation is enriched in the PSD. ....	81
Figure 3.18 Isoproterenol/ $\beta$ AR stimulation increases S1166 phosphorylation. ....	82
Figure 3.19 Isoproterenol induced S1166 phosphorylation is independent of AKAP150. ....	84
Figure 3.20 Forced swim-induced stress increases S1166 phosphorylation. ....	85
Figure 3.21 I.p. injection of propranolol inhibits forced swim induced phosphorylation of S845, but not S1166. ....	87
Figure 3.22 D <sub>1</sub> /D <sub>5</sub> receptor stimulation increases S1166 phosphorylation. ....	89
Figure 3.23 I.p. injection of SCH23390 has no effect on forced swim-induced phosphorylation. ....	90
Figure 3.24 Combined i.p. injection of propranolol and SCH23390 reduces basal S1166 phosphorylation. ....	91
Figure 3.25 I.p. injection of a combination of propranolol and SCH23390 does not block forced swim-induced S1166 phosphorylation. ....	92
Figure 3.26 I.p. injection of the A <sub>2A</sub> R antagonist SCH58261 does not effect forced swim-induced phosphorylation. ....	94
Figure 3.27 Milder forced swim stress results in reduced phosphorylation levels. ....	96
Figure 3.28 Hippocampal injection of Rp-cAMPs blocks stress-induced phosphorylation of S1166. ....	98
Figure 3.29 The 11R cell penetrating peptide is cytotoxic at a concentration of 10 $\mu$ M, but not 1 $\mu$ M. ....	101
Figure 3.30 The 11R cell penetrating peptide, but not myristoylation, inhibits CaMKII kinase activity. ....	104
Figure 3.31 The 11R cell penetrating peptide, but neither myristoylation nor the Tat Sequence, inhibits PKA kinase activity. ....	107

## Acknowledgements/Danksagung

Of course this work would not have been possible in this way without the help and support of a lot of people (I will hopefully remember to mention them all).

First I want to thank the two people who made this external Ph.D. thesis possible, Prof. Dr. Johannes Hell and Prof. Dr. Gabriele Fischer von Mollard.

Thank you, Johannes for all of your guidance and support during many exciting projects. I am grateful for all the knowledge and direction you have given me, and will always remember your open and positive nature. Your scientific and personal input and the flexibility you granted me not only let me grow as a scientist, but also personally.

I am deeply grateful to Gabi, who made all of this possible and supported me when I was taking my first baby steps in her lab during my Diploma thesis.

A special thank you goes to our collaborators Prof. Dr. Suzanne Zukin and Dr. Jessica Murphy for the fruitful and exciting collaboration on the S1166 phosphorylation of the NMDAR. I also want to thank Prof. Dr. Magdalena Sanhueza and Prof. Dr. John Lisman, who involved us in the investigation of the CaMKII/NMDAR complex and its role in the maintenance of synaptic strength. And last but not least Prof. Dr. Karen Zito and Andrew Hamilton for the collaboration on the proteasome regulated activity-dependent outgrowth of new dendritic spines (which is of course depending on the NMDAR and CaMKII).

I want to thank the Department of Chemistry at the University of Bielefeld, the Department of Pharmacology at the University of Iowa and the Department of Pharmacology at UC Davis as well as their members for the support and the thriving environment they have provided me with.

Despite the fun we sometimes make of the name, the Hell Lab was always an exciting and joyful place to be part of; thanks to all the great past and present members I had the pleasure to work with (Duane, Rob, Amy, Jason, Hui, Diana, Cigdem, Tommaso, Mingxu, Zee, Pang-Yen). I thank you

all for the good times in the lab and the even better ones after work. I “especially” want to thank Michaela Donaldson, curiously the only current native speaker for proofreading this thesis and her help with the mice husbandry. I want to thank the Matts for proof reading parts of this thesis, and having good times in and outside of the lab. I also want to thank Sharon, Yen and Cheston for their valuable help in the lab.

Und natürlich ganz besonders bedanken möchte ich mich bei meinen allerersten Vorbildern, meinen Eltern. Vielen Dank für die immerwährende Unterstützung in all dem was war und auch immer noch kommen mag.

Abschließend danke ich Maïke für ihre Unterstützung und Geduld, so wie bislang sieben wundervolle Jahre.

## Curriculum Vitae

### Sebastian Ivar Stein

#### Education

---

General qualification for University entrance, Städtisches Gymnasium, Gütersloh	09/91-06/00
Military duty at Deutsche Bundeswehr, Transport unit Lippstadt	06/00-04/01
University of Bielefeld, Department of Chemistry, Bielefeld, Germany	10/01-03/07
Diploma thesis/Master of Science in the Department of Chemistry (University of Bielefeld), Advisor Prof. Dr. Gabriele Fischer von Mollard - Chair of Biochemistry III Topic: Identification of interacting proteins of the yeast SNARE Vti1p via Suppressor-Screening and analysis of the N-terminal function of Vti1p via synthesis and characterization of mutants	06/06-03/07
Visiting Scholar/Internship, The University of Iowa College of Medicine, Department of Pharmacology, Iowa City, Iowa	04/07-06/07
External Ph.D. work, University of Bielefeld, Department of Chemistry, Bielefeld, Germany	11/07-present
Advisor Prof. Dr. Gabriele Fischer von Mollard - Chair of Biochemistry III and Prof. Dr. Johannes Hell University of California, Davis, School of Medicine, Department of Pharmacology	

#### Appointments

---

Visiting Scholar, University of Iowa College of Medicine, Department of Pharmacology, Prof. Dr. Johannes Hell	04/07-06/07
Visiting Scholar/Research Assistant III, University of Iowa College of Medicine, Department of Pharmacology, Prof. Dr. Johannes Hell	11/07-08/09
Visiting Scholar/Junior Specialist, University of California, Davis, School of Medicine, Department of Pharmacology, Prof. Dr. Johannes Hell	09/09-01/10
Visiting Scholar/Assistant Specialist, University of California, Davis, School of Medicine, Department of Pharmacology, Prof. Dr. Johannes Hell	01/10-present

#### Honors and Awards

---

Academic Federation Research Travel Grant, Society for Neuroscience Annual Meeting 2011, Washington DC	11/11
---	-------

---

**Professional Affiliations**

---

Member of the Society for Neuroscience since 2008

---

**Publications**

---

1. **Stein, I.S.**, A. Gottfried, J. Zimmermann, and G. Fischer von Mollard, *TVP23 interacts genetically with the yeast SNARE VTI1 and functions in retrograde transport from the early endosome to the late Golgi*. *Biochem J*, 2009. **419**(1): p. 229-36.
2. **Stein, I.S.** and J.W. Hell, *CaMKII hunkers down on the muscarinic M4 receptor to help curb cocaine-induced hyperlocomotion*. *EMBO J*, 2010. **29**(12): p. 1943-5.
3. Xu, H., K.S. Ginsburg, D.D. Hall, M. Zimmermann, **I.S. Stein**, M. Zhang, S. Tandan, J.A. Hill, M.C. Horne, D. Bers, and J.W. Hell, *Targeting of protein phosphatases PP2A and PP2B to the C-terminus of the L-type calcium channel Ca v1.2*. *Biochemistry*, 2010. **49**(48): p. 10298-307.
4. Sanhueza, M., G. Fernandez-Villalobos, **I.S. Stein**, G. Kasumova, P. Zhang, K.U. Bayer, N. Otmakhov, J.W. Hell, and J. Lisman, *Role of the CaMKII/NMDA receptor complex in the maintenance of synaptic strength*. *J Neurosci*, 2011. **31**(25): p. 9170-8.
5. Halt, A.R., R.F. Dallapiazza, Y. Zhou, **I.S. Stein**, H. Qian, S. Juntti, S. Wojcik, N. Brose, A.J. Silva, and J.W. Hell, *CaMKII binding to GluN2B is critical during memory consolidation*. *EMBO J*, 2012. **31**(5): p. 1203-16.
6. Hamilton, A.M., W.C. Oh, H. Vega-Ramirez, **I.S. Stein**, J.W. Hell, G.N. Patrick, and K. Zito, *Activity-dependent growth of new dendritic spines is regulated by the proteasome*. *Neuron*, 2012. **accepted**.
7. **Stein, I.S.**, M.S. Donaldson, and J.W. Hell, *CaMKII binding to GluN2B is important for massed spatial learning but not fear conditioning*. *Genes, Brain and Behavior*, 2012. **submitted**.

---

**Abstracts**

---

1. **Stein I. S.**, C.Y., Hell J. W. *Activity-driven postsynaptic clustering of endogenous CaMKII in high quality hippocampal cultures with the reformulated B27/NS21 supplement in Society for Neuroscience Annual Meeting*. 2008. Washington, DC.
2. Murphy J. A., L.C.G., **Stein I. S.**, Suadicani S. O., Bennett M. V. L., Hell J. W., Zukin R. S. *Identification of a serine residue in the carboxy-terminal domain of NR2B critical to the regulation of NMDA receptor calcium permeability by PKA in Society for Neuroscience Annual Meeting*. 2010. San Diego, California.
3. **Stein I. S.**, H.A.R., Dallapiazza R. F., Brose N., Hell J. W. *The interaction between CaMKII and GluN2B is critical for contextual memory consolidation in Society for Neuroscience Annual Meeting*. 2010. San Diego, California.
4. **Stein I. S.**, H.A.R., Dallapiazza R. F., Brose N., Hell J. W. *The role of the interaction between CaMKII and GluN2B in learning and memory in Society for Neuroscience Annual Meeting*. 2011. Washington, DC.

## Erklärung

Die vorliegende Arbeit wurde unter der wissenschaftlichen Betreuung von Prof. Dr. Johannes Hell an der University of California Davis, Department of Pharmacology und von Prof. Dr. Gabriele Fischer von Mollard, Arbeitsgruppe Biochemie III an der Fakultät für Chemie der Universität Bielefeld angefertigt. Ich versichere hiermit, dass ich die vorliegende Dissertation selbstständig verfasst habe und keine anderen außer den angegebenen Hilfsmitteln und Quellen benutzt habe. Ich habe an keiner anderen Fakultät oder Hochschule einen Antrag auf Zulassung zur Promotion eingereicht und die vorliegende Dissertation weder in der gegenwärtigen noch in einer anderen Fassung vorgelegt.



---

Sebastian Ivar Stein (19. Mai 2012)